2009

Functional Silane Based Co-Polymers for Biofunctionalization Studies, Chemical Sensing and Separations

Swapna Addagulla
University of Rhode Island

FUNCTIONAL SILANE BASED CO-POLYMERS FOR BIOFUNCTIONALIZATION STUDIES, CHEMICAL SENSING AND SEPARATIONS

BY

SWAPNA ADDAGULLA

A DISSERTATION SUBMITTED IN PARTIAL FULFILLMENT OF THE REQUIREMENTS FOR THE DEGREE OF

DOCTOR OF PHILOSOPHY

IN

DEPARTMENT OF CHEMISTRY

UNIVERSITY OF RHODE ISLAND

2009

DOCTOR OF PHILOSOPHY DISSERTATION

OF

SWAPNA ADDAGULLA

APPROVED:

Thesis Committee:

Major Professor 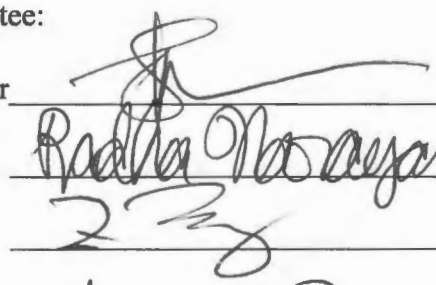

DEAN OF THE GRADUATE SCHOOL

UNIVERSITY OF RHODE ISLAND
2009

ABSTRACT

The focus of the research reported in this dissertation has focused on two areas: (1) Synthesis of silane-containing polymers and (2) the application of these polymers to surface modification of substrates such as PDMS (for microfluidic applications), glass, quartz, silicon wafers and various nanoparticles (magnetic iron oxide, silica) for use in chemical and biological sensing and separation applications as well as in biofunctionalization of magnetic nanoparticles.

Chapter 1 of this dissertation described the preparation of a library of silane containing co- and terpolymer prepared with various susbtitued maleimides along with their characterization by FTIR, UV-Visible, ^{1}H- and ^{13}C-NMR, TGA and DSC. The ability to control the reactive functionalities incorporated into the polymer structure affords direct control over the resulting properties of the materials. Chapter 2 describes the conversion of the polymers prepared in chapter 1 into various functional forms that can be used in the design of different sensing and separation platforms. More specifically, this chapter lays out the conversion of these polymers into polymer thin-films, polymer-silica composites, polymer-coated nanoparticles and polymer facilitated nanoparticle arrays. In all cases the conversion or assembly of these polymers into these structures is made possible through the reaction of the alkoxysilane side groups of the polymers forming very robust siloxane bonds. These structures are being explored for their use in chemical sensing and separations of

explosive and amines and other species as described in other chapters of this dissertation. The conversion of the polymer into thin-films is accomplished through either dip-coating using a layer-by-layer deposition scheme or through a spin-coating scheme. The layer-by-layer scheme allowed for a controlled deposition of the polymers into films of desired dimension where a constant loading density is observed as a function of the deposition cycle (i.e. number of layers). A facile biofunctionalization of magnetic and silica nanoparticles is also describe in this dissertation. The ability to biofunctionalize these materials allows for their potenital application in the biomedical field where they can be used in detection and in targeted drug delivery.

Also described herein is the functionalization of microfluidics systems for bioanalysis. Surface modification with silica nanoparticles would be a promising technique to provide an excellent interface on the conventional polymer surface. A sensitive biofunctionalization is carried in microfluidic chips. The antigens attached to the surface modified silanes via urea linkage and successful binding of antigens and antibodies is observed and can preserve the bioactivity of the antigens and antibodies and resist non specific adsorption. This study can be extended for a high-throughput system for bio-marker proteins.

Finally, we demonstrated the applicability of these polymers for sensing amines and nitro compounds. Substitutions on the phenyl ring help in tuning the sensitivity of these polymers to various amines including very weak aromatic amines. Increase in the intensity of fluorescence and a very noticeable change in color of the polymer solutions in presence of amines helps in their detection. The color of the

solution depended on two factors: identity of the polymer and identity of the base. For different polymers, the color varied with the electron withdrawing/donating power of the substitutions on the phenyl ring and also the variation in the side chain allyl vs. vinyl and ethoxy vs. methoxy. Also the nature of the amines 1^0 vs. 2^0 vs. 3^0 affected the rate at which the polymers reacted with those amines and formed the final yellow product. The colored polymer solutions with high fluorescence intensity have been used to detect the presence of nitro compounds as their presence brought the fluorescence down and was directly proportional to the amount of nitro compound present. This work represents our ability to design, control and utilize novel materials for various applications.

DEDICATION

My Devotion and Education Is Most Humbly and Respectfully

Dedicated to The Lotus Feet of

SRI SHIRDI SAI BABA

My Parents Ashok Addagulla and Nagarani Addagulla

My Most Lovely Husband Sreenivasa Sanikommu

ACKNOWLEDGEMENTS

Without the help of others, nothing worthwhile can be accomplished. I would like to thank a few people for helping me through out this thesis process.

First and foremost my advisor, Assistant Professor Jaycoda. S. Major for his guidance and encouragement during this study and for his invaluable mentorship through out my stay in graduate school. He not only guided me in academics, research but also in my career. It is not often that one finds an advisor and colleague that always finds the time for listening to the little problems and roadblocks that unavoidably crop up in the course of performing research. His technical and editorial advice was essential to the completion of this dissertation and has taught me innumerable lessons and insights on the workings of academic research in general.

I would also like to thank all my committee members for their support and useful suggestions. Special sincere acknowledgements to Dr. Martin Bide for his valuable time. I am also thankful to Dr.Sze Yang, Dr. Brenton Deboef who helped me with useful discussions and suggestions.

I would also like to thank Dr. Radha Narayanan for giving me access to the instruments in your laboratory.

My thanks also goes to Dr. Zhang and Dr. Mohammed Faghri for supporting my research by funding me during my research. I am very grateful to Dr. Sue Geldart from whom I learned better teaching skills. Thanks Sue for teaching me to take things as they come.

I would like to acknowledge my colleagues Deidre Blackwell, Louis Marchetti, Matthew Belisle and Deanna Silva for the most useful discussions and helpful suggestions with my research. Thank you all for making my stay in this lab a cherishable one. A special sincere gratitude to Shathaverdhan Potavathri for helping me through out my stay in school.

I would like to thank all the faculty and staff of chemistry department who have been helpful either directly or indirectly towards the completion of my degree.

I am also thankful to my best friend Shravan Jalli for the support, suggestions and help I received from him in my research. I wish him all the best and success in all his endeavors in future.

I cannot end without thanking my family, on whose constant encouragement and love I have relied throughout my time at the Academy. I am grateful also to the examples of my brother, Nagaraju Addagulla, Sister-in-law, Kalpana Addagulla, my father, Ashok Addagulla, and my mother, Nagarani Addagulla. Their unflinching courage and conviction will always inspire me, and I hope to continue, in my own small way, the noble mission to which they gave their lives. It is to them that I dedicate this work.

Last, but not least I would like to thank my husband Sreenivasa Reddy Sanikommu for his understanding and love during the past few years. His support and encouragement was in the end what made this dissertation possible.

Preface

This dissertation has been prepared in the manuscript format in accordance with section 11-3 of the Graduate Manual of the University of Rhode Island. Some redundancy is inevitably introduced into the dissertation e.g.; references that appear at the end of the chapter must also appear in bibliography.

This dissertation is divided into seven chapters. Chapter one contains a general introduction about the design of materials and their applications. Chapter two contains the details of synthesis and characterization of novel silane-based polymer materials which bear silane side-groups which have been modified into various other forms and studies. Chapter three describes the conversion of these polymeric materials into nanocomposites and their assembly onto thin films by a Layer-by-Layer strategy using "dip-coating" and "spin-coating" methods. Chapter four describes how the polymers prepared in Chapter 2 were used to facilitate the attachment of proteins to the surface of magnetic (iron oxide) nanoparticles. Chapter five is aimed at developing novel ways of functionalizing microfluidic systems for bioanalysis. A sensitive biofunctionalization is carried in microfluidic chips. The antigens attached to the surface modified silanes via urea linkage and successful binding of antigens and antibodies is observed and can preserve the bioactivity of the antigens and antibodies and resist non specific adsorption.

This study can be extended for a high-throughput system for bio-marker proteins. Chapter six is about the use of these polymers as sensors for detecting primary, secondary and tertiary amines based on the color changes and finally Chapter seven is about the conclusions and future work. This is followed by a bibliography.

Table of Contents

List of Tables

List of Schemes

List of Figures

CHAPTER 1

INTRODUCTION

The recent advances in simulation, chemistry, processing techniques, and analytical instrumentation allow a whole host of new types of polymer particles and polymer nanotechnology applications to be realized. Particles include; hollow, multi-lobed, magnetic, functionalized with reactive groups on the surface, conductive, etc. Our ability to devise new process control strategies have led to the ability to control the shape, chemical composition, internal structure, and morphology of the nanoparticles so as to develop new levels of product performance and application[1].

Nanotechnology enables us to create functional materials, devices, and systems by controlling matter at the atomic and molecular scales, and to exploit novel properties and phenomena[2]. Nanosensors and nano-enabled sensors have applications in many industries, among them transportation, communications, building and facilities, medicine, safety, and national security, including both homeland defense and military operations. Consider nanowire sensors that detect chemicals and biologics[3], nanosensors placed in blood cells to detect early radiation damage in astronauts[4], and nanoshells that detect and destroy tumors[5]. Nanomaterials and nanostructures are other promising application areas.

Two functions often separated in many sensors, especially those for chemicals and biological substances, are recognition of the molecule or other object of interest and transduction of that recognition event into a useful signal. Nanotechnology will

enable us to design sensors that are much smaller, less power hungry, and more sensitive than current micro- or macrosensors.

Recent advances in top-down manufacturing processes have spurred both micro- and nanotechnologies. Makers of leading-edge ICs use lithography, etching, and deposition to sculpt a substrate such as silicon and build structures on it. Conventional microelectronics has approached the nanometer scale—line widths in chips are near the 100 nm level and are continuing to shrink. MEMS (Micro Electromechanical Systems) devices are constructed in a similar top-down process. As these processes begin working on smaller and smaller dimensions, they can be used to make a variety of nanotechnology components, much as a large lathe can be used to make small parts in a machine shop.

In the nano arena, various bottom-up methods use individual atoms and molecules to build useful structures. Under the right conditions, the atoms, molecules, and larger units can self-assemble[6]. Alternatively, directed assembly can be used[7]. In either case, the combination of nano-scale top-down and bottom-up processes gives materials and device designers a wide variety of old and new tools. Designers can also combine micro- and nanotechnologies to develop new sensor systems.

Few sensors today are based on pure nanoscience, and the development of nano-enabled sensors is in the early stages; yet we can already foresee some of the possible devices and applications. Sensors for physical properties were the focus of some early development efforts, but nanotechnology will contribute most heavily to realizing the potential of chemical and biosensors for safety, medical, and other purposes[8].

Nanotechnology will also enable the very selective, sensitive detection of a broad range of biomolecules[9]. Other areas we expect to benefit from nanotechnology-based sensors include transportation (land, sea, air, and space); communications (wired and wireless, optical, and RF); buildings and facilities (homes, offices, factories); humans (especially for health and medical monitoring); and robotics of all types[11]. We'll also see nano-enabled sensors increasingly integrated into commercial and military products. Many new companies will make nano materials and some will make sensors based on them. Nanotechnology is certain to improve existing sensors and be a strong force in developing new ones. The field is progressing, but considerable work must be done before we see its full impact. Among the obvious challenges are reducing the cost of materials and devices, improving reliability, and packaging the devices into useful products. Nevertheless, we are beginning to see nano-scale materials and devices being integrated into real-world systems, and the future looks very bright indeed for technology on a tiny scale[12].

Polymer materials offer important advantages for sensing applications including (1) mechanical robustness compared with Silicon and other semiconductor materials; (2) potentially lower cost of preparation and processing; (3) low temperature processing and enhanced biocompatibility; (4) new methods of processing including molding, embossing, melt processing, and imprinting[13].

Microfluidic systems have also become important platforms for diagnostics and therapeutic applications. The use of microfluidic devices to conduct biomedical research and create clinically useful technologies has a number of significant advantages. First, because the volume of fluids within these channels is very small,

usually several nanoliters, the amount of reagents and analytes used is quite small. This is especially significant for expensive reagents. Microfluidic technologies enable the fabrication of highly integrated devices for performing several different functions on the same substrate chip include specific binding of proteins, isoelectric focusing[14,15,16], DNA analysis[17-20] and cell separation[21].

The second step in characterization of material after its design is its assembly. The importance of self-assembly as a synthetic tool in the fabrication of polymeric materials has increased dramatically due to the complex chemical nature of current materials[22]. A very limited number of synthetic polymeric systems that have either been fabricated through simulating nature's self-assembly methodologies or have been suggested have begun to emerge in the literature[22].Typical forces that are used for the assembly include Hydrogen bonding, van der waal's, electrostatic, capillary and hydrophobic forces; metal-ligand interactions; and covalent chemical bonds e.g. covalent Si-O-Si interactions[23]. A number of techniques have been developed for modification of surfaces such as atmospheric plasma treatments[24], vacuum plasma treatments[24], microwave plasma[25], corona discharge[26], ion beam irradiation[27], plasma deposition[28], photolithography[29] and immobilization of biologically active molecules/ligands[30]. All these methods leave the bulk material properties unaffected, from a practical standpoint, each suffers from lack of operating conditions and lack of controllability. Much of research is done on nanocomposite thin films. Nanocomposite materials are multiphase materials and thin film deposition methods have proven very useful in producing nanocomposites with very sensitive microstructural control. Owing to the very small structural length scale, nanocomposites often display unusual

and enhanced properties compared to bulk materials that have potentially important technological applications[31]. Nanocomposites of silica particles in a polymer matrix have received a great deal of interest. Depending on the polymer composition and structure, such nanocomposites exhibit a unique combination of desirable properties (for example, physical, chemical, mechanical, optical, magnetic and electrical) that are otherwise unattainable[32].

The main goal of this research work is to design and develop novel materials (polymers) using simpler, convenient techniques and which could be easily prepared. Theses materials have unique properties and multiple applications which allow their use as thin films, be modified into polymer nanocomposites and used as multifunctional sensors all made of the same materials[33-37]. The preparation of polymers, their characterization and its conversion into various forms for various applications has been mentioned below concisely and dealt with in detail in the following chapters[37-46].

In chapter two of this dissertation, we report the facile synthesis of a wide range of silane based copolymers. The work described in this chapter focuses on our ability to design materials which allows us to introduce various functional moieties into the matrix of the bulk materials which is finally used to tune the macroscopic material selectivity. Synthesis of these polymers has been carried out in three steps, In the first step, the maleic anhydride is reacted with various functionalized anilines to synthesize the maleamic acid and followed by the ring closure by dehydration to give the respective substitututed N-Phenylmaleimide. In the final step, the phenylmaleimide is copolymerized with a variety of allyl/vinyl alkoxy silanes to result

in the desired polymers. The polymerization is achieved by radical initiator AIBN, the amount of initiator used can control the chain lengths and also the molecular weights of the polymers. A variety of methods have been used to characterize these materials. FTIR, ^{1}H NMR and ^{13}C NMR have been used to determine the structure of these polymers. DSC (Differential Scanning Calorimetry) was used to study the thermal properties in order to understand the thermal behavior and robustness of these polymers. GPC (Gel Permeation Chromatography) to determine the molecular weights of the polymers.

In Chapter 3 we report how the prepared silane based copolymers are converted into various functional forms such as polymer-silica composite nanoparticles and modification of various substrates by deposition and by a facile layer-by-layer approach. These nanocomposite particles and thin-films were shown to be effective in the detection of amino and nitro containing compounds using fluorescence and fluorescence quenching as the detection scheme. UV-Visible Spectroscopy was used to confirm material deposition with each cycle when preparing polymer thin-films. We observe an increase in the intensity of the absorption band of the chromophore in the UV-Visible spectra with increase in the amount deposited with each deposition cycle in all the cases. Since the chemistries of the surfaces used such as silicon and glass is similar to those of capillaries (CE or CEC) the polymers deposited on these surfaces provided a two dimensional environment of how the polymer is effected under different conditions when these materials are made into columns. The modification of the surfaces has been accomplished by a facile spin-

coating or dip-coating method and provides a very convenient alternative to the laborious lithographic techniques for preparation of arrayed interfaces.

In Chapter 4 we report facile attachment of proteins to the surface of magnetic iron oxide nanoparticles using our polymers as well as other simple silane compounds. It was possible to demonstrate the retention of the biofunctionality of the proteins when a polymer underlayer is employed. This is most likely due to the polymer providing a cushion that protects the protein from the surface of the particles, where surface effects may adversely affect the protein. This work also demonstrated the successful attachment of antigens and antibody that can be used to design biosensors, as well as allowing for the design of targeted drug delivery and imagining systems.

In Chapter 5 we developed novel ways of functionalizing microfluidics systems for bioanalysis. Through the sensitive biofunctionalization carried in microfluidics chips, successful binding of antigens and antibodies is observed and can preserve the bioactivity of the antigens and antibodies and resist non-specific adsorption and prevents the surface fouling of proteins in the channels.

Chapter 6 describes the application of the polymers reported in chapter 2 for sensing organic molecules such as amines and nitro compounds. The polymers not the monomers or their precursors were found to be sensitive to the presence of amines. These polymers were found to react with primary, secondary and tertiary amines at different rates giving rise to colored intermediates which finally turns to a yellow colored final product.

Both ^{1}H and ^{13}C NMR studies confirmed the formation of Imines when the polymers react with primary amines and enamine formation with secondary amines.

This work also describes how the properties of the bulk can be tuned by introducing different groups on the phenyl ring. More electronegative the group is more sensitive the polymer is to the presence of weak bases such as aromatic amines. Another advantage of these polymers as sensors is the dependence of the sensitivity on the polymer concentration rather than the amine. Hence even very low concentrations of amines can be detected by increased polymer concentration.

The distinct advantages of the materials reported in this dissertation are the ease of preparation and the reproducibility of method used for polymer preparation. The simplicity of maleimides chemistry allows the introduction of a variety of functional groups which allows the materials to be used as sensors for a variety of organic molecules. The tunability of side chains also provides an advantage as they help in forming strong and stable Si-O-Si covalent bonds and also provides control on materials deposition.

These polymers are hence very easy to be modified into thin films which are very robust under harsh oxidizing conditions. The modification of these polymers to nanocomposites can be done by employing simple siloxane chemistry[33]. This property of the materials can have a variety of applications for useful functional devices such as improved sensor design for lab on a chip and better materials for columns in separation chemistry.

References

1. Jamie Hobbs, Depts. of Chemistry & Physics & Astronomy, University of Sheffield, UK, Real-time Structural Analysis for Soft Nanotechnology, NSTI, Nanotech, The National Technology and Conference Trade Show., June, 2006.
2. "Small Wonders, Endless Frontiers: A Review of the National Nanotechnology Initiative," National Academy Press, 2002.
3. Cui, Y., et al., "Nanowire Nanosensors for Highly Sensitive and Selective Detection of Biological and Chemical Species," *Science*, Vol. 293, Aug. 17, 2001, pp. 1289-1292.
4. "Space Mission for Nanosensors," *The Futurist*, Nov./Dec. 2002, p. 13.
5. Cassell, J.A., "DoD grants $3M to Study Nanoshells for Early Detection, Treatment of Breast Cancer," *NanoBiotech News*, Vol. 1, No. 3, Aug. 13, 2003.
6. Bernt, I., et al., "Molecular Self-Assembly: Organic Versus Inorganic Approaches," Springer Verlag, M. Fujita, ed., 1st Ed., May 15, 2000.
7. Nanotechnology at Zyvex Capabilities
8. Vo-Dinh, T., B.M. Cullum, and D.L. Stokes, "Nanosensors and Biochips: Frontiers in Biomolecular Diagnosis," *Sensors and Actuators B*, 74 (2001) pp. 2-11.

9. Nicewarner-Pena, R., et al., "Submicrometer Metallic Barcodes," *Science*, Vol. 294, 2001, p. 137.

10. Freemantle, F., "Nano Bar Coding for Bioanalysis," C&EN: News of the Week, *Science*, Vol. 79, No. 41, Oct. 8, 2001, p. 13.

11. Smalley, E., "Chip Senses Trace DNA," *Technology Research News*, Jul. 30/Aug. 6, 2003.

12. "Ultralight device analyzes gases immediately. Flying SnifferSTAR may aid civilians and U.S. Military," Sandia National Laboratories, Press Release, Jan. 23, 2003.

13. Fan, Kee Ryu, Kashan Shaikh, David Bullen., Chang, Liu., Jack, Chen., Polymer Micromachining and Applications in Sensors, Microfluidics, and Nanotechnology. Journal of Micromechanics and Engineering, 2000, 10, 80-84.

14. Macounova, K., Cabrera, C. R., Holl, M. R. & Yager, P. Generation of natural pH gradients in microfluidic channels for use in isoelectric focusing. Analytical Chemistry 72, 3745-3751 (2000).

15. Xu, J., Lee, C. S. & Locascio, L. E. Isoelectric focusing of green fluorescence proteins in plastic microfluid channels. Abstracts of Papers of the American Chemical Society 219, 9-ANYL (2000).

16. Macounova, K., Cabrera, C. R. & Yager, P. Concentration and separation of proteins in microfluidic channels on the basis of transverse IEF. Analytical Chemistry 73, 1627-1633 (2001).

17. Buchholz, B. A. et al. Microchannel DNA sequencing matrices with a thermally controlled "viscosity switch". Analytical Chemistry 73, 157-164 (2001).

18. Fan, Z. H. et al. Dynamic DNA hybridization on a chip using paramagnetic beads. Analytical Chemistry 71, 4851-4859 (1999).

19. Koutny, L. et al. Eight hundred base sequencing in a microfabricated electrophoretic device. Analytical Chemistry 72, 3388-3391 (2000).

20. Lee, G. B., Chen, S. H., Huang, G. R., Sung, W. C. & Lin, Y. H. Microfabricated plastic chips by hot embossing methods and their applications for DNA separation and detection. Sensors and Actuators B-Chemical 75, 142-148 (2001).

21. Yang, J., Huang, Y., Wang, X. B., Becker, F. F. & Gascoyne, P. R. C. Cell separation on microfabricated electrodes using dielectrophoretic/gravitational field flow fractionation. Analytical Chemistry 71, 911-918 (1999).

22. Warren Gerhardt, Matija Carne, and MarcusW eck., Multifunctionalization of Synthetic Polymer Systems though Self-Assembly., Chemistry-A European Journal., 10, 24, 6212-6221.

23. Iwasaki, Y., Sawada, S., Nakabayashi, N., Khang, G., Lee, H.B., Ishihara, K., Biomaterials, 1999, 20, 2185.

24. Shenton, M.J., Surface Modification of Polymer Surfaces: atmospheric plasma versus vacuum plasma treatments, Journal of Physics D: Applied Physics, 18, 34, 2001, 2761-2768.

25. Dong H. Shin, Chan U. Bang, Jong H. Kim, Kun H. Han, Yong C. Hong, Han S. Uhm, Dae K. Park and Ki H.Kim., Modification of metal surfaces by microwave plasma at atmospheric pressure, Surface and Coatings Technology, 201, 9-11, 2007, 4939-4942.

26. Mittal, K.L., A text book Polymer Surface Modification: relevance to adhesion, Volume 2.

27. Ito, Y., Materials Science and Engineering C, 1998, 6, 267.

28. B.Pignataro, E.Conte, A.Scandurra and G.Marletta, Biomaterials, 1997, 18, 1461.

29. Sherlock, R.J., Bhogal, D.N., Ball, M., Glynn, T.J., Proceedings of Society of Photooptical Instrumentation Engineers, 2003, 4876.

30. Dewez, J., Lhoest, J.B., Detrait, E., Berger, V., Dupont-Gillain, C.C., Vincet, L.M., Schneider, Y.J., Bertrand, P., Rouxhet, P.G., Biomaterials, 1999, 19,1441.

31. Robert, Cammaratta., Processing and Mechanical Behavior of Nanocomposite Thin Films, Material Science and Engineering, Seminar, 2006.

32. Abhikit, Biswas., The challenge of fabricating nanocomposite thin films, Nanowerk., July 10, 2007.

33. Aruna, M.Velamakanni, Functional Silane Based Polymers for Sensing and Separations, Thesis Dissertation, University of Rhode Island, 2006.

34. Sertchook, H., Elimech, H., Avnir, D., Composite Particles of Silica/Polydimethylsiloxane , Chemistry of Materials, 2005, 17, 4711-4716.

35. Major, J.S., Blanchard, G.J., Strategies for Covalent Multilayer Growth.1. Polymer Design and Characterization, Chemistry of Materials, 2002, 14, 2567-2573.

36. Sagiv, J., Journal of American Chemical Society, 1980, 102, 92-98.

37. De, G., Karmakar, B., Ganguli, D., Journal of Materials Chemistry, 2000, 10, 2289-2293.

38. Rodriguez Gutierrez, J.A., Petit Dominguez, M.D., Pinilla Macais, J.M., "Development of ion-selective electrochemical sensors by using the sol-gel process." Analytica Chimica Acta (2004) 524 (1-2), 339-346.

39. Ito, A.; Shinkai, M.; Honda, H.; Kobayashi, T. Medical Application of Functionalized Magnetic Nanoparticles. *Journal of Bioscience and Bioengineering* **2005**, *100*, 1-11.

40. Ito, A.; Shinkai, M.; Honda, H.; Kobayashi, T. Medical Application of Functionalized Magnetic Nanoparticles. *Journal of Bioscience and Bioengineering* **2005**, *100*, 1-11.

41. The Future of Sensors, Electronic Design, The Authority on Emerging Technologies for Design Solutions, July 5, 2004.

42. Jones, R.M., Lu, L., Helgeson, R., Bergstedt, R.S., McBranch, D.W., Whitten, D.G., Proceedings of National Academy of Sciences, 2001, 98, 14769.

43. Bastos, C., Mgan, N., Sensors and Actuators, B. Chemical, 2006, 116, 151.

44. Ailamaki, A., Faloustos, C., Fischbeck, P.S., Small, M.J., Small, J., Sigmod Record, 2003, 32, 47.

45. A Textbook by Jiri Janata, Principles of Chemical Sensors.

46. A textbook by Rameier Narayanaswamy, Optical .Sensors: Industrial, Environmental and Diagnostic Applications.

Functional Silane-Based Polymers for Chemical Sensing and Separations

CHAPTER 2

Preparation and Characterization of Silane-Based Polymers

Abstract

In this chapter, the preparation and characterization of a group of silane-based copolymers are presented. The copolymers were all designed in-house through radical polymerization of various phenylmaleimides with either vinyl/allyl alkoxy silanes which are capable of being incorporated into covalently bound multilayer synthesis, polymer nanocomposites monolithic columns and sensors. We report on the co-polymerization of allyltrimethoxy, allyltriethoxy, vinyltriethoxy and vinyltrimethoxy acid monomers with a variety of N-Phenyl substituted maleimides in chloroform with AIBN as a radical initiator. The substituted maleimides were prepared by reaction of maleic anhydride with selected aromatic amines. Polymerization results are typically in the range of 60-95% consumption of monomers. ^{1}H NMR, FTIR, UV, TGA, DSC, GPC and Fluorescence were used to characterize the polymers. The materials reported in this chapter have been used to modify substrates by growing covalently bound multilayers, develop sensors and also been made into polymer composite nanoparticles and their assembly and these findings are reported in the following chapters in this dissertation.

Introduction

Hybrid materials are one of the most expanding material classes based on sol-gel process. The synergistic combination of the various components in one material leads to properties and processing possibilities that cannot be reached by other materials. Particular advantages of hybrid materials are that they can be produced under mild reaction conditions in usual organic solvents[1]. Our work reports on the incorporation of polymer into the silica to form hybrid materials [2,3]. Polymer materials have been successfully used in preparation of electrodes, catalytic supports, separation techniques an sensors[2,4,5]. For biological sensing applications many biological entities have also been successfully entrapped. Because of their versatility of these materials have been used in both sensing and separation applications[6]. As in sensing, large number of materials has been studies to be used as a stationary phase in chromatographic separations[6]. In separation techniques silica based stationary phases are the most popular. The dominance of silica in the chromatographic industry reflects the many desirable properties that silica affords the chromatographer[7]. Silica can be prepared in a wide variety of pore size and particle size materials, and can be easily modified to yield stationary phases with a wide range of differing properties. The C18 column displays vastly different retention behavior relative to that of native silica, and is the most widely employed reversed phase liquid chromatography column. Some of the unique advantages of silica as a support include the ease by which it can be chemically modified to present various chemistries and, the high mechanical strength[6.7] provided. Historically these materials have provided separation media with

acceptable separation efficiency for specific classes of analyte. However, there are some disadvantages of silica based materials, including silica has a high solubility in an alkaline environment and these materials have limited application at basic pH[6,7]. Silicon based polymers is in its advanced research and technological innovations using macromolecular organosilicon compounds. Silicon containing polymers are used all over the world and in a variety of industries, domestic products and high technology applications. All the silicon based polymers can adopt very different structures like chains, nanocomposites, physical and chemical gels[1]. Organic polymer based materials have also been used as a stationary phase in reversed phase liquid chromatographic separations[8-10]. These materials have advantages over silica based materials as they provide possibility of variety of chemical modifications. The advantages of organic polymeric materials offers chemical stability over a wide range of pH. Also free from secondary effects, like surface silanol activity. These materials however, due to their physical nature, pose a problem as they may form mesopores[11].

These polymeric materials effectively limits the use of many solvents as they undergo swelling and shrinking depending on the use of some solvents in the mobile phase. Materials based on wet chemical technology processing, the so-called Sol-Gel process, paves the way to the versatility and ease of liquid film deposition on many types of substrates for a variety of inorganic and hybrid coatings materials. Many techniques have been developed and are in practical use for laboratory and industrial applications[12]. Materials based on the sol-gel technology provide an alternative to polymeric hybrid materials and organic polymeric materials[13]. The modern concept of organic-inorganic hybrid materials emerged only very recently, when the research

turned to more sophisticated materials with a higher added value, associated to the development of composites and molecular materials where the organic and inorganic component interact at a molecular level[14]. In this hybrid materials, silica and organosilanes provide materials properties which are intermediate between pure organics and pure inorganic materials. Moreover materials based on sol-gel technology provide good mechanical strength to the column, their method of preparation is simple[15], and resulting materials are thermally, chemically and mechanically robust[16-18].

Different criteria are applied for selecting materials to be used for sensing and separation applications. For example, analyte selectivity is advantageous for sensing applications; it is prime requirement for separations[19]. Materials should have transducing properties for sensing, for separation it should have ability to influence mass transfer behavior and phase partitioning of analyte. For sensing applications materials should have the ability to achieve near complete resolution of analyte within shortest possible time, as well as it should provide predictable response over a wide range of operating conditions.

In this work we report the preparation and characterization of a group of stable polymers that have been designed to incorporate silane side-groups directly into the polymer backbone. These polymers allow the preparation of polymeric sol-gels, where the polymers are capable of participating directly in the sol-gel formation process, which we demonstrate in following chapter. We expect these materials to afford control over both the physical and chemical properties (selectivity, for example) of the resulting sol-gels by the judicious choice of the various moieties like allyl and

vinylalkoxysilanes that can be incorporated into the polymer matrix[20]. We therefore intend to tailor the materials to specific sensing and separating applications. Incorporation of the silane groups into the polymer backbone is expected to minimize or eliminate phase segregation, a common problem with polymer blending. When these alkoxysilane side groups are hydrolyzed, they can bond covalently within the sol-gel matrix, to give a more uniform sol-gel matrix with minimal or no phase separation. Phase separation would lead to micro heterogeneity in the sol-gel matrix, and would affect the properties of the material. If these materials were employed as a stationary phase in RP-LC, it would adversely affect the mass transfer of the analyte throughout the column and thus affect the separation. Similarly, if these non homogeneous materials were used in sensing application, they would not give uniform sensitivity in its microenvironment.

The ability to vary/control the functional moieties incorporated into the polymer backbone, as well as the molecular weights of the polymers through a simple synthetic scheme, has been described elsewhere in the literature [21]. The polymers prepared here were found to be insoluble in water and stable for extended periods in solution, with no evidence of cross-linking of the silane groups except in the presence of a catalyst (aqueous base, for example). This was confirmed with FTIR spectra which showed no evidence of –Si-O-Si band which would occur in the region of 1020-1090 cm^{-1}. Thus no special protocols are required to handle or store these polymers[22]. In the following chapter, we describe the conversion of these polymers into stable sol-gel materials, where we use tetraethoxysilane (TEOS) to promote conversion to the sol-gel. We also report in the chapter on the ability of these polymers to participate

directly in sol-gel formation, even in the absence of any promoter (TEOS) through the cross-linking of the silane side groups which are an integral part of the polymer, describe the application of these polymers for various uses such as arrays, thin films their assembly and characterization, conversion to nano composites and their applications as sensors.

Experimental

The preparation of polymers in this study was accomplished by radical polymerization using 2, 2'-azobisisobutyronitrile (AIBN) as initiator of the various monomer units. The polymers were characterized using Gel Permeation Chromatography (GPC), solution phase ^{1}H-NMR, ^{13}C-NMR, thermogravimetric analysis (TGA), differential scanning calorimetry (DSC), and Infrared spectroscopy (FTIR-ATR). The results obtained by the above studies are presented below along with a discussion of the results following.

Monomer Preparation:

The maleimide monomers were prepared by reacting maleic anhydride with a substituted aniline in a two step reaction as described in Scheme 1 in cases where the moiety was not commercially available. The reaction of a functionalized aniline with maleic anhydride leads to the formation of the corresponding maleamic acid (**Scheme 2.1**). A 1:1 mole ratio of maleic anhydride and functionalized aniline was dissolved in chloroform and stirred overnight at ambient conditions until the maleamic acid

precipitated out of the solution. This was filtered, washed with excess chloroform and dried before use for next step.

Scheme 2.1: Reaction of Maleic Anhydride with functonalized amine to give Maleamic acid

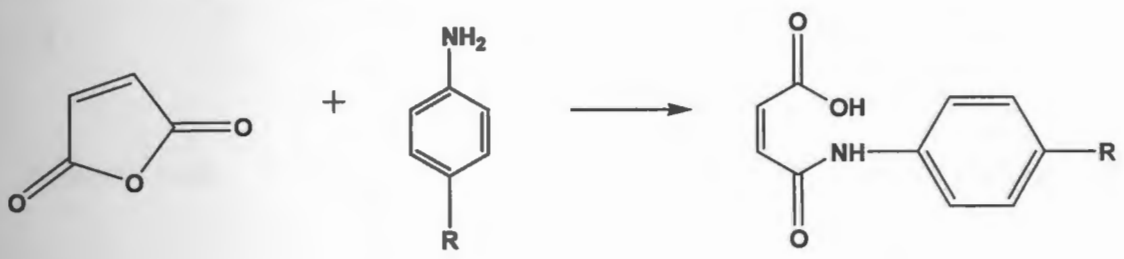

Maleic Anhydride **Functionalized Aniline** **Maleamic acid**

Cyclization of the maleamic acid (**Scheme 2.2**) is accomplished by reaction with sodium acetate in acetic anhydride. Acetic Anhydride was used to dissolve the solid and a 1:1 mole ratio of sodium acetate. The mixture was refluxed at 70 degrees Celsius for 2-3 hours. After ring closure, the maleimide monomers are collected from ice-cold water with stirring, followed by filtration and rinsing with cold water and purified for further use.

Scheme 2.2: Ring closure reaction of Maleamic acid

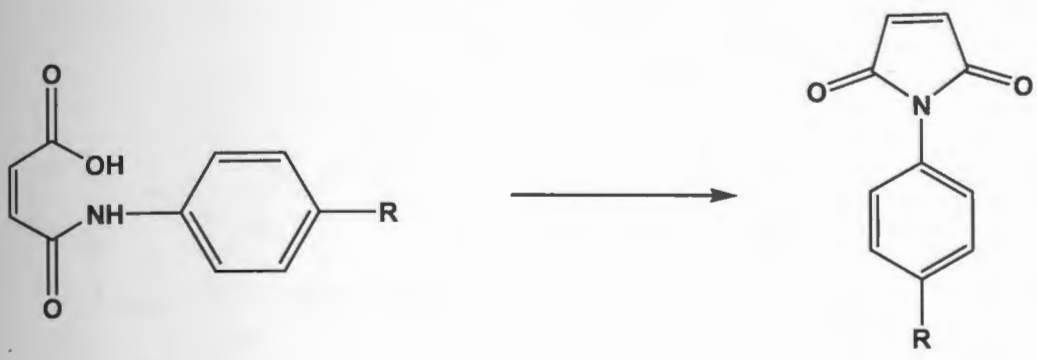

Maleamic acid **N-Phenyl Maleimide**

Polymer Preparation:

The polymers described in this work were prepared by reacting N-Phenyl maleimide (NPM) with vinyltrimethoxy/ethoxy silanes or allylmethoxy/ethoxy silanes using AIBN as the radical initiator. The NPM Monomers was dissolved in chloroform in a round bottom flask. VTMS (1:1 mole ratio) and AIBN (10% w/w) were added to the flask and refluxed at 50-60 degrees Celsius for 24 hours. Upon completion of the reaction, excess solvent was removed by rotary evaporation and the resulting solution was diluted with hexanes and stirred for ~ 30 min to separate residual monomer from the polymer product. The resulting polymer was collected by filtration and air dried.

The polymer preparation of some of the representative polymers has been described in detail below.

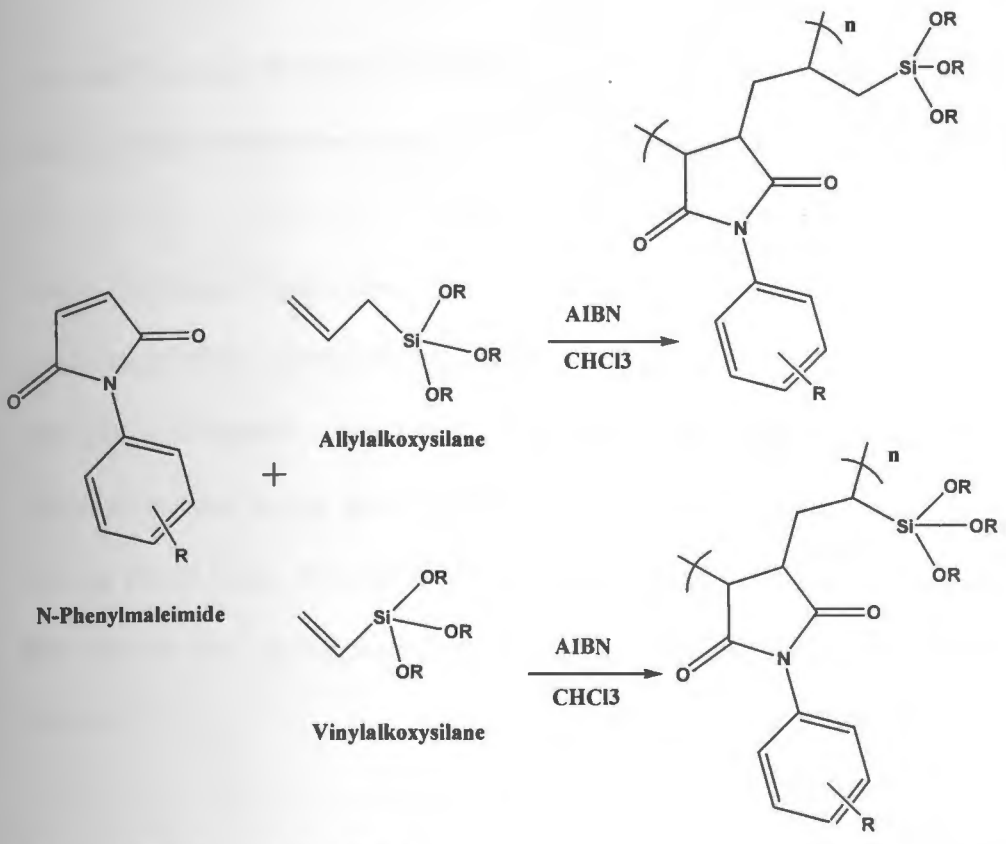

Scheme 2.3: Synthesis of Polymer

Poly (N-Phenylmaleimide-vinyltrimethoxy silane): Poly(N-Phenylmaleimide-vinyltrimethoxy silane), poly (NPM-VTMS), was prepared by reacting equimolar amounts of N-phenyl maleimide with vinyltrimethoxy silane in the presence of AIBN. Refluxed at 50-60 degrees Celsius for 24 hours. Purification of the product was accomplished by dissolution in chloroform and collection from hexane. Typical yield for this polymerization is 80% with 10% w/w AIBN initiator, 85% with 5 mole % AIBN initiator and >85% with 1 mole % AIBN initiator.

Poly (N-Phenylmaleimide-allyltrimethoxy silane): Poly (N-Phenylmaleimide-allyltrimethoxy silane), poly (NPM-ATMS), was prepared by reacting equimolar amounts of N-Phenyl maleimide with allyltrimethoxy silane in the presence of AIBN,

a radical initiator. Refluxed at 50-60 degrees Celsius for 24 hours. Purification of the product was accomplished by dissolution in chloroform and collection from hexane.

Poly (4-Chloro-N-phenylmaleimide-vinyltrimethoxy silane): Poly (4-Chloro-N-phenylmaleimide-vinyltrimethoxy silane), (poly (4-Cl-NPM-VTMS), was prepared by reacting equimolar amounts of 4-Chloro-N-phenylmaleimide with vinyl trimethoxysilane in the presence of AIBN (10% w/w). Refluxed at 50-60 degrees Celsius for 24 hours. Typical yield for this polymerization was ~80%. Purification of the product was accomplished by dissolution in chloroform and collection from hexane.

Poly (4-fluoro-N-phenylmaleimide-vinyltrimethoxy silane): Poly (4-fluoro-N-phenylmaleimide-vinyltrimethoxy silane), (poly (4-Fl-NPM-VTMS), was prepared by reacting 4-Fluoro-N-phenylmaleimide with vinyl trimethoxy silane in chloroform in presence of the initiator AIBN (10 mole%). Reaction conditions and procedures were same as reported above. Typical yield for this polymerization was ~80%.

Poly (4-Bromo-N-phenylmaleimide-vinyltrimethoxy silane): Poly (4-Bromo-N-phenylmaleimide-vinyltrimethoxy silane), (poly (4-Br-NPM-VTMS), was prepared by reacting 4-Bromo-N-phenylmaleimide with vinyl trimethoxy silane in chloroform in presence of the initiator AIBN (10 mole%). Reaction conditions and procedures were same as reported above. Typical yield for this polymerization was ~80%.

Poly (1-aminopyrene-N-phenylmaleimide-vinyltrimethoxy silane): Poly(1-aminopyrene-N-phenylmaleimide-vinyltrimethoxy silane), poly(1-aminopyrene-NPM-VTMS), was prepared by reacting 1-aminopyrene-N-phenylmaleimide with vinyl trimethoxy silane in chloroform in presence of the initiator AIBN (10% w/w). Reaction conditions and procedures were same as reported above. Typical yield for this polymerization was ~ 70%.

Poly (2,3,4,5,6-Pentafluoroaniline-N-phenylmaleimide-vinyltrimethoxy silane): Poly(2,3,4,5,6-Pentafluoroaniline-N-phenylmaleimide-vinyltrimethoxy silane), poly (2,3,4,5,6-NPM-VTMS) was prepared by reacting 2,3,4,5,6-N-phenylmaleimide with vinyl trimethoxy silane in chloroform in presence of the initiator AIBN (10% w/w). Reaction conditions and procedures were same as reported above. Typical yield for this polymerization was ~ 60%.

Poly (Styrene – vinyltrimethoxy silane): Poly (Styrene – vinyltrimethoxy silane) was prepared by reacting equimolar amounts of styrene with vinyl trimethoxy silane in toluene in the presence of the initiator AIBN (10% w/w). Refluxed for one hour at 100 degrees Celsius and recrystallized by dissolving in methanol and extracting with hexane. Typical yield for this polymer was ~ 60%.

Poly (Maleic anhydride – vinyltrimethoxy silane): Poly (Maleic Anhydride – vinyltrimethoxy silane) was prepared by reacting equimolar quantities of Maleic

anhydride with vinyl trimethoxy silane in chloroform in the presence of the initiator AIBN (10% w/w). The polymer was recrystallized by dissolving in chloroform and extracting with hexane. Typical yield for this polymer was ~ 80%.

Poly (N-Phenylmaleimide allyl isothiocyanate – vinyl trimethoxy silane): Poly (N-Phenylmaleimide allyl isothiocyanate – vinyl trimethoxy silane), poly (NPM-AISCN-VTMS), was prepared by reacting N-Phenyl maleimide with allyl isothiocyanate in equimolar quantities in the presence of the initiator AIBN (10% w/w). The polymer was recrystallized by dissolving in chloroform and extracting with hexane. Typical yield for this polymer was ~ 85%.

By introduction of various electron donating and electron withdrawing groups on the phenyl ring of the above mentioned copolymers made the resulting materials amenable to a variety of sensing applications. All the functionalized monomers employed in the work are prepared in house and used after recrystallization with ethanol.

Terpolymer Preparation:

The terpolymer in this study to demonstrate a layer-by-layer deposition scheme was prepared by radical polymerization of n-phenylmaleimide, vinyltrimethoxysilane (VTMS) and pyrenemaleimide Scheme 2.4. In a fashion similar to the copolymers, this terpolymer is given the acronym n-Pyrenylmaleimide-VTMS. AIBN is used as initiator for preparation of this polymer and greater than 85% yield of this polymer was realized.

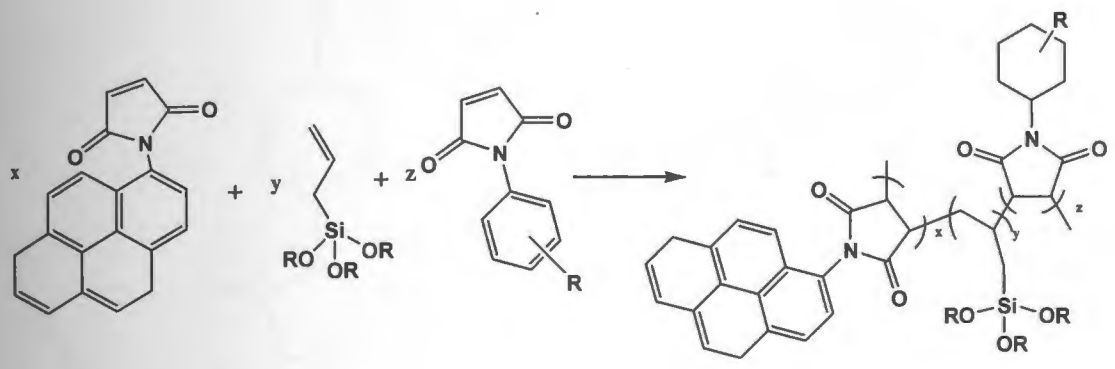

x = 2 mole%
y = 50 mole%
z = 48 mole%

R = -OCH3, -OC2H5

Scheme 2.4: Preparation of n-Pyrenylmaleimide-Vinyltrimethoxysilane copolymer

[redacted]*phenylmaleimide-vinyltimethoxysilane-AllylIsothiocyanate Copolymer* (CPM-VTMS-AITC): CPM-VTMS-AITC is a terpolymer prepared by radical polymerization of chlorophenylmaleimide (CPM), vinyltrimethoxysilane (VTMS) and allylisothiocyanate (AITC) using AIBN as the radical initiator. Polymerization was carried out under similar conditions as described above. The polymer was collected as a powdery precipitate from hexanes and used in the studies as described below. The typical yields were greater than 50 percent. The structure of CPM-VTMS-AITC is shown in Figure 2.1.

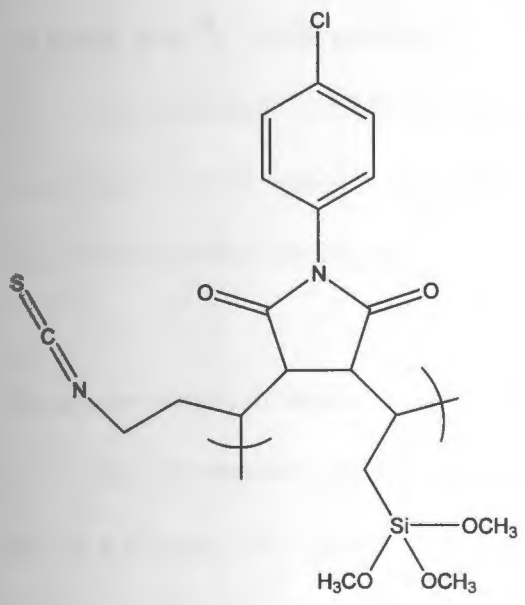

Figure 2.1 : Structure of NPM-VTMS-AITC.

FTIR Analysis:

FTIR-ATR analysis of the material was performed on a Thermo Nicolet Nexus 870 FT-IR E.S.P. using OMNIC® computer software from the Thermo Electron Corporation. With the help of FT-IR analysis, we were able to characterize different groups. Monomer and polymer products were verified by IR spectra. We were also able to distinguish difference between allylalkoxy and vinylalkoxy polymers. It was also used to confirm that no hydrolysis has occurred by the absence of O-H stretches. An absence of hydrolysis proves the stability of the polymer in ambient conditions.

^{1}H NMR and ^{13}C NMR analysis:

^{1}H NMR and ^{13}C NMR analysis was performed using Bruker 300 MHz NMR spectrometer. NMR analysis was used to confirm the structures of polymers. This study also helped to confirm the stability of polymers against hydrolysis.

Molecular weight determination:

Gel permeation chromatography (Agilent 1100) was used in which THF was used as a solvent, with a flow rate of 0.5 ml per minute and a refractive index detector. Effect of different AIBN concentration (10%, 5% and 1%), on molecular weight was also studied using GPC analysis.

Thermal analysis:

Thermal stability of the polymers was studied using a DSC (Q 100 V8 build 261). At heating rate of 10°C/min, the polymers were analyzed in the temperature range of 30 to 450^{0}C. Thermal properties were studied in order to understand the thermal behavior and robustness of these polymers as these materials will be used in separation and sensing applications, they should be stable and perform efficiently under various conditions such as high temperatures.

Results and Discussion:

The ultimate goal of the work was the preparation of stable polymeric materials and that can also be used in the preparation of polymeric sol-gels. Through the facile synthesis of the maleimides a variety of functional groups can be added for

a variety of sensing applications. Some examples of maleimides prepared are listed in Figure 2.2.

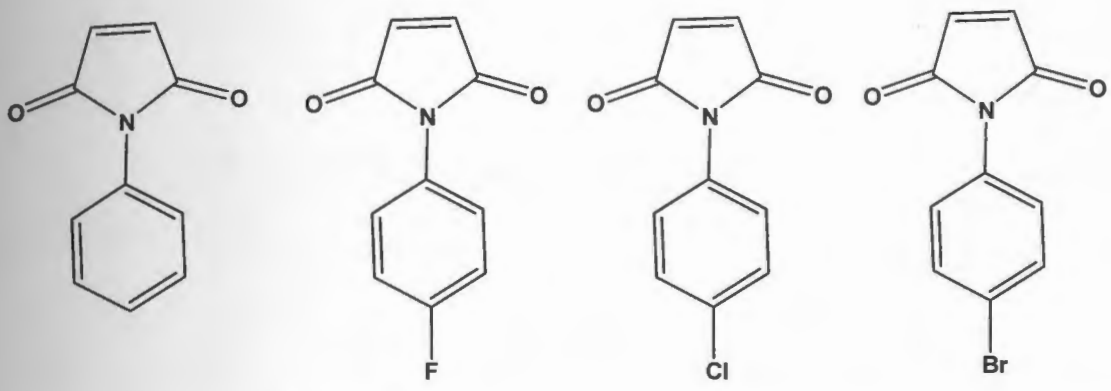

Figure 2.2: Various maleimides prepared showing the ability to change the group in the para position of the benzene ring such as a) n-Phenylmaleimide (NPM), b) 4-Chlorophenylmaleimide (4-ClPM), c) 4-Bromophenylmaleimide (4-BrPM).

These polymeric materials will find use in the design of various tailored materials for use in separation media and sensors within the Major research group. The polymers prepared in house, the silane side-groups form an integral component of the polymer through direct incorporation into the polymer backbone is the difference in the work we report relative to the other works reported in the literature. Thus the preparation of sol-gel with minimum problems of phase separation as these polymers achieved, owing to the presence of silane side groups would be able to bind covalently with the sol-gel matrix. This accomplished by co-polymerizing allyl (ii) and vinyl (iii) alkoxysilane monomers with N-Phenylmaleimide (i) as shown in Figure 2.3.

N-Phenylmaleimide

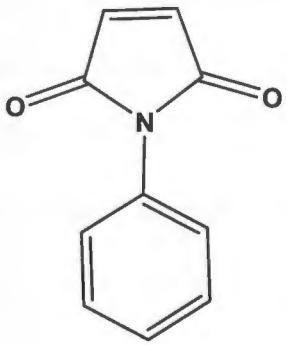

(a)

Allylalkoxy silanes

(b)

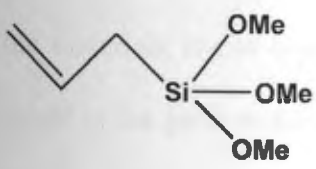

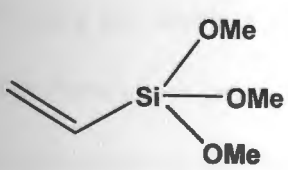

(c)

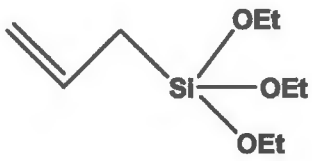

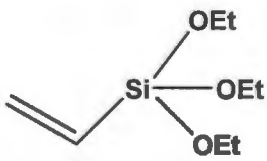

Figure 2.3: List of some monomers used to prepare polymers in this study.

By incorporating the silane side groups diresctly into the copolymer backbone allowed for the direct participation of the polymers in the sol-gel formation process. As expected the phase separation was very negligible, which can prove to be a significant problem using other methods to incorporate polymers into the sol-gel matrix. This finding was particularly important as these materials were prepared for predetermined applications such as chromatographic separation and sensing. These polymers can be incorporated in the tetraethoxysilane (TEOS) matrix to form sol-gel or the polymers itself can be converted to sol-gels. Eventually when preparing the polymer, maleimides tend to form alternating copolymers which ensures a regular structure to the polymers as well as having consistent properties. Having consistent properties in a polymer provides the stationary phase with uniform selectivity leading to a more reproducible separation. A non-uniform matrix, this will affect the interaction of the stationary and mobile phase with the analyte under investigation. Hence the separation results will not be reproducible. Similar is true if these materials are used in sensing applications, the response of the materials will not be uniform if the materials is not homogeneous. Therefore, phase separation could pose a major threat to the performance of these materials, but owing to the presence of silane side groups in the polymer backbone they can covalently bind with the sol-gel matrix reducing the problem of phase separation to minimum. Additionally, the preparation of polymeric sol-gels affords us the ability to tailor the properties of the end product, by incorporating different polymers in TEOS matrix and by using different conditions for making materials. This allows us exquisite control over the design of materials with pre-determined functions.

To confirm the structures, the IR spectrum was taken of the monomer where Fig 2.4 shows the results of N-Phenylmaleimide (NPM). NPM was the most frequently used in making the polymers presented in this work. As shown in the spectrum, there is a carbonyl peak (~1700 cm^{-1}) and the absence of H-N stretch (3300-3500 cm^{-1}) from the amine as the $-NH_2$ group, from aniline, was converted to maleimides. The absence of amine group is particularly important ensuring the ring closure reaction of maleamic acid. Stretches of C-N (1180-1360 cm^{-1}) and C-H (3000-3100 cm^{-1}) insure that benzene ring is still present in the monomers.

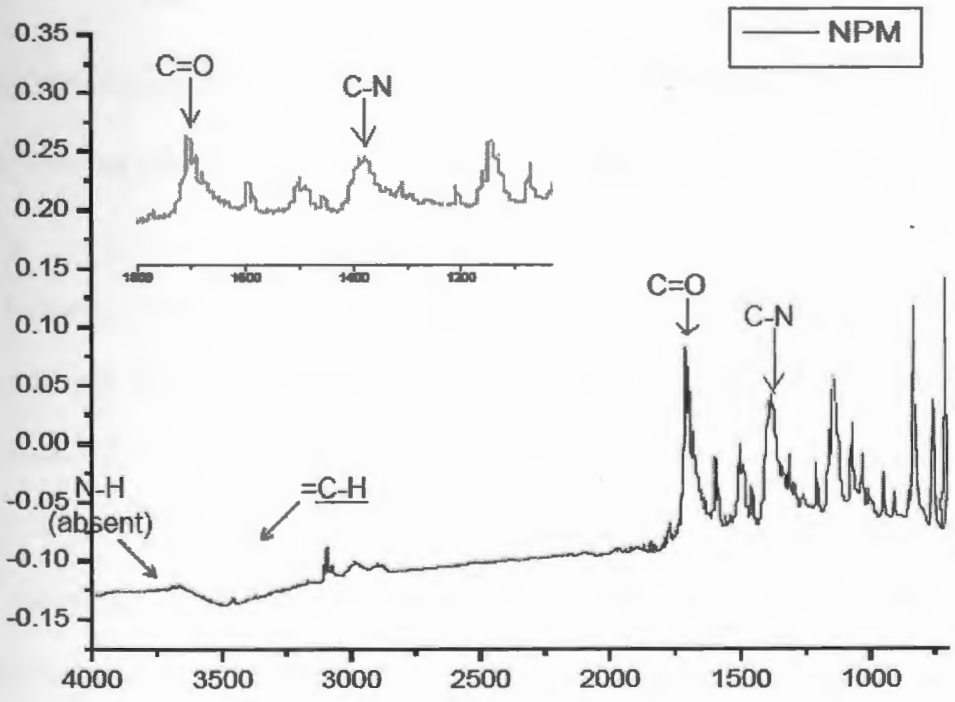

Figure 2.4: FTIR Spectrum of the monomer, NPM with an inset in the range of 1000-1800 cm^{-1}.

For the second monomer, the alkoxysilanes bring their own benefits for the copolymer. In this work, vinyltrimethoxysilane was the main silane used although polymers have been made with different alkoxysilanes as presented in Fig 2.5.

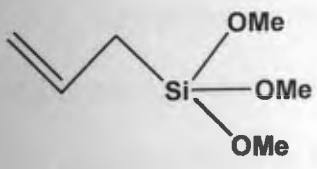

Allyltrimethoxysilane (ATMS)

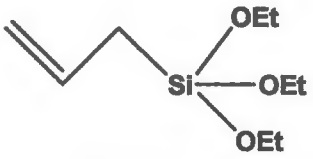

Allyltriethoxysilane (ATES)

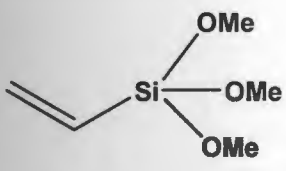

Vinyltrimethoxysilane (VTMS)

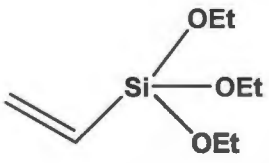

Vinyltriethoxysilane(VTES)

Fig 2.5: Various alkoxysilanes used to introduce silane groups to the copolymer.

However, when choosing the alkoxysilanes, the type of alkoxy and silane groups can give different properties. An allyl or vinyl group can be used to vary the chain length and influence the pore size within the copolymer. Depending on whether methoxy or ethoxy is utilized, will affect the reactivity of the polymers. These silane groups ($SiOCH_3$ or $SiOC_2H_5$) are the most important part of the copolymer by allowing the polymer to covalently link to a silica surface such as a silica particle or capillary wall. A methoxy group is more reactive than an ethoxy which determines how quickly the polymer can deposit or attach itself to silica. Silica particles and capillary walls contain silanol groups (Si-OH) which can react with the polymer when

its silane groups are hydrolyzed into silanols. Combining all these properties provides a copolymer that can be tuned and attached to silica surface in order to prepare different forms of stationary phases for separation techniques.

The polymers prepared in this work were found to be very stable, showing no significant hydrolysis of the silane side groups as evidenced by the absence of the Si-OH stretching bands at 3200-3700 cm^{-1} in the FTIR spectrum. In the one-pot synthesis of polymer, a stable powdery precipitate was obtained. All polymers prepared in this study were solid powder-like materials that were found to be insoluble in water and in most organic solvents.

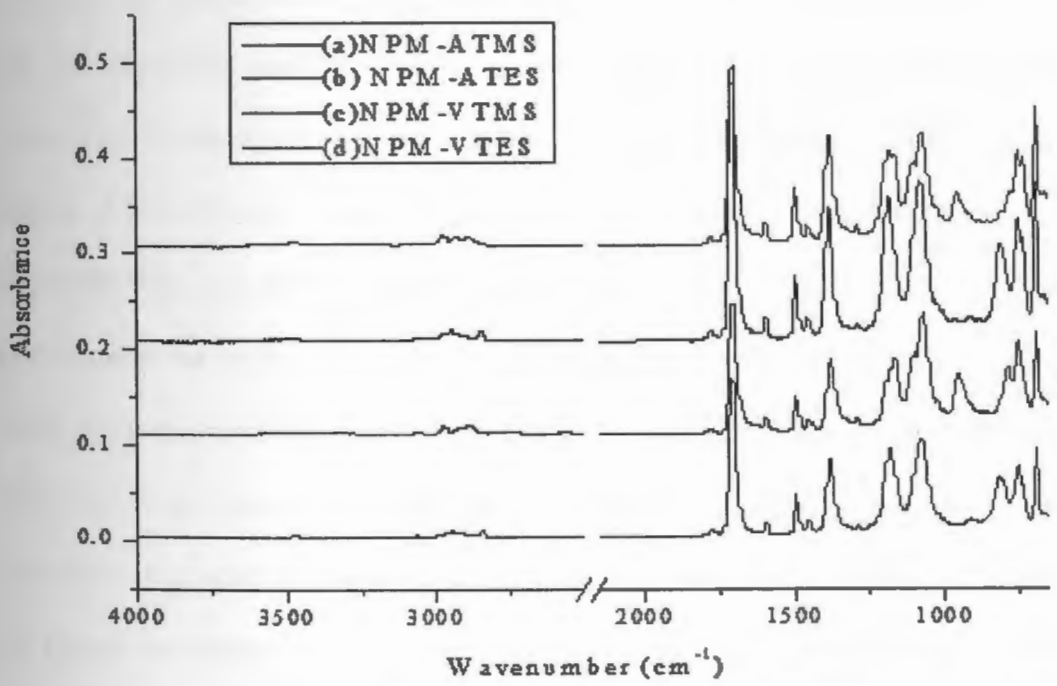

Figure 2.6: FTIR spectra of polymer (a) NPM-ATMS, (b) NPM-ATES, (c) NPM-VTMS and (d) NPM-VTES.

The common bands in the region 2800-3000 cm^{-1} in all four of the spectra can be attributed to –C-H stretch in the aromatic ring. The stretches around 1450-1500 cm^{-}

$^{-1}$ are because of the C=C stretch in the aromatic structure. A single band around 1300-1350 cm^{-1} can be attributed to aryl C-N stretches. All the polymers showed the presence of carbonyl group –C=O around the 1680-1750 cm^{-1}. Stretches around 1110-1060 cm^{-1} are characteristic of the –Si-O-R groups. Allyl and vinyl methoxysilane polymers showed difference in the spectrum. In Figure 2.6 spectrums (a) NPM-ATMS and (c) NPM-VTMS show two distinct bands at 1080 cm^{-1} and 1190 cm^{-1} which are of same intensity, on the other hand spectrum (b) NPM-ATES and (d) NPM-VTES show two similar bands at 1080 cm^{-1} and 1190 cm^{-1} but these bands are not of same intensity. The spectrums (b) NPM-ATES and (d) NPM-VTES distinct bands at 960-940 cm-1 is characteristic band of ethoxy silane (-Si-OEt). From the FTIR spectrum we can distinctly identify different groups in polymer structure. The absence of hydrolysis of alkoxysilane groups is confirmed by the absence of the band in the region of 920-830 cm^{-1} in any of the above four spectrums. This finding was a very important that no special handling protocols are required as with their liquid counterparts due to the reactivity of the silane groups, particularly in the presence of water. No presence of broad stretch around the region 3200-3700 cm^{-1} which indicates that there is no presence of –OH group confirms that the polymers are stable for hydrolysis. But after hydrolysis in the presence of a catalyst such as an acid or a base, we expect the change in the intensity of the –Si-OR stretch in the region 1040-1100 cm^{-1}. This is because after the hydrolysis, the alkoxysilane groups will be removed from the chain and subsequently will be converted into –Si-OH group. This was confirmed by increase in the intensity of the –Si-OH stretch in the region of 3200-

3700 cm^{-1}. Over a period of time the silanol groups will be interlinked to form –Si-O-Si- linkage which we expect to show in FTIR spectra in the region of 1000-1100 cm^{-1}.

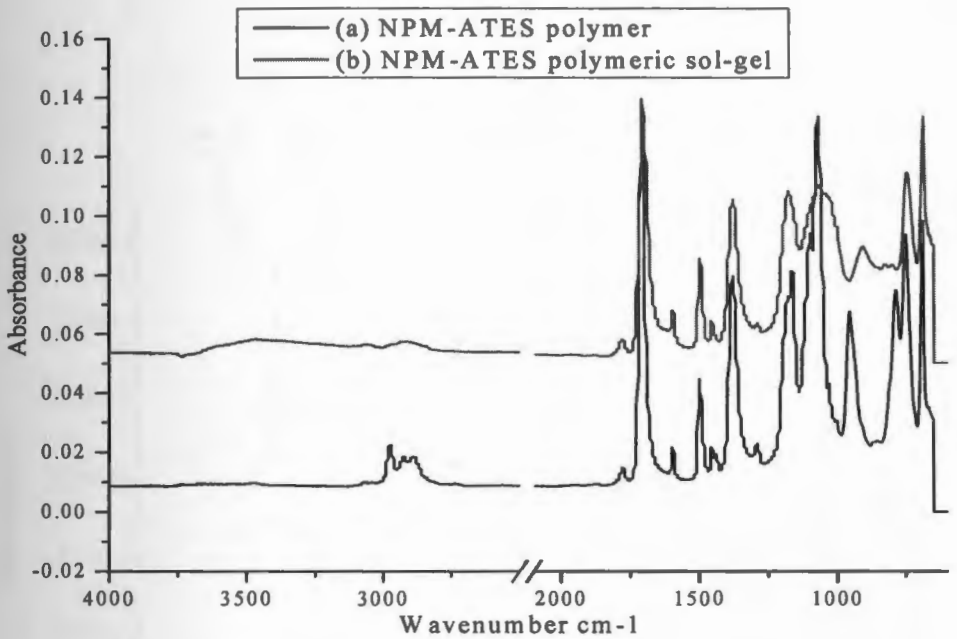

Figure 2.7: FT-IR spectra of (a) polymer NPM-ATES and (b) Conversion of polymer into sol-gel.

Figure 2.7 FTIR spectra shows polymer NPM-ATES and its subsequent conversion to sol-gel over a period of time by a base catalyzed reaction. In spectrum (b) of figure 2.6 after treating the polymer with suitable catalyst, in this case a base, the ethoxysilane groups are hydrolyzed and the intensity of the stretch of ethoxysilane groups around 960 cm^{-1} decreases. There is also appearance of a small band at 920 cm^{-1} which indicates the formation of the silanol (-Si-OH) bonds. The silanol bonds, over a period of time, undergo condensation to form siloxane bonds. After the formation of sol-gel there will be cross linking of –Si-O-Si- bonds which s conformed by the

presence of the broad band between 1093 cm^{-1} and 1070 cm^{-1} in spectrum (b) of Figure 2.7 which is characteristic of siloxane stretches.

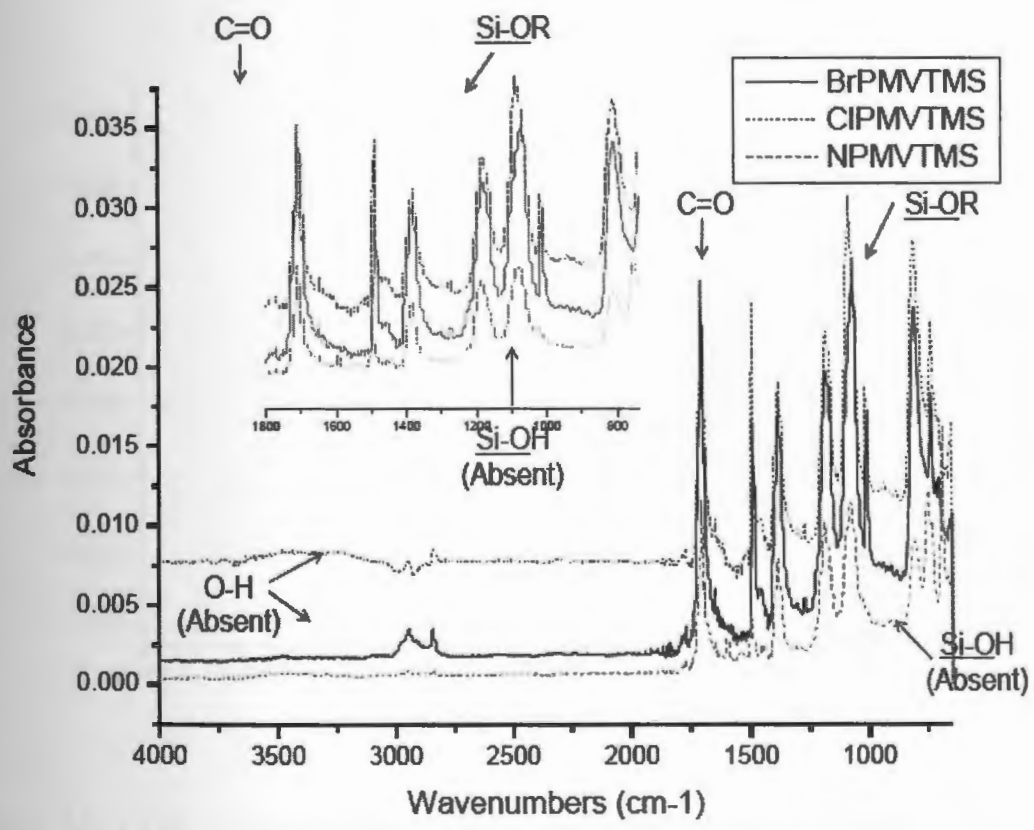

Figure 2.8: FTIR spectra of the polymers: NPM-VTMS (green), ClPM-VTMS (red), and BrPM-VTMS (black) with an inset in the range of 650-1800 cm^{-1}.

It is evident from the Figure 2.8 that polymers were not hydrolyzed uner preparation conditions by the absence of OH stretch in the region 3200-3500 cm^{-1} or Si-O (of the Si-OH) stretch at 920 cm^{-1} in the FTIR spectra. This confirms that the polymer termination is still alkoxysilanes that are used in the preparation of the materials. If hydrolysis had occurred, the polymer would begin reacting with itself

instead of the silica surface. The peaks associated with the carbonyl groups of the Phenylmaleimide and the Si-O (of the Si-OR) of the alkoxysilane are apparent at ~1720 cm^{-1} and 1100 cm^{-1} respectively. Copolymers used, in this work, were assorted types of maleimides and VTMS.

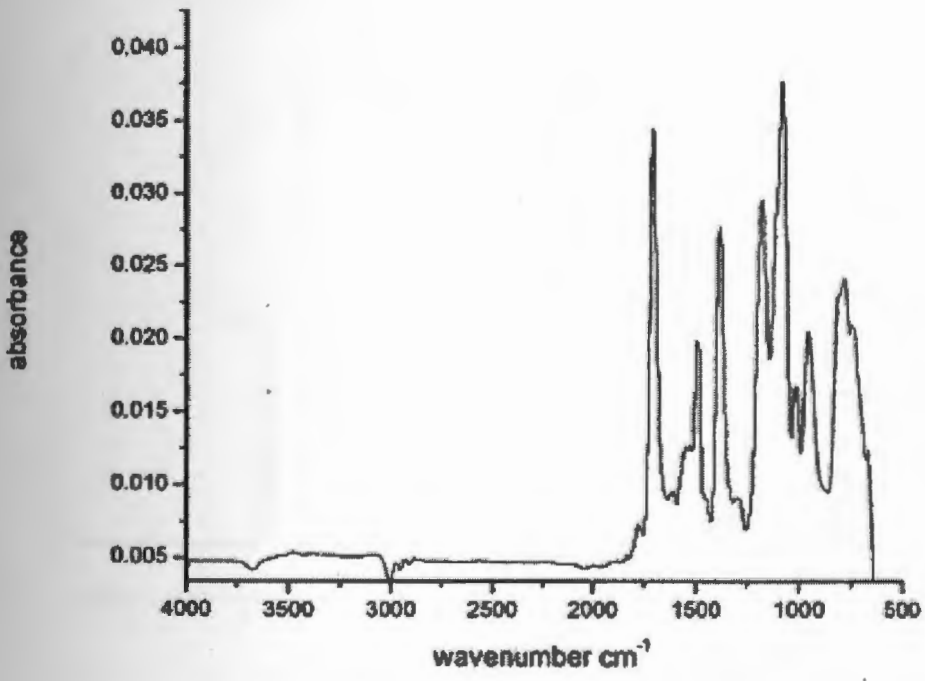

Figure 2.9: FTIR spectrum of the polymer poly(4-Br-NPM-VTES).

In Figure 2.9, the presence of VTES side chain is indicated by the two bands at 1080 cm^{-1} and 1190 cm^{-1} of different intensity and the band at 960 cm-1 distinctive of the (Si-OEt) ethoxysilane. Other bands are similar to the other silane polymers, the Ar-Br band lies at below 400 cm^{-1} is not seen. But the strong band at 800 cm^{-1} show that the benzene is para substituted.

In the ^1H NMR spectra, the resonance of the proton is influenced by other protons in its vicinity. In all ^1H NMR spectra no resonance of the proton around $\delta = 5.0$ was observed, which is the resonance value of the proton in the –Si-OH group. Fig 2.9 shows ^1H NMR of monomer NPM.

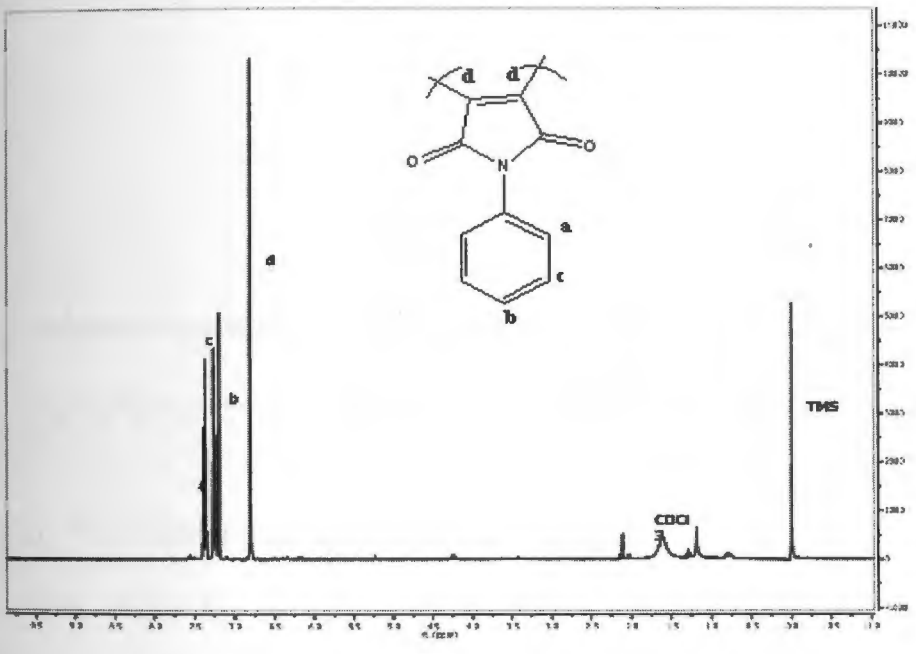

Figure 2.10: ^1H NMR of Monomer N-Phenylmaleimide

The Figure 2.10 NMR spectra shows the typical aromatic proton resonance at $\delta = 7.36$, 7.34 and $\delta = 7.46$ ppm. The maleimide protons were observed as a singlet at $\delta = 6.836$ ppm indicating the successful attachment of maleic anhydride moiety and functionalized aniline with a complete ring closure reaction of maleamic acid.

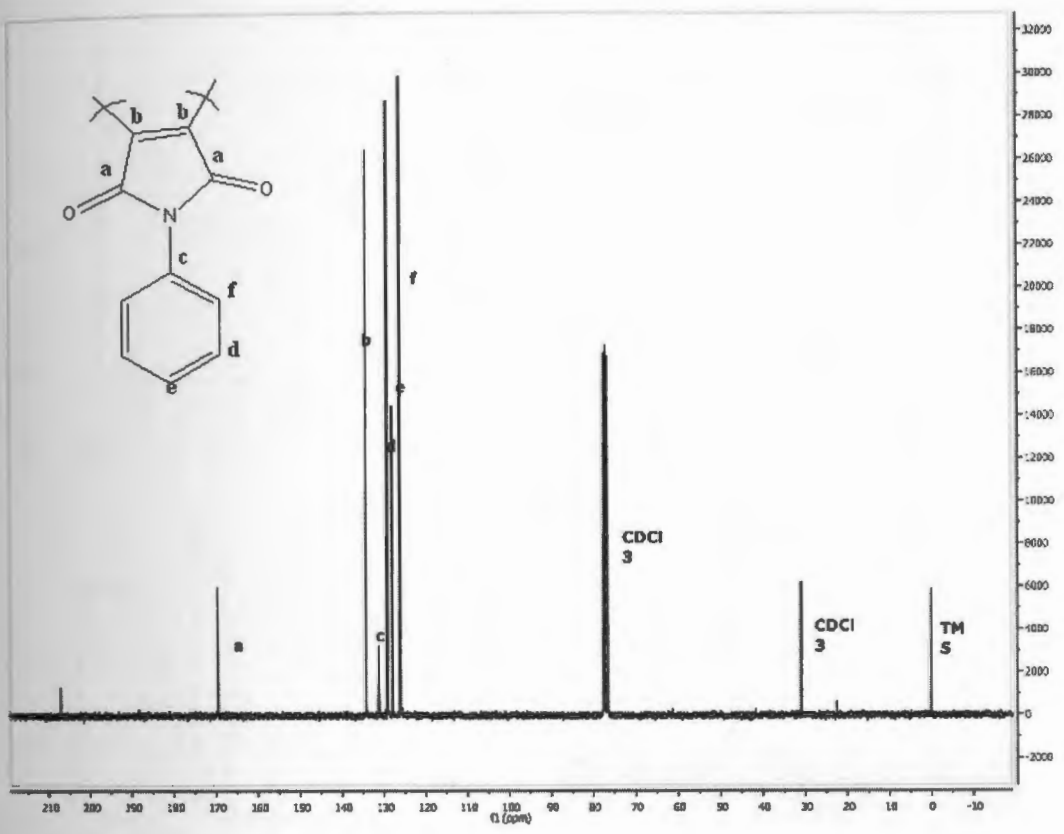

Fig 2.11: ^{13}C NMR of Monomer N-Phenylmaleimide

The spectra Figure 2.11 shows the typical aromatic carbon resonance at δ = 124 to 132 ppm. The peak at δ = 170 ppm confirms the presence of carbonyl group of maleimide ring. The aliphatic protons on the maleamide ring were observed at δ = 138.

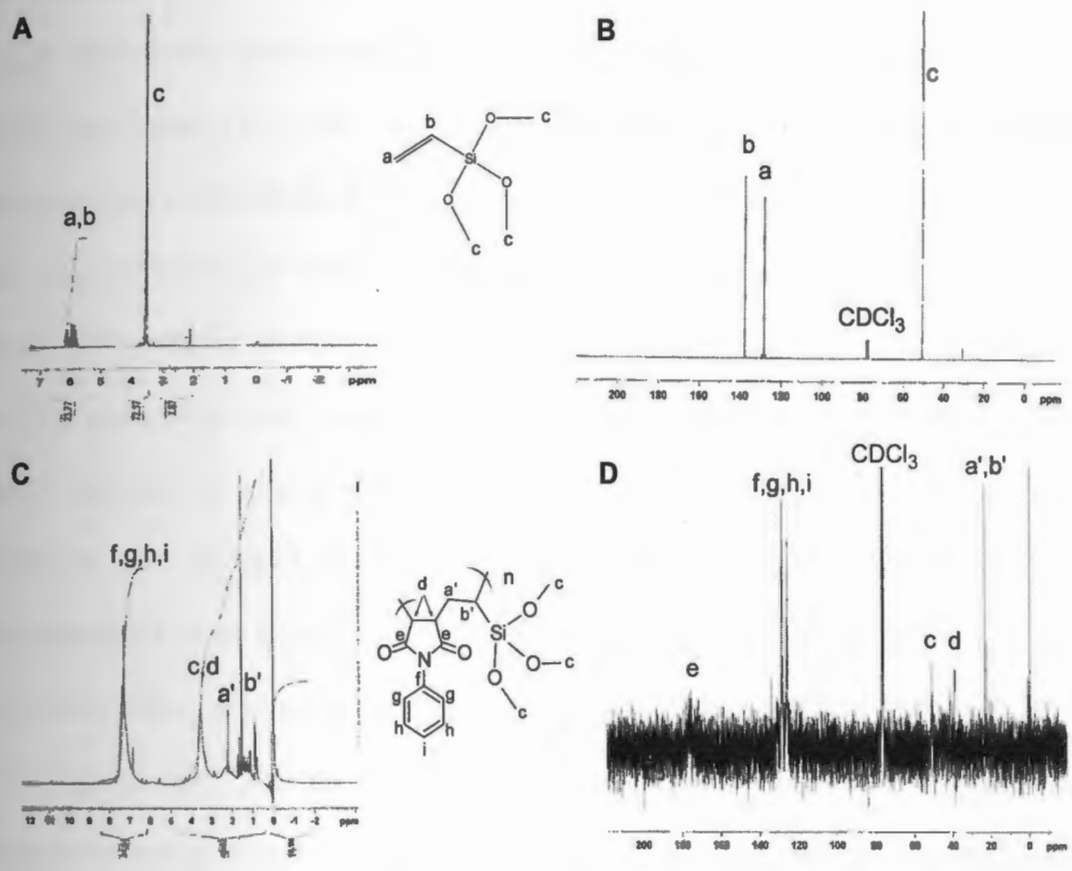

Figure 2.12: (A) ^{1}H-NMR spectrum of VTMS in $CDCl_3$, (B) ^{13}C-NMR spectrum of VTMS in $CDCl_3$, (C) ^{1}H-NMR spectrum of NPM-VTMS in $CDCl_3$, and (D) ^{13}C-NMR spectrum of NPM-VTMS in $CDCl_3$ with the structures of vinyltrimethoxysilane (VTMS, top) and n-phenylmaleimide-co-vinyltrimethoxysilane (NPM-VTMS, bottom).

Proton NMR was taken of the alkoxysilane monomer, VTMS (Fig. 2.12(A)), where resonance from the protons on the vinyl (5.7-6.3 ppm) and methoxysilane, Si-OCH_3, (3.5 ppm) are observed along with some impurities between 2 and 3 ppm. Fig. 2.12 B is the ^{13}C-NMR spectrum of VTMS with its characteristic peaks from the vinyl (128 and 137 ppm) and methoxysilane (~ 51 ppm) carbons. Proton NMR was taken of the copolymer, NPM-VTMS, is presented in Fig. 2.12 C. A broad peak at 7.1-7.6 ppm

is representative of aromatic protons from the phenyl ring. Succinimide protons, which are between carbonyl groups on the maleimide ring, were detected at 3.5 ppm, where the chemical shift can vary with cis (3.2 ppm) or trans (2.7 ppm), proving the disappearance of the alkene through the polymerization process. At the attachment of the alkoxysilane to the maleimide ring there are methylene protons (δ = 2.3 ppm) along with a methine proton at 1.7 ppm showing loss of the vinyl moiety. Terminal $-OCH_3$ groups are intact through resonance at 3.5 ppm due to the methyl groups which can also be seen in the proton NMR of VTMS. The silane peaks are also visible in the ^{13}C-NMR spectrum of NPM-VTMS (Fig. 2.12 D) at 51.13 ppm. Representative peaks from the phenyl ring are present at 126-129 ppm. The carbonyl and succinimide carbons, on the maleimide ring were detected at 176.62 and 39.34 ppm respectively. Successfully preparation of the copolymer is also confirmed through the loss of the vinyl moiety and peaks from the $-CH_2$ and $-CH$ (22-23.5 ppm) between the maleimide and alkoxysilane. With this data, in combination with the IR spectra, it is proven that the copolymer was prepared successfully as well as stable under normal laboratory conditions with its methoxysilane side groups intact.

The polymers were characterized for their molecular weights using Gel Permeation Chromatography (GPC). The polymers in this study were synthesized using different concentrations of AIBN as a radical initiator. The purpose of GPC study was done to compare the number average molecular weight, weight average molecular weight, and polydispersity of different polymers with 5% and 10% radical initiator.

Table 2.1 represents molecular weights of polymers NPM-ATMS, NPM-ATES, NPM-VTMS, and NPM-VTES which were prepared using different concentrations of AIBN 5 mole % and 10 mol %. M_n shows number average molecular weight, M_w weight average molecular weight and D, the polydispersity of the polymers.

Table 2.1: Represents molecular weights of polymers NPM-ATMS, NPM-ATES, NPM-VTMS and NPM-VTES prepared using different concentrations of AIBN 5 mol % and 10 mol %.

Polymer (initiator conc)	Mol Wt (M_n)	Mol Wt (M_w)	D
NPM-ATMS (5%)	2684	5043	1.878
NPM-ATMS (10%)	2470	5215	2.111
NPM-VTMS (5%)	10723	27376	2.45
NPM-VTMS (10%)	6064	17747	2.92
NPM-ATES (5%)	2441	5567	2.28
NPM-ATES (10%)	8543	21043	2.46
NPM-VTES (5%)	5756	16607	2.88
NPM-VTES (10%)	8488	25982	3.06

AIBN affects polymer molecular weights with different alkoxysilanes as well as their poydispersity with Gel Permeation Chromatography (GPC). M_n is the number

of molecules of each weight in the sample is counted. M_w is sum of the weight fractions of each species times its molecular weight. N_i is the number of molecules or moles of those molecules having molecular weights M_i. Polydispersity (D) is the ratio of weight average molecular weight to numver average molecular weight.

$$\bar{M}_n = \frac{\sum_i N_i M_i}{\sum_i N_i} \quad \bar{M}_w = \frac{\sum_i N_i M_i^2}{\sum_i N_i M_i} \quad D = M_w / M_n$$

Polydispersity measures the distribution of molecular weights, A value of 1 represents a copolymer is monodispersed meaning there is a uniform molecular weight. Typical values in the range 2 -100. In the polymer studies values close to 1 is considered good. All the values shown in Table 2.1 represent polymers with narrow distribution of molecular weight. As expected having lower M_w yields coolymers with a more narrow distribution which is shown when comparing allyl versus vinyl copolymers. The results show that polymer synthesis give a reasonable distribution of molecular weights that can be controlled by varying the concentration of radical initiator.

The important observation here was, an increase in polydispersity of each polymer, when we increased concentration of AIBN radical used for the polymerization process. When the initiator, used for polymerization process was increased, the polydispersity values increased. This suggest that as the initiator concentration increased, distribution range of molecular weights increases. This observation explained by the mechanism of radical polymerization process. The radical polymerization process occurs in three main steps. First step being the radical

initiation, radicals are generated and initiates the polymerization reaction. Second step is the chain propagation, the polymer chain increases by addition of monomers to the chain. The third step is chain termination, when two radicals in the reaction mixture react to neutralize each other thereby stopping the process of increasing chain length. As the higher concentrations of AIBN are used, the number of radicals generated during polymerization are more and subsequently the probability of two radicals neutralizing each other in the polymerization mixture is higher. The GPC data of these polymers shows similar observations. As the AIBN concentration used for polymerization process increased, polydispersity values were found to be increased. The polydispersity values for NPM-VTMS and for NPM-VTES were found to be higher than for NPM-ATMS and NPM-ATES. This observation can be explained by the fact that vinylalkoxysilanes are more reactive than allylalkoxysilanes. Therefore polymerization reaction of vinylalkoxysialnes will terminate faster than the allylalkoxysilanes, resulting in a wide distribution of molecular weights for vinylalkoxysilanes polymers.

Thermogravimetric analysis of the polymers show that the polymers were stable upto the temperature of 380^0C . Figure 2.13 shows the Thermogravimetric (TG) analysis of polymers NPM-ATES and NPM-VTES.

Figure 2.13 shows the Thermogravimetric (TG) analysis of polymers NPM-ATES (a) and NPM-VTES (b). Changes in sample mass are plotted as a function of temperature, and as we can see from figure polymer NPM-VTES changes in mass above temperatures of 150^0 C. NPM-ATES polymer does not show any loss in weight until after 400^0 C.

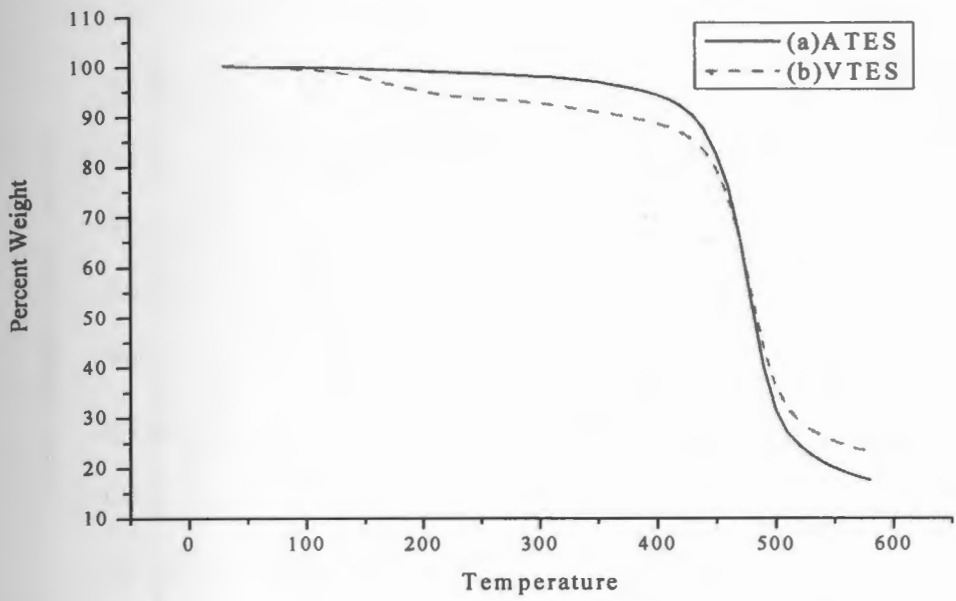

Figure 2.13: TGA curve of (a) NPM-ATES and (b) NPM-VTES. Figure shows that the weight loss for NPM-VTES (b) starts early at temperatures less than 200^0 C and NPM-ATES (a) is stable until the temperature of 400^0 C.

This observation can be confirmed from differential thermal analysis (DTA). In DTA change in mass with respect to temperature (dm/dT) is plotted against temperature or time. DTA are derivative plots and any small changes in mass are clearly observed. Figure 2.14 shows the DTA curves of polymers NPM-ATES and NPM-VTES.

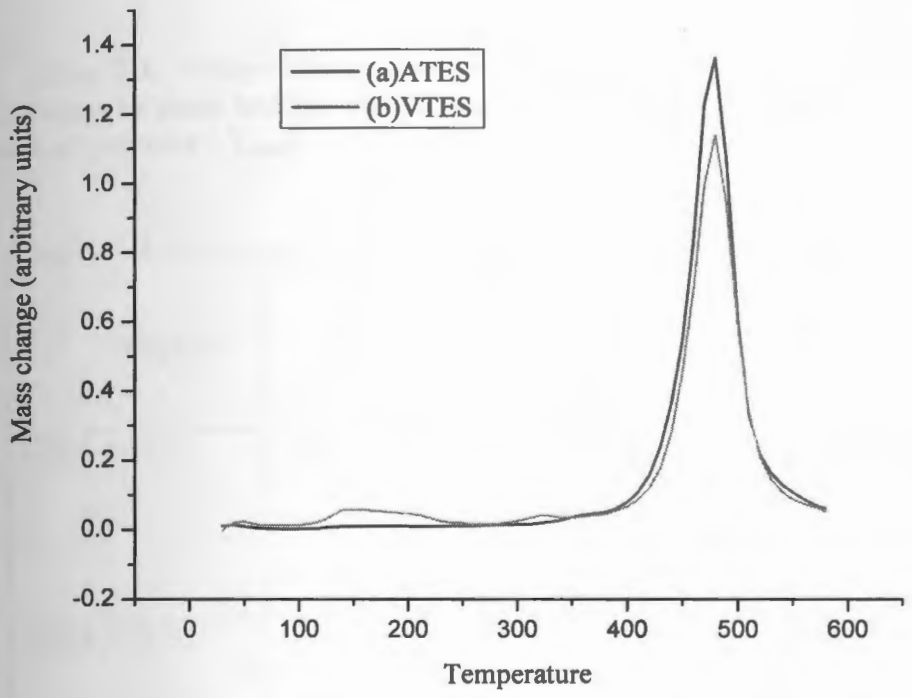

Figure 2.14: DTA curve of polymers NPM-ATES (a) and NPM-VTES (b)

Fig. 2.14 again clearly shows that change in mass for NPM-VTES begins at temperature of 150^0 C whereas for NPM-VTES, the mass change does not occur until after temperature of 400^0 C. Initial decomposition temperature is the temperature at which there is loss in weight of more than 10 % of the initial weight of the polymer. Based on the initial decomposition temperature TGA revealed that the allyl polymers are thermally more stable than the vinyl polymers. The data suggests that the initial decomposition temperature is less in vinyl polymers as compared to allyl polymers. Allyl polymers showed no sign of thermal degradation below temperatures of 420^0 to

430^0 C while the vinyl polymers show change in mass at temperatures of 150^0 C and at temperatures after 330^0 C there is significant change in mass (more than 10%).

Table 2.2: Temperatures required for 10% ($T_{10\%}$), 50% ($T_{50\%}$), 70% ($T_{70\%}$), change in mass and the temperature at which there is maximum change in the mass of polymer (T_{max}).

Polymer	$T_{10\%}$	$T_{50\%}$	$T_{70\%}$	T_{max}
NPM-ATMS	420	490	540	500(53%)
NPM-ATES	430	480	480	480(52%)
NPM-VTMS	330	480	510	470(56%)
NPM-VTES	340	480	520	480(54%)

Table 2.2 shows the values of temperatures required for 10% change is mass ($T_{10\%}$), temperature required for 50% change in mass ($T_{50\%}$), temperature required for

70% change in mass ($T_{70\%}$) and the temperature at which there is maximum rate of change in the mass of polymer (T_{max}). For vinylmethoxy and vinylethoxy polymers the $T_{10\%}$ was 330^0 C and 340^0 C respectively and for allylmethoxy and allylethoxy polymers $T_{10\%}$ was 420^0 C and 430^0 C in that order. $T_{50\%}$ for all the polymers was observed to be similar which was 480^0-490^0 C and T_{max} for all the polymers was in the range of 480^0-500^0 C. These data suggest that the only difference is in the initial degradation of the polymers. In later stages of their thermal decomposition they show a similar trend. These changes in the initial degradation temperatures might be due to the difference in their structures. In allyl silanes the presence of one more carbon in alkoxysilane side chain reduces steric restriction, refer to structures in Figure 2.15.

Allylalkoxysilane

Vinylalkoxysilane

Figure 2.15: Structural difference between allylalkoxysilane and vinylalkoxysilane monomers.

This effectively allows allylalkoxy polymer chains to change their orientation when (increase in random arrangement) they are heated, but since vinylalkoxy polymer chains have comparative steric restriction, they have limitations to change orientation. This suggests that entropy (randomness in arrangement of polymer chains) for allylalkoxy polymers is more than vinylalkoxy polymers. When these polymers are heated, in case of allylalkoxy heat energy is used to change the arrangement of

polymer chains in space and therefore it's melting enthalpy i.e. energy required to melt the polymer is less as compared to vinylalkoxy polymers. This observation is in accordance with the transition enthalpies of the melting which is energy required to melt these polymers. The enthalpies of the melting for ally polymers were in the range of 96-118 J/g while these values for vinyl polymers were in the range of 295-405 J/g. This again suggests that the entropy of the allyl polymers is more than the entropy of vinyl polymers, which can attributed to the structural difference between the two polymers. Therefore the enthalpy required for melting vinyl polymers is more than the allyl polymers which is confirmed by differential scanning calorimetry.

CONCLUSION

Synthesis of phenylmaleimide monomers, silane-based copolymers and the materials that can be used in the efficient preparation of polymeric sol-gel materials have been achieved. The phenylmaleimides were created by reacting a functionalized aniline and maleic anhydride. Through IR spectra, the full conversion of the amine group from the aniline derivatives to the maleimide is verified by the absence of N-H stretches. With IR spectra, peaks from the carbonyl (maleimide) and silane (alkoxysilane) groups are visible. It also shows no silanol groups which would be present if any hydrolysis had taken place. This proves the stability of the copolymer in synthesis and ambient conditions. NMR reports further supports that there is no hydrolysis of the copolymer with the absence of resonance of the silanols. The resonance of the proton also confirms that the alkoxysilane is attached to the maleimide at the double bond between the two carbonyl groups. In the synthesis of the

polymers, molecular weights were controlled by the amount of radical initiator, AIBN. The molecular weights were higher as the AIBN concentration increased. Vinylalkoxysilane polymers were found to be more polydisperse than allylalkoxysilane polymers. The thermo gravimetric analysis suggests that the polymers are very much stable upto a temperature of 350^0C. The allylalkoxysilane polymers were found to be thermally more stable than the vinylalkoxysilane polymers owing to difference in the structure of side chain. Due to the low polydispersity and enhanced thermal stability, allylalkoxy silane polymers are more suitable for use in the preparation of sol-gel materials. The properties of the polymers can be manipulated by selective monomers and polymerization conditions, thus we have the ability to control the extent of cross-linking of the matrix as well as control over the potential applications of the end-products. The data suggest that the polymers prepared are very stable and can be easily converted to the corresponding sol-gel in the presence of a simple catalyst such as an aqueous base.

References

1. Ulrich Schubert., Organo functional metal oxide clusters as building blocks for Inorganic-Organic Hybrid Materials, Journal of Sol-Gel Science and Technology, 2004, 31, 1-3.
2. Bing. Yan., Sol-gel preparation and luminescence of silica polymer/hybrid material incorporated with terbium complex, Materials Letters, 57,16-17,2003,2535- 2539.
3. A Text Book by Ganachaud, Franicois., Boileau, Sylvie., Boury, Bruno., Silicon Based Polymers , Advances in Synthesis andSupra Molecular Organization, 2008, Page 285.
4. Kirkland J.J., Truszkowski, F.A.,R.D., A typical silica based colum packing for High-Performance Liquid Chromatography, Journal of Chromatography A., 2002,965,25-34.
5. Kirkland, J.J., Development of some stationary phases for reversed-phase HPLC, Journal of Chromatography A, 2004, 1060, 9-21.
6. Aruna, Velamakanni., Functional Silane Based Polymers for Sensing and Separations, Thesis Dissertation, University of Rhode Island, 2006.
7. Jack Cazes., Encyclopedia of Chromatography., R.Andrew Shalliker, Sindy Kayillo., Zirconia-Silica stationary phases for HPLC, Overview and Applications, pages 349-359.
8. Hosoya, K., Kubo, T., Takahashi, K., Ikegami, T., Tanaka, T., Novel Surface modification of polymer-based separation media controlling separation

selectivity, retentivity and generation of electroosmotic flow, Journal of Chromatography A, 2002, 979, 1-2,3-10.

9. Hosoya, K., Teramachi, M., Tanaka, N., Koboyashi, A., Kanda, T., Ohtsu, Y., Preparation Strategy for Uniformly Sized, Polymer-Based HPLC Packing Materials Having Practically Acceptable Column Efficiency. 1. Copolymerization Technique, Analytical Chemsitry, 2001, 7, 5852-5857.
10. Hosoya, K., Watabe, Y., Kubo, T., Hoshino, N., Tanaka, N., Sono, T., Kaya, K., Novel surface-modification techniques for polymer-based separation media: Stimulus responsive phenomena based on double polymeric selectors, Journal of Chromatography A, 2004, 1030, 237-239.
11. Claesens, H.A., Van traten, M.A., and Review on the chemical and thermal stability of stationary phases for reversed-pase liquid chromatography, Journal of Chromatography A, 2004, 1060, 23-41.
12. Liu, M., Liu, Y., Zeng, Z., Peng, T., Preparation and Characteristics of high pH-resistant sol-gel alumina-based hybrid organic-inorganic coating for solid-phase microextraction of polar compounds. Journal of Chromatography A, 2006, 1108, 149-157.
13. Buchmeiser, M.R., New synthetic ways for the preparation of high-performance liquid chromatography supports, Journal of Chromatography A, 2001, 918, 233-266.
14. Sertchook, H., Elimech, H., Avnir, D., Composite Particles of Silica/Polydimethylsiloxane , Chemistry of Materials, 2005, 17, 4711-4716.

15. Constantin, S., Freitag, R., Solignac, D., Sayah, A., Gijs, M.A., Utilization of the sol-gel technique for the development of novel stationary phases for capillary electrochromatography on a chip, Sensors and Actuators B: Chemical, 2001, 78, 267-272.

16. Li, X., Zeng, Z., Gao, S., Li, H., Preparation and Characteristics of sol-gel-coated calixfarene fiber for solid-phase microextraction, Journal of Chromatography A., 2004, 1023, 15-25.

17. Wyndham, K.D., O'Gara, J.E., Walter, T.H., Glose, K.H., Lawrence, N.L., Alden, B.A., Izzo, G.S., Hudalla, C.J., Iraneta, P.C., Characterization and Evaluation of C18 HPLC Stationary Phases Based on Ethyl-Bridged Hybrid Organic/Inorganic Partcles, Analytical Chemistry, 2003, 75, 6781-6788.

18. Kim, T.Y., Alhooshami, K., Kabir, A., Fries, D.P., Malik, A., High pH Resistant surface-bonded sol-gel titania hybrid organic-inorganic coating for effective on-line hyphenation of capillary microextraction in-tube solid-phase microextraction with high-performace liquid chromatography, Journal of Chromatography A, 2004, 1047, 165-174.

19. He, L., Chee-seng Toh., Recent advances in analytical chemistry – A Materials approach, Analytica Chimica Acta, 2006, 556, 1-15.

20. Hodgson, R.J., Chen, Y., Zhang, Z., Tleugabulova, D., Long, H., Zhao, X., Organ, M., M.A., Brennan, J.D., Protein-doped monolithic silica columns for capillary liquid chromatography prepared by the sol-gel method : applications to frontal affinity chromatography, Analytical Chemistry, 2004, 76, 2780-2790.

21. Major, J.S., Blanchard, G.J., Strategies for Covalent Multilayer Growth.1. Polymer Design and Characterization, Chemistry of Materials, 2002, 14, 2567-2573.

22. Sunil, Sonawane., Synthesis and Characterization of Silane Based Polymers for Chemical Separation, Thesis Dissertation, University of Rhode Island, 2007.

CHAPTER 3

Preparation of Polymeric Superstructures for Sensing and Separation Applications

ABSTRACT

In this work we prepared variety of copolymers that bear silane and alkoxysilane side groups converted into polymer-silica composite particles using a modified sol-gel protocol and their self-assembly at various interfaces such as silicon and glass. In this work we also employ the self-assembly of those polymers to prepare surfaces capable of templating/directing the assembly of nanoparticles and polymer composites into organized assemblies that will later be used in the preparation of arrays that are intended for sensing applications. In this work we also demonstrate the preparation and characterization of a group of pyrene-functionalized silane-based copolymers that have been converted into polymer particles and polymer-silica nanocomposites. Measurements employing these particles were shown to be an effective detection and quantification technique for amino- and nitro-containing compounds using fluorescence quenching as the detection scheme. In addition, we have demonstrated a facile method for the self-assembly of these particles onto various surfaces. This assembly protocol will be investigated for non-lithographic surface patterning for the development of array-based sensors.

Introduction

In recent years the materials chemistry and nanochemistry has gained significant attention due to the ability to design materials with unique properties on the scale and that can be assembled [1, 2] in a controlled manner by providing materials that are both thermally[3,4] and chemically robust[5, 6].

The drive has seen the development of a number of different types of materials and methods to assemble them into useful forms. Material science has witnessed major developments with the emergence of sol-gel chemistry. The popularity of the sol-gels stems from their ease of preparation, their robustness (chemical and thermal) and the ease with which they can be tailored for specific applications. The sol-gel method has been used extensively to prepare a variety of novel glasses[7, 8, 9], ceramics[10, 11], and zeolites[12, 13], however, recent interest in sol-gels, has been fueled by the preparation and use of tailored sol-gels as potential catalytic supports[14], electrodes[15, 16] and sensors[17-19]. Enzymes[20-22] and antibodies[23, 24] have been successfully entrapped in sol-gel matrices for biological applications[25, 26]. Recent work has also demonstrated the incorporation of polymeric materials[27-29] within the sol-gel matrix. Extensive research continues in the design of novel high performance materials for specific target applications.

Much of this research has involved particle self-assembly at various interfaces. Recently, ordered particle arrays have found use in a number of technologies, including high-density storage[30], chemical and biological sensing[31-33], photonic band gap devices[34, 35] and optoelectronic devices[36, 37]. Various methods, such as Langmuir-Blodgett[38, 39], controlled evaporation[40-43], directed assembly by templating onto modified substrates[44,45] or nanolithographic techniques[46], have been investigated and have successfully produced ordered particle arrays, both 2D and 3D. In many cases, however, nanoparticles must first be modified to increase hydrophobicity or increase van der Waals interactions, allowing particles to self-assemble during deposition. Many of the available methods are also time-consuming, taking upwards of several weeks in some cases, and long-range order is still often not achieved. The inclusion of a post-deposition ordering step may remedy this problem.

In this work we demonstrate a facile and robust method for the preparation and surface modification/patterning of interfaces able to facilitate nanoparticle self assembly via a non-lithographic technique. Nanoparticles have been modified to present various functionalities can be placed onto surfaces in an array pattern. The ability to assemble organized structures of nanoparticles, where these nanoparticles can be selectively modified will find use in the fields of chemical and biological sensing.

In this work the silane-based polymers were allowed to react directly with the surface silanol groups of glass and silica through the formation of siloxane (Si-O-Si) bonds as described elsewhere[47, 48]. Subsequent to polymer deposition the modified surfaces were exposed to a suspension of preformed silica nanoparticles or polymer silica nanocomposites. These particles were prepared via two major routes based on methods originally demonstrated by Stober et al[49] and De et al[50]. The modified Stober method is considered more efficient for the assembly of ordered arrays arising from the ability to form discrete particles of controllable size. Particle deposition was accomplished by one of the two facile techniques. The first was "dip-coating" method and the second a "spin-coating" method. Both were investigated to determine which of these simple methods would be more appropriate for ultimately producing ordered particle arrays. Again, ordered arrays are of great interest for several of the applications mentioned above. Ordered arrays produced by this self-assembly method would be desirable due to its facile and inexpensive nature.

EXPERIMENTAL

Polymer Preparation:

The preparation of the polymers employed in this study was described in chapter 2 of this dissertation. For example a copolymer was prepared by radical copolymerization of *n*-phenylmaleimide and vinyltrimethoxysilane (NPM-VTMS) using AIBN as radical initiator with chloroform as solvent. A terpolymer of 1-pyrenylmaleimide with NPM and VTMS was also prepared as described in chapter 2 and used to prepare both particulate and thin-films in this work. Subsequent to polymerization the polymers were collected as powdered precipitates from hexane. After purification the polymers were then used as described below. The alkoxysilane side groups were used as the functionality of attachment of the polymers to the various interfaces. Additionally, the side-groups facilitated the formation of the composite particles as the alkoxysilane groups were converted to siloxane cross-links.

Preparation of various functional forms:

Using the polymers prepared as above various functional forms can be prepared by simply modifying experimental conditions. Example structure include (1) polymer-silica nanocomposites, (2) Coated nanoparticles, (3) polymer thin-films and (4) polymer-facilitated nanoparticle arrays.

Polymer-silica nanocomposite particle Preparation:

Different amount of the appropriate polymer (0.1g, 0.5g, and 1.0g) was dissolved in 10ml of acetone followed by the addition of 0.2 ml of concentrated HCl to the solution and stirred for approximately 5 minutes. The addition of the acid to the polymer solution was to ensure the hydrolysis of alkoxysilane side groups. In previous studies we have found that the pre-hydrolysis of the alkoxysilane side groups allows for the efficient incorporation of the polymer into the silica matrix which prevents the phase separation, a common problem when attempting to incorporate organic components into an inorganic matrix. In a separate vial, a mixture of water, tetraethoxysilane (TEOS) and either hydrochloric acid or ammonium hydroxide was stirred. The choice of hydrochloric acid or ammonium hydroxide depended upon whether an acidic or basic mechanism was being employed to prepare the particles. In either case, TEOS was added in the last step and this mixture was stirred for 2-3 minutes. The prehydrolyzed polymer mixture from the first vial was slowly added into the TEOS solution with vigorous mixing. The sol-gel procedure is described in reaction scheme in Figure 3.1. This mixture was capped and allowed to stir until the mixture formed a gel.

Reaction scheme: TEOS sol-gel preparation.

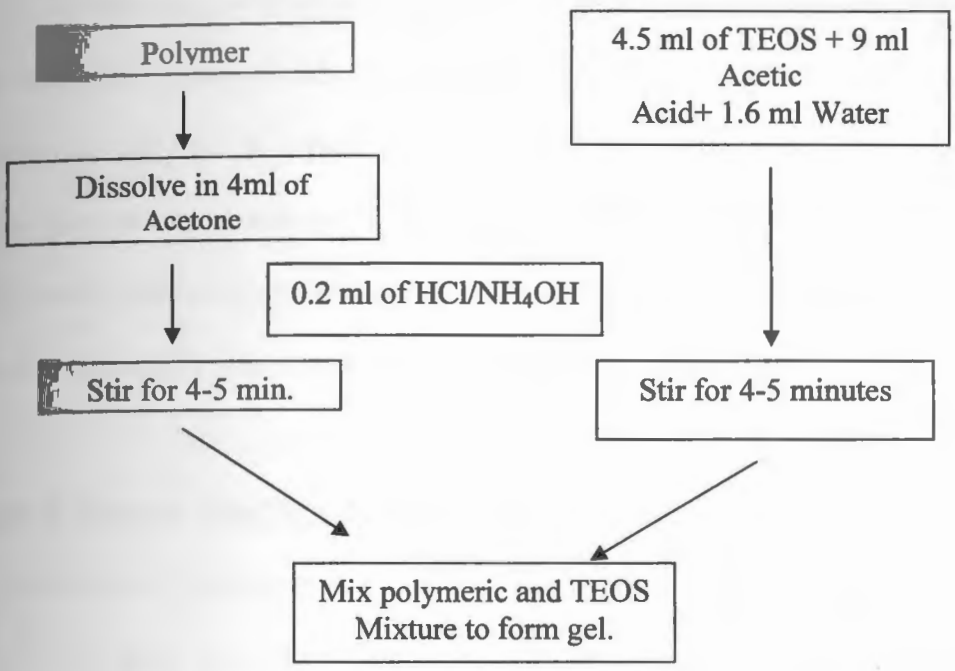

Scheme 3.1: Preparation scheme of polymer-TEOS sol-gel materials.

Scheme 3.1 shows the conversion of polymers into the polymer-silica composites. After sitting for 2-3 days the gelatinous matrix become more firm. At this point, the caps are removed and the material is allowed to air dry. After drying, the resulting material becomes a very powdery matrix that is collected and used in subsequent studies as described below. FTIR studies were conducted on the composite materials over time which confirmed the further crosslinking of the matrix over time as expected. This confirmation was possible due to the increasing intensity of the siloxane bonds observed in the spectrum over time and the corresponding decrease in silanol peaks.

2. Preparation of polymer coated nanoparticles:

In this step, commercially available or in-house prepared silica nanoparticles are employed. The polymer solutions are prepared as described above in Form 1, where each polymer is initially prehydrolyzed. To a flask containing the prepared silica nanoparticles suspended in a solution of either toluene or ethanol, the prepared polymer solution is slowly added and stirred overnight. The polymer coated particles are then collected by vacuum suction and stored until further needed.

Form 3. Polymer thin-film preparation:

a. Preparation of interfaces for thin-film deposition:

The glass and silicon interfaces used in this study were cleaned in piranha solution (a mixture of 1:3 30% H_2O_2 and concentrated H_2SO_4 – this mixture is very corrosive and can be explosive if exposed to organics, extreme care should be exercised) followed by extensive washing in distilled water. The interfaces were then used in the thin-film schemes as described below.

b. Polymer modified interfaces (dip-coating):

In this case of polymer-modified interfaces, the polymers prepared as described above were dissolved in 1:10 acetone:toluene mixture to which the piranha-cleaned surfaces were introduced. The surfaces remained in the polymer solutions with gentle heating (50 – 60^{0}C) overnight. The surfaces were subsequently withdrawn and rinsed with acetone and allowed to dry and stored until need. The polymer deposited on glass or quartz was used to collect UV-Visible spectra to confirm the

deposition of the polymers on the interfaces. Polymer deposition onto the silicon wafers was confirmed by ellipsometry. Ellipsometric measurements allow the determination of the thickness of the polymer thin-films as a function of the number of deposition cycles.

c. Polymer modified interfaces (spin-coating):

Spin coating is done by a spin coater, Model # WS-400-6NPP/LITE (Laurell Technologies Corporation). Spin coating is a process during which substrate spins around an axis perpendicular to the coating area. The polymer composite particles is dispensed onto the interfaces such as glass or silicon wafer and is spread across the interface by spinning at approximately 500 rpm. The interface is then spun at a higher speed of 2000-4000 rpm for 3-5 minutes as ethanol is used as solvent it evaporates very quickly. Ethanol was chosen as the evaporative solvent as it would evaporate at room temperature in minimal time (less than 3 minutes) while still affording adequate time for the particles to obtain a small degree of order. Other solvents, acetone in particular, evaporated too rapidly resulting in larger agglomerates. The objective of the spin-coating scheme is to develop a method that proves facile, time-efficient and reproducible. We have chosen this method to achieve two specific goals. The first was that the method should be time-efficient and uncomplicated. The second goal was that we desired to maintain a uniform deposition on the interface.

[redacted]: Nanoparticle Arrays - Nanoparticle Self-Assembly:

The deposition of the various nanoparticles into organized arrays was accomplished in one of two schemes, either dip-coating or spin-coating similar to polymer thin-film preparation as described in Form 3 above.

a. Nanoparticle self-assembly – dip-coating:

In the first scheme a simple "dip-coating" method is employed. Here, the polymer-silica composites or the polymer coated nanoparticles prepared as described in Forms 1 and 2 above are suspend in an appropriate solvent (toluene or ethanol) to which a thin-film coated silicon or glass wafer is added. The wafer is left suspended in the stirring particulate suspension overnight. The surfaces withdrawn and rinsed with acetone and distilled water and stored until further studies. It should be noted that the deposition of the nanoparticles onto the surfaces is facilitated by the formation of siloxane bonds between the alkoxysilane side groups of the polymer already deposited on the surface and the surface silanol groups of the nanoparticles. It is also very likely that the surface of the nanoparticles also bear alkoxysilane side groups since they also contain the same polymers that are used to prepare the polymer thin-films.

b. Nanoparticle self-assembly – Spin-coating:

Using the same spin-coating apparatus as described above, nanoparticles can be organized on the surface by spin-coating. In this scheme, the particles (polymer-silica composites or polymer-coated) are suspended in ethanol and then added to a flat glass substrate that had been affixed to the spin-coating apparatus. The mixture was

then spun at a rate of 500 rpm for 2-3 minutes. The spinning was allowed to continue until excess fluid spins off the edges of the substrates at 2000-4000 rpm for 4-5 minutes, yielding the desired thickness. During the spin-coating process a volatile solvent is usually employed to allow for the simultaneous evaporation of the solvent from the surface during the process. It should be noted that in this spin-coating scheme, the glass substrate (or silicon wafer) can either be functionalized with a polymer-thin film prior to the nanoparticles being spun. The polymer would facilitate the deposition of the particles in the exact manner as described above under the dip-coating scheme. The resulting thickness of the film depends on the concentration of the solution and the choice of solvent.

Images of the interfaces were acquired using AFM and/or SEM – both dip coating and spin coating deposition techniques confirmed the deposition of particles at the interfaces. The thickness of the films were measured by ellipsometry and data is represented in the results section of this chapter.

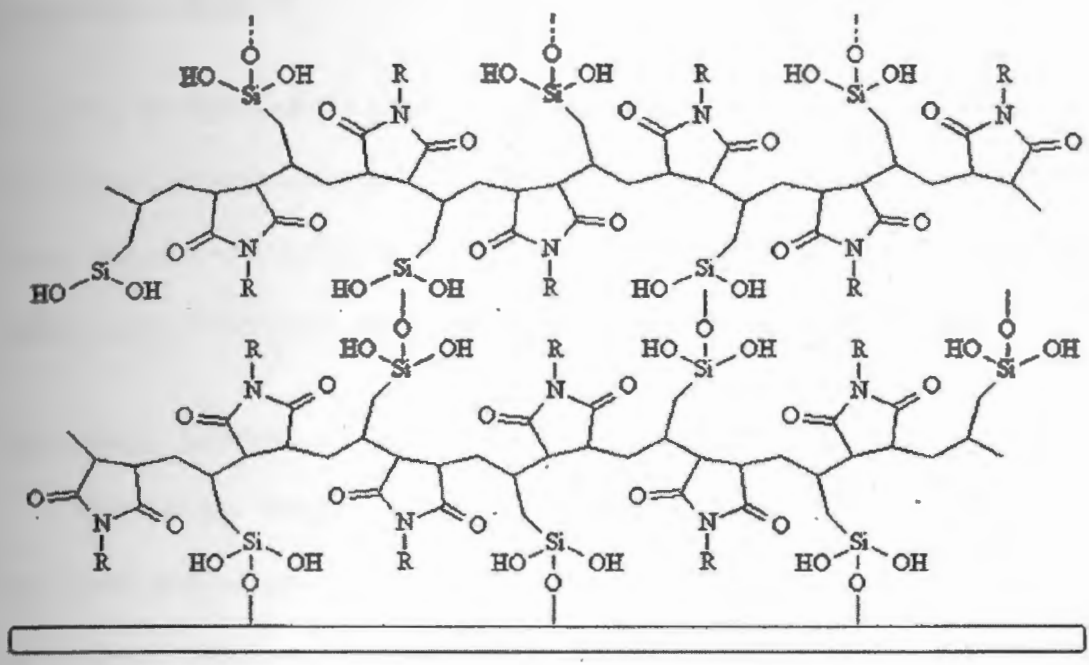

R = phenyl

Figure 3.1: Depiction of "idealized" polymer assembly onto substrates showing likely linkage.

FTIR analysis:

FTIR analysis was performed on Thermo Nicolet instrument. The materials thus prepared were analyzed after 1 hour and then after every week using FTIR to find out the extent of hydrolysis of alkoxysilane groups and simultaneous formation of new –Si-O-Si- bonds. FTIR studies confirmed the significant formation of siloxane bonds in the sol-gel matrix after a period of three weeks.

Ellipsometric Analysis:

The thickness of the polymer thin-films coated onto the silicon wafers was accomplished through Gaertner L116C Ellipsometer using the surface characterization lab at University of Massachusetts – Amherst. It is based on the measurement of the variation of the polarization state of the light after reflection on a plane surface.

Fluorescence Analysis:

Fluorescence analysis of the pyrene labeled polymers was accomplish through steady-state analysis using a PTI-QuantaMaster system. Here we used an excitation wavelength of 340nm and scanned the emission monochromator from 350 to 650nm to collect the emission spectrum.

Microscopic Imaging

Scanning electron microscopic (SEM) images were collected on an FEI Quanta 200 instrument. Particle-deposited interfaces were sputtered with gold prior to analysis with SEM. Images were collected at voltages between 15 kV and 25 kV depending on particle composition.

Atomic force microscope (AFM) images were collected on a Park Instruments AFM/STM. AFM images of both the polymer-free and polymer-modified surfaces and particle-deposited surfaces were collected. Surface area and surface roughness of both polymer-free and polymer-modified interfaces were obtained from AFM also.

RESULTS and DISCUSSIONS

The aim of the work described in this chapter is the facile conversion of the polymer prepared in-house into various functional forms that can be used in the development of sensing and separation platforms. All of the polymer employed in this work were designed and synthesized within our research group as described in chapter 2 of this dissertation. Using these polymers that bear alkoxysilane side groups facilitated the conversion into the various functional forms through the formation of very robust siloxane bonds.

The ability to prepare and assemble organized structures of nanoparticles, where selectivity of the resulting structures can be achieved through the judicious choice of the polymer chosen. The ability to introduce selectivity in such a facile manner allows for the tailoring of these thin-films and arrays to find application in diverse fields such as chemical/biological sensing and combinatorial studies. In this chapter we briefly demonstrate an example of the use of these materials in the sensing/detection of explosive and explosive-like compounds using fluorescence quenching as a detection method.

It should further be noted that the scope of this work was not to form well organized arrays based on deposition method alone, but rather how the polymers (both deposited on various surfaces and polymers within composite particles) influence the self-assembly. As previously mentioned, we intend to explore the self-assembly of nanoparticles at polymer modified interfaces in an attempt to develop patterned interfaces that can be tailored to specific sensing applications. The specifics of this

work – polymer preparation and surface modification and particle self-assembly are described below.

The presence of silane side groups in the polymeric chains helps in achieving a uniform blend. While preparing organic-inorganic materials the polymers were separately dissolved in acetone and treated with the hydrolyzing agents e.g. acid or a base (HCl or NH_4OH in this case). This step ensured the hydrolysis of alkoxysilane groups in the polymer chains. TEOS is treated separately by making a mixture of 2 ml of water, 4 mL of 95% ethanol and 1ml of hydrochloric acid, 4 mL TEOS is added to this mixture in the last step. The hydrolysis of alkoxysilane groups before mixing with the TEOS solution minimizes the problem of phase separation. This is because the hydrolyzed polymers form silanol groups which can easily form bond with the TEOS matrix ensuring the uniform composition of the matrix.

In acid catalyzed reactions the acidic proton along with the water molecule forms a complex with the central Si atom along with the water molecule. After breaking one of the alkoxy groups this complex is converted into a silanol (-Si-OH) group. These silanol groups undergo condensation to form siloxane (-Si-O-Si-) bonds. The base catalyzed reaction occurs according to the S_N2 mechanism. A complex is formed and after breaking one of the alkoxy groups, it is converted to silanol (-Si-OH) group. Again these silanol groups undergo condensation reaction to form siloxane (-Si-O-Si-) bonds.

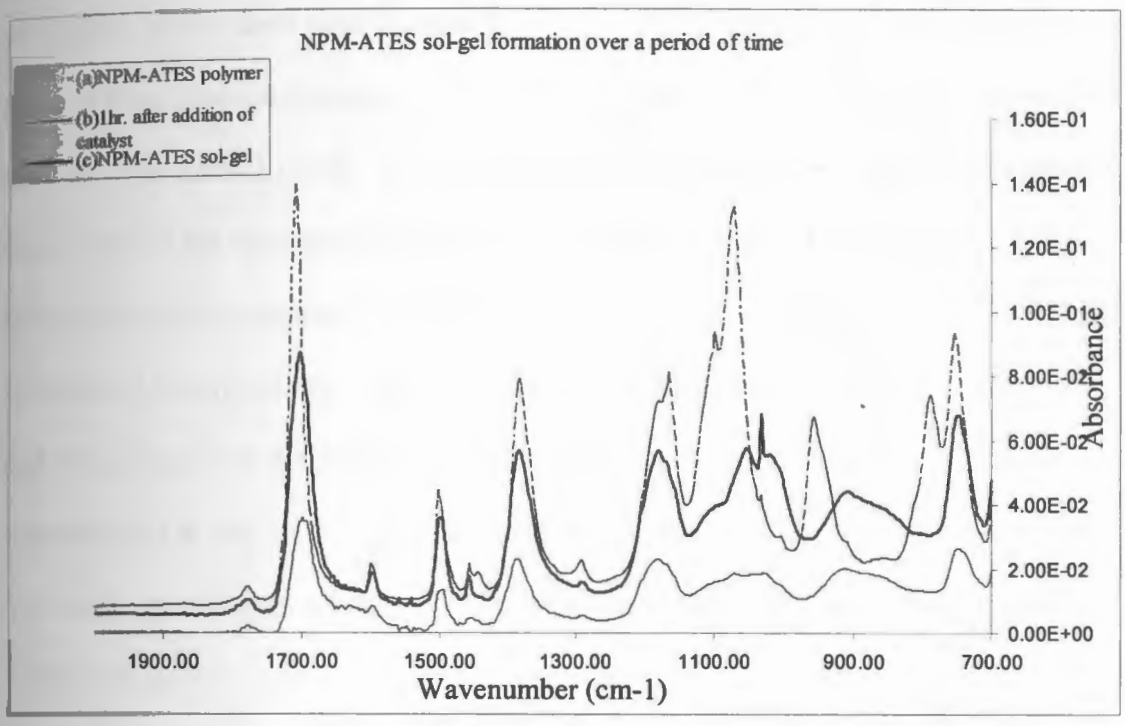

Figure 3.2: Figure shows part of FTIR spectra of (a) polymer NPM-ATES (b) after hydrolysis of alkoxy groups on the polymer (c) and conversion of polymer into sol-gel.

Figure 3.2 shows a part of FTIR spectra of the polymer NPM-ATES and its subsequent conversion into sol-gel. Spectra (a) is of polymer NPM-ATES, (b) is 1 hour after its hydrolysis using an acid and spectra (c) is that after the formation of polymeric sol-gel. Curve (b) shows that 1 hour after treating with the hydrolyzing agent the intensity of the bands around 1070 and 1170 cm^{-1}, which are characteristic bands for alkoxy group, decreases. This indicates the hydrolysis of alkoxy silane side groups. These are then converted into silanol groups, confirmed by the appearance of a broad stretch around 3200-3700 cm^{-1}. This confirms the presence of –Si-OH in the matrix. As the material dries out the silanol groups condense to form siloxane network (-Si-O-Si-) confirmed in Figure 3.1, (c) by appearance of band in the region of 1020-

1060 cm^{-1}. While there is an increase in the intensity of these bands at 1020-1060 cm^{-1} there is simultaneous decrease in the intensity of the silanol bands around 3200-3700 cm^{-1} as these silanol groups are condensed into siloxane bonds. Similar observations were made in the base catalyzed polymeric sol-gel materials; used to prepare organic-inorganic hybrid materials. As described in Scheme 3.1, polymer and TEOS were hydrolyzed before mixing. Figure 3.3 shows the FTIR spectra polymer NPM-VTES and its analysis over the period of three weeks as the material is converted into sol-gel. Spectrum (a) is that of the polymer NPM-VTES, spectrum (b) is of the sol-gel after one week, showing the presence of silanols in the matrix by the broad stretch around 3200-3700 cm^{-1}.

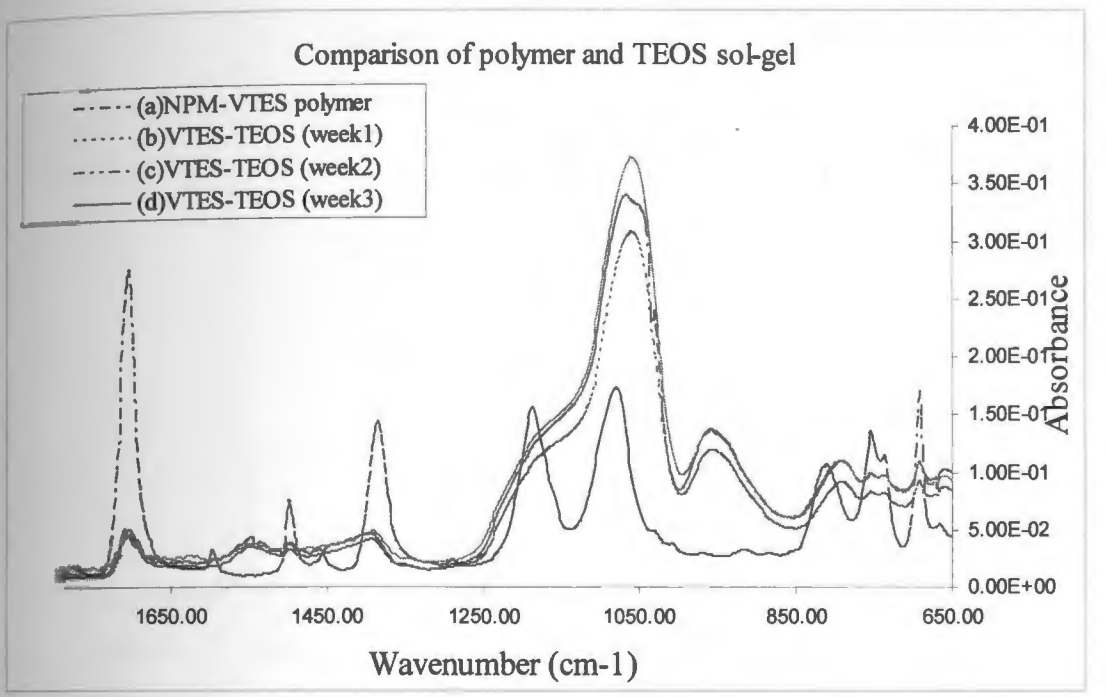

Figure 3.3: FTIR spectra of polymer NPM-VTES (a) one week after hydrolysis (b) two weeks after hydrolysis (c) and 3 weeks after hydrolysis (d) to form sol-gel.

There is also an appearance of a small band at 800 cm^{-1}, which can be attributed to the formation of long chain of siloxane bonds (-Si-O-Si).

Over a period of three weeks the intensity of the band at 800 cm^{-1} increased, along with the intensity of the band at 1030-1100 cm^{-1}. This confirmed the condensation of –Si-OH bonds and increase in the (–Si-O-Si-) siloxane groups.

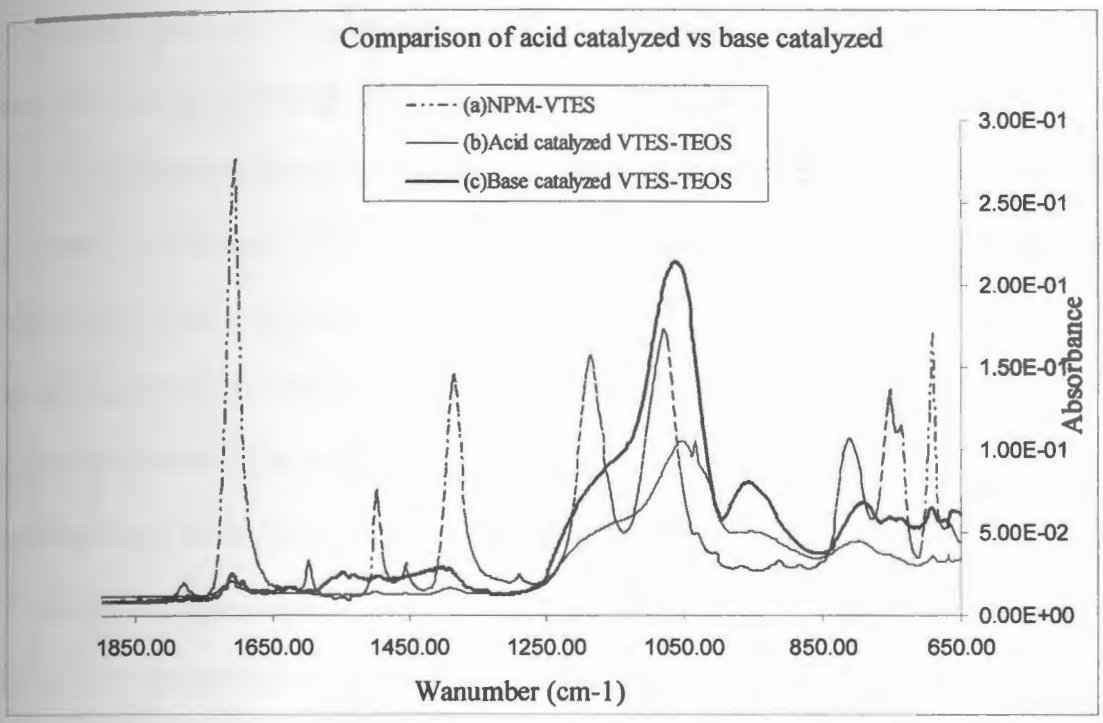

Figure 3.4: FTIR spectra of sol-gel of the polymer NPM-VTES (a), prepared by acid catalysis (b), and prepared by base catalysis mechanism (c).

The conversion of silanols into siloxane bonds was faster in base catalyzed than in acid catalyzed sol-gels. Figure 3.4 shows the comparison of acid catalyzed (b) and base catalyzed (c) spectra at the end of third week. In the base catalyzed sol-gel the intensity of the band at 1030-1100 cm^{-1} is very high as compared to the acid catalyzed sol-gel (b). Also the intensity of the band at 800 cm^{-1} is high in base catalyzed sol-gel than the acid catalyzed at the end of third week. This indicates that the siloxane bond network is formed faster in the base catalyzed sol-gels than acid catalyzed sol-gels. There was also a difference in the texture of acid and base catalyzed sol-gels. The base-catalyzed sol-gels appeared to be porous with a smaller particle size than the materials prepared through acid-catalyzed mechanism. A suitable

catalyzing agent can thus be used depending on desired properties in the material. Base also has the advantage of making sol-gel process faster.

Polymers prepared in house by a facile method which allows a choice of polymer functionality. In this work, we have chosen to work with the phenylmaleimide moiety to allow confirmation of polymer deposition spectroscopically by monitoring the aromatic band centered at 220 nm in the UV-Vis spectrum. Assembly at the surfaces employed in this work (glass or silicon wafer) was accomplished through the formation of siloxane (Si-O-Si) bonds between the silane (Si-OH) and alkoxysilane (Si-OR) side-groups of the polymer and the surface silanol groups of the surfaces. From the UV data, it is clear that polymer deposition is accomplished. We have also observed that absorbance at the aromatic band increases as a function of deposition cycle indicating the ability to deposit multiple layers of the polymer at the interface Figure 3.5.

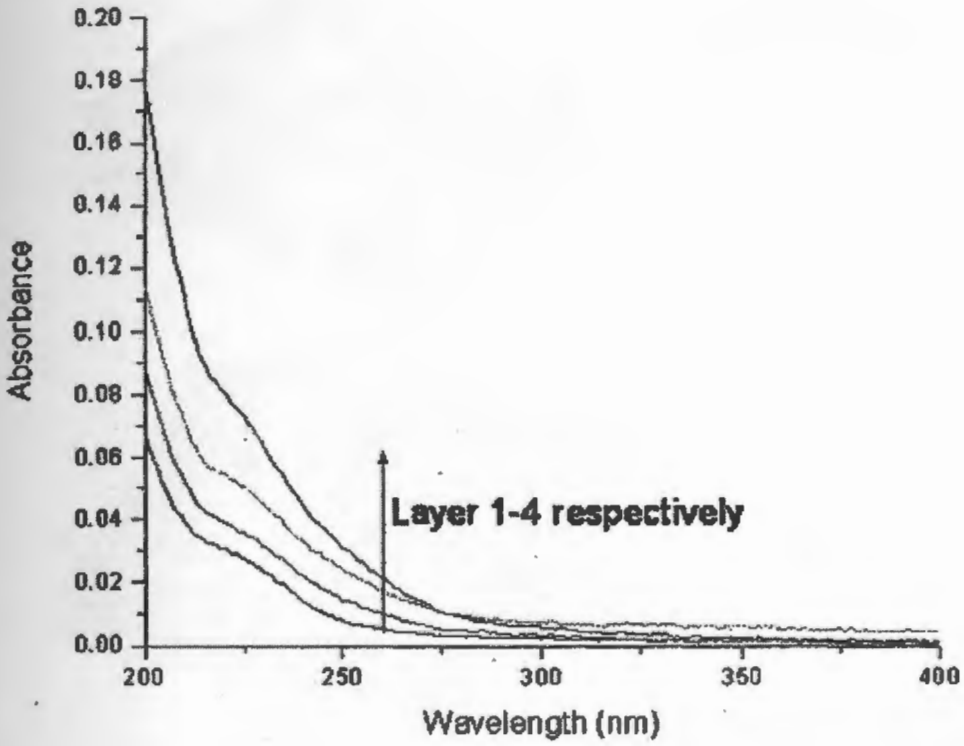

Figure 3.5: UV-Visible Absorption versus deposition cycle.

Analysis of the AFM images reveals an increase in the surface area and roughness of the polymer-modified surfaces relative to the polymer-free surfaces confirming polymer deposition. Figure 3.6 a shows the flat nature of the polymer-free interfaces, while Figure 3.6 b exhibits clearly defined high and low elevation points.

This increased surface area and surface roughness could account for the enhancement in particle deposition on the polymer-modified surfaces over the deposition on polymer-free surfaces.

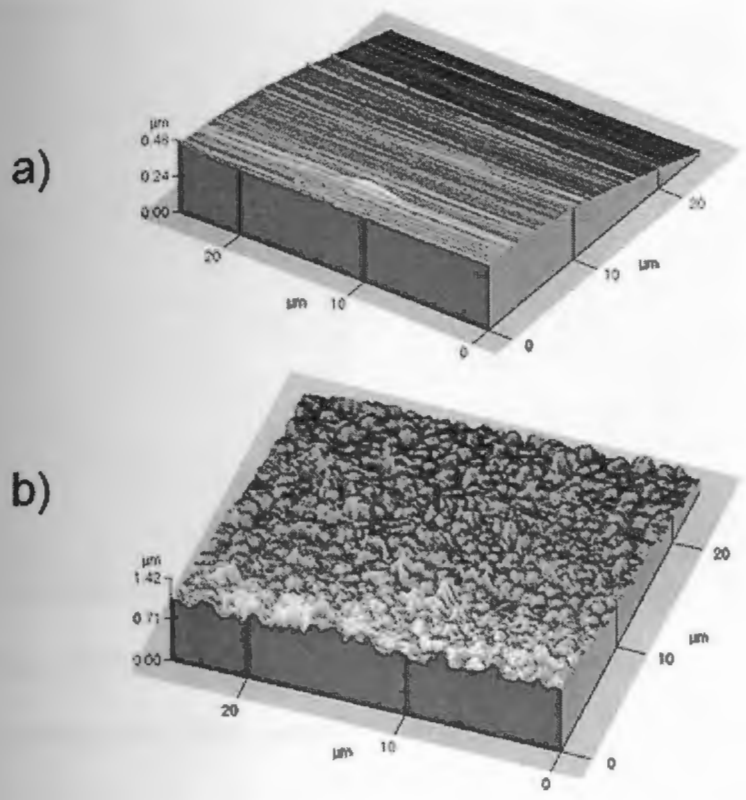

Figure 3.6: AFM images of (a) plain silicon wafer (b) polymer-modified silicon wafer.

We were also able to realize the deposition of polymer-silica composite nanoparticles at the polymer-modified interfaces as shown in Figure 3.7. Figure 3.7 is an SEM image of these deposited particles showing an irregular deposition pattern. The irregularity does not however, disqualify this method for use in sensing technologies, as irregular arrays have been utilized in the past. The SEM image also reveals the polydispersity of the size of the polymer-silica composite nanoparticles, where the sizes ranged from about 500 to 1,500 nm. Again, we observed the highest deposition of these particles from toluene as the deposition solvent. In future work we intend to attempt to better organize these assemblies by annealing the polymers at temperatures beyond the glass transition temperature (T_g).

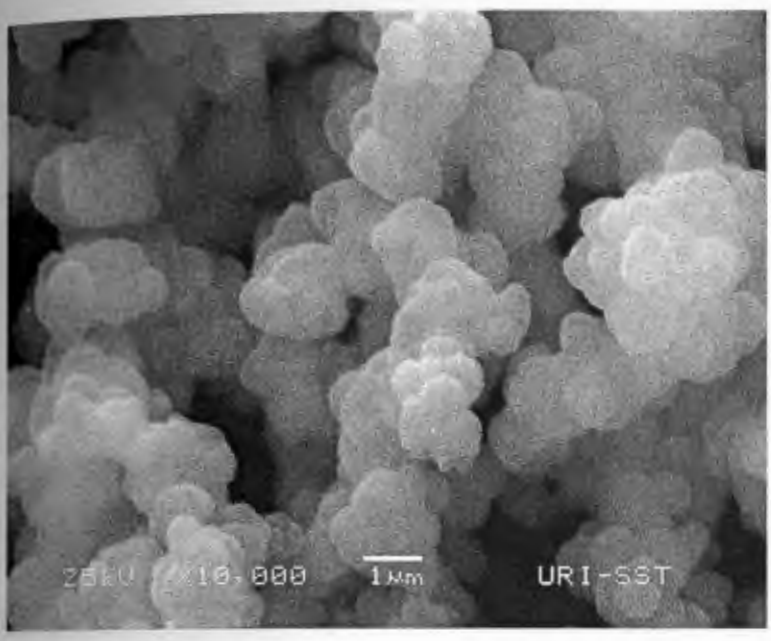

Figure 3.7: SEM image of polymer-silica composite nanoparticles deposited onto a polymer-modified interface.

Ellipsometric thickness data confirms that we are able to deposit these polymers in a controlled manner where plots of film thickness versus time of exposure to the polymer yields a linear plot with slope of ~ 28nm/30minute exposure with an R^2 value of 0.99. Additionally thickness data collected for the base catalyzed reaction yield a film thickness approximately twice that of the non catalyzed initial layer, while the acid catalyzed reaction yields a film thickness of approximately three times the non-catalyzed. These results confirm that we are indeed able to control film thickness. The table below summarizes the collected ellipsometric thickness data. The plot of film thickness versus deposition cycle (30 minute per deposition cycle) is also presented below.

Table 3.1: Ellipsometric thickness (nm) as a function of deposition cycle (per 30 minutes) for CPM-VTMS. Deposition was perform at 40^0C from a mixture of 2:8 acetone:toluene. Base = base catalyzed reaction, Acid = acid catalyzed and Regular = no base/acid added.

	Regular (nm)	Base (nm)	Acid (nm)
Cycle 1	23	38	71
Cycle 2	49	64	
Cycle 3	80		
Cycle 4	98		

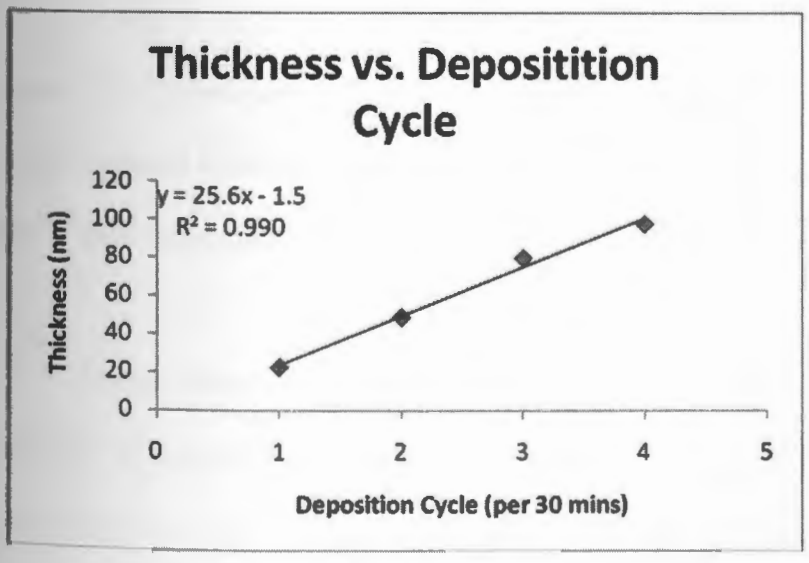

Figure 3.8. Plot of ellipsometric thickness data (nm) as a function of deposition cycle (per 30 minutes).

Explosives Detection:

Using the surfaces prepared as described in the chapter the detection of explosives is demonstrated. To accomplish this study, the polymer that was chosen was a terpolymer that contained pyrenemaleimide. This polymer was used to prepare polymer thin-films, polymer-silica composites and polymer-coated silica nanoparticles. These materials were used to detect the presence of various nitro-containing explosive, namely picric acid (2,4,6-trinitrophenol), trinitrotoluene(TNT), nitrobenzene (NB) and 2-nitrotoluene (2-NT) as depicted in Figure 3.9 below.

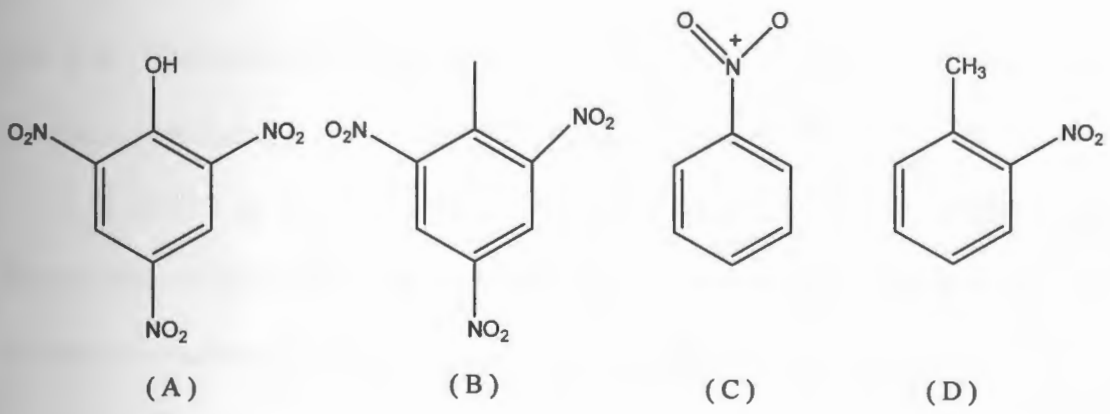

Figure 3.9: Structures of the various nitro explosives used for study. (A). Trinitrophenol (Picric acid) (B). Trinitrotoluene (TNT) (C). Nitrobenzene (D). 2, -Nitrotoluene (2-NT).

Nitroaromatics and Nitramines classes of compounds are of interest due to their use in explosives. These compounds are ideally detected by fluorescence quenching due to their strong electron-withdrawing groups that are capable of forming charge-transfer complexes with pyrene leading to the quenching of its emission by either a static or dynamic quenching mechanism. In the studies performed in this

work a dynamic mechanism is evident due to the decreasing intensity as the concentration of the quencher is increased. Further confirmation was possible due to the decrease in the fluorescence lifetime, a finding that is consistent with a dynamic mechanism.

The collisional/dynamic fluorescenc quenching mechanism is defined by the Stern-Volmer relationship:

$$F_0/F = \tau_0/\tau = 1 + kq\tau_0\,[Q]$$

Where F_0 and F are fluorescence intensities in absence and presence of quencher, τ_0 and τ are fluorescence lifetime in absence and presence of quencher, kq is the bimolecular quenching constant and [Q] is quencher concentration.

It should be noted that in a static mechanism there is no change in the fluorescence lifetime, only a change in the fluorescence intensity is observed. In a dynamic mechanism, the lifetime is quenched upon the collision of the quencher with the excited fluorophore. In all the below spectra Fig 3.10 and 3.11 it is observed that by increasing the quencher concentration the fluorescence intensity is decreased.

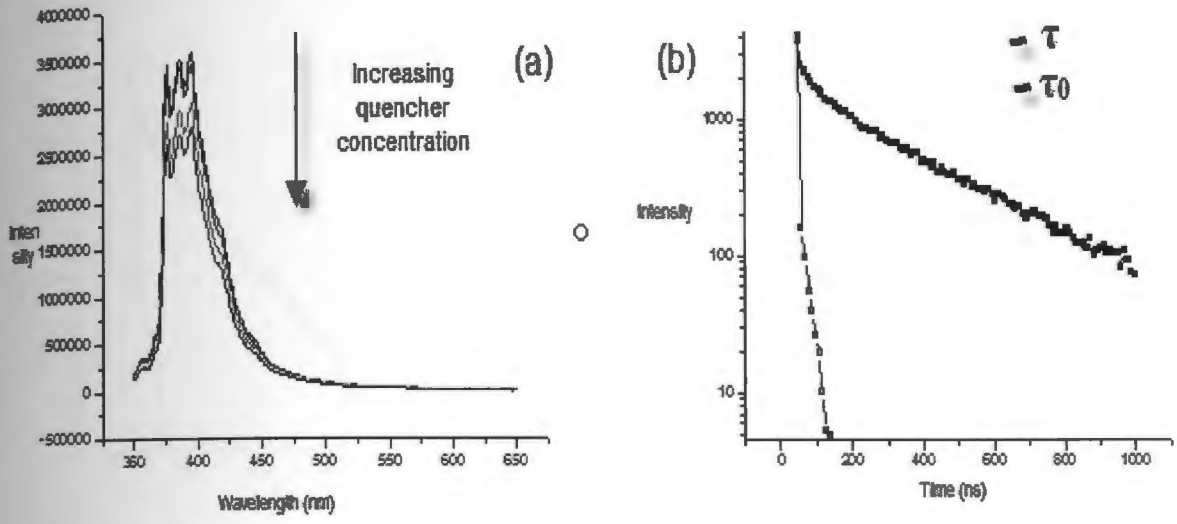

Figure 3.10: (a). Explosive 2-Nitrotoluene fluorescence spectrum pyrene signal intensity quenched upon increasing the quencher concentration. (b). Plot of Intensity vs. time (ns) clearly show that the lifetime of fluorophore is quenched in the presence of nitro-containing compounds.

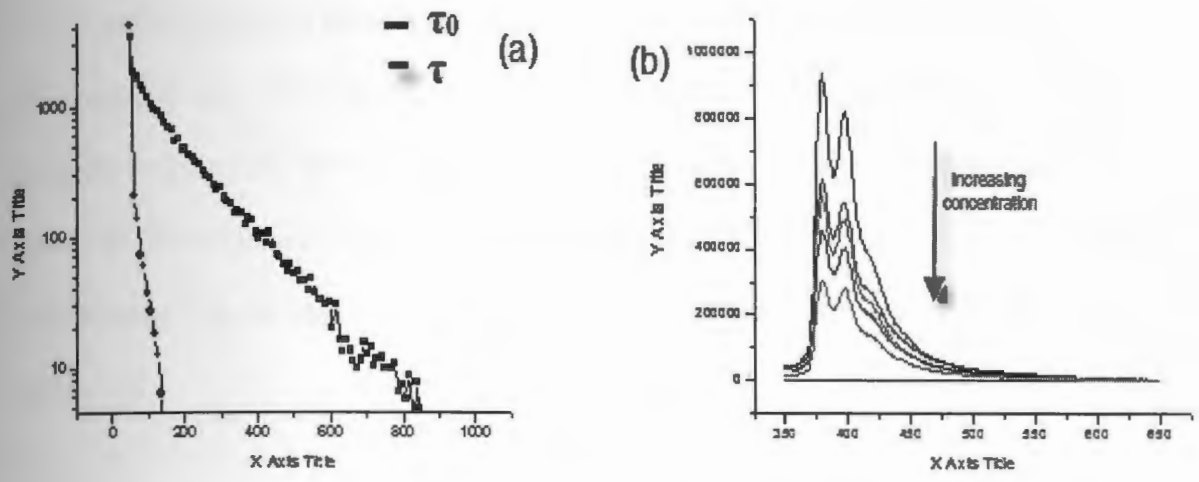

Figure 3.11: (a). Plot is a plot of the lifetime of pyrene showing the change in lifetime in the absence of fluorophore (τ_0) and in the presence of the quencher (τ). Plot (b) is the steady-state fluorescence spectra of pyrene showing the quenching of the emission as the quencher concentration is increased. In this case, the quencher is nitrobenzene.

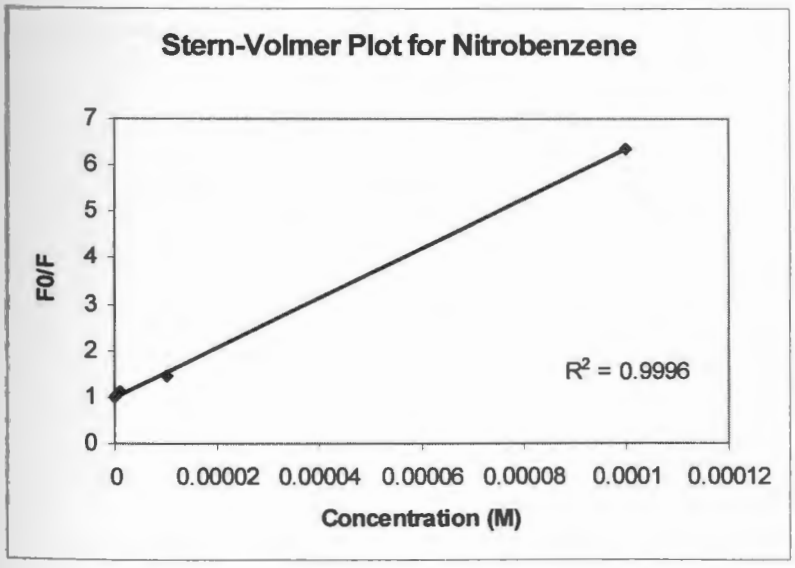

Figure 3.12: Stern-Volmer Plot of Nitrobenzene.

In Stern-Volmer plots the quenching data are usually presented as plots of F_0 /F versus [Q]. The 1/KSV is the quencher concentration at which F_0 /F = 50% of the intensity is quenched. If we look at the values in Table 3.2 the quenching constant value of Nitrobenzene is much higher than the other explosives hence the Nitrobenzene shows rapid quenching at increasing concentrations than the other explosives.

Table 3.2: Shows the quenching constant values of different explosives.

Quencher	***K*SV (M^{-1})**
Nitrobenzene	4.29×10^6
2,6-Dinitroaniline	1.44×10^6
2-Nitrotoluene	1.16×10^5

Conclusion

In this work we have a demonstrated the facile conversion of the silane-containing polymers prepared in this work into various functional forms. By simply varying experimental conditions, it is possible to convert these polymers into polymer-silica composites, polymer-coated nanoparticles, polymer thin-films and polymer-facilitated arrays. By simply choosing an appropriate polymer, it is possible to tailor the resulting assembly to a specific application. In this work we have demonstrated the use of these structures in the detection of explosives and explosive like molecules using a fluorescence quenching mechanism. The ability to prepare these polymers and structures opens up the possibility of using them in a variety of biological and chemical sensing and separations platforms

References

1. Hupp, T., Nguyen, S.T., Functional Nanostructured Molecular Materials, Interface, 2001, 10, 28.
2. Srinivasa, U., Leipmann, D., Howe, R.T., Microstructure to substrate self-assembly using capillary forces, Journal of Microelectromechanical Systems, 2001, 10, 17-24.
3. Donskoi, A.A., Shashkina, M.A., Zaikov, G.E., Fire Resistant and Thermally Stable Materials Derived From Chlorinated Polyethylene, October 2003 VSP.
4. Birner, A., Luetzen, J., Foster, K., Simmonds, M., Waeterloos, J., Millis, M., A Fourth Material: Thermally Stable Organic gap-fill spin-on-polymer enabling new integration concepts [DRAM example], Electronic Devices Meeting, International Electronic Devices Meeting Technical Digest, Institute of Electric and Electronic Engineers International, 2003, 28.4.1 – 28.4.4.
5. Hatgerink, et al., Self-Assembly and Mineralization of Peptide-Amphiphile Nanofibers, Science, 2001, 1684.
6. Fan, Hangyou., Yang, Kai., Boye, Daniel. M., Sigmon, Thomas., Malloy, Kevin.J., Xui, Huifang., Lopez, Gabriel.P., Brinker.C.Jeffrey., Self-Assembly of Ordered, Robust, Three-Dimensional Gold Nanocrystal/Silica Arrays, Science, 2004, 304, 567-571.
7. Parashar, V.K., Sahaya, A., Pfefferb, M., Schochb, F., Gobrechtc, J., Gijsa, M.A.M., "Nano-replication of diffractive optical elements in sol-gel derived glasses."Microelectronic Engineering (2003), 67-68, 710-719.

8. Li, C., Murase, N., "Synthesis of Highly Luminescent Glasses Incorporating CdTe Nanocrystals through Sol-Gel Processing," Langmuir (2004), 20(1),1-4.

9. Meneseza, W.G., Pedro, H.C., Camaroga, Oliveiraa, M.M., Evans, D.J., Soaresa, J.F., Zarbena, A.J.G., "Sol-gel processing of a bimetallic alkoxide precursor confined in a porous glass matrix: A route to novel glass/metal oxide nanocomposites." Journal of Colloid and Interface Science (2006) 299 (1), 291-296.

10. Rambo, C.R., Cao, J., Rusina, O., Sieber, H., "Manufacturing of bimorphic (Sc, Ti, Zr)-carbide ceramics by sol-gel processing." Carbon (2005) 43, 1174-1183.

11. Roman, J., Padilla, S., Vallet-Regi, M., "Sol-Gel Glasses as Precursors of Bioactive Glass Ceramics." Chemistry of Materials (2003) 15, 798-806.

12. Pradhan, A.R., Macnaughtan, M.A., Raftery, D., "Preparation of Zeolites Supported on Optical Microfibers." Chemistry of Materials (2002) 14 (7), 3022-3027.

13. Berger, C., Glaser, R., Rakoczy, R.A., Weitkamp, J.,"The synthesis of large crytals of zeolite Y re-visited." Microporous and Mesoporous Materials (2005) 83 (1-3), 333-344.

14. Tursiloadi, S., Imai, H., Hirashima, H., "Preparation and characterization of mesoporous titania-alumina ceramic by modified sol-gel method." Journal of Non-Crystalline Solids (2004) 350, 271-276.

15. Gong, K., Zhang, M., Yan, Y., Su, L., mao, L., Xiong, S., Chen, Y., "Sl-Gel Derived Ceramic-Carbon Nanotube Nanocomposite Electrodes: Tunable Electrode

Dimension and Potential Electrochemical Applications." Analytical Chemistry (2004) 76 (21), 6500-6505.

16. Mazloum Ardakania, M., Khayat Kishania, M., Salavati-Niasaria, M., Ensafi, A.A., "Lead ion-selective electrode prepared by sol-gel and PVC membrane techniques." Sensors and Actuators B: Chemical (2005) 107 (1), 438-445.
17. Walcarius, A., "Electrochemical Applications of Silica-Based Organic-Inorganic Hybrid Materials." Chemistry of Materials (2001) 13, 3351-3372.
18. Rodriguez Gutierrez, J.A., Petit Dominguez, M.D., Pinilla Macais, J.M., "Development of ion-selective electrochemical sensors by using the sol-gel process." Analytica Chimica Acta (2004) 524 (1-2), 339-346.
19. Marxer, S.M., Schoenfisch, M.H., "Sol-gel derived potentiometric pH sensors." Analytical Chemistry (2005) 77 (3), 848-853.
20. Lei, C., Shin, Y., Liu, J., Ackerman, E.J.,"Entrapping Enzyme in a Functionalized Nanoporous Support." Journal o American Chemical Society (2002) 124 (38), 11242-11243.
21. Btancor, L., Lopez-Gallego, F., Hidalgo, A., Fuentes, M., Podrasky, O., Kuncova, G., Guisan, J.M., Fernandez-Lafunete, R., "Advantages of the Pre-Immobilization of Enzymes on Porous Supports for their Entrapment in Sol-Gels." Biomacromolecules (2005) 6 (2), 1027-1030.
22. Cleide, M.F., Soaresa, Oneila, A., dos Santosa, de Castrob, H.F., de Moraesa, F.F., Zanina, G.M., "Characterization of sol-gel encapsulated lipase using tetraethoxysilane as precursor." Journal of Molecular Catalysis B: Enzymatic (2006) 39, 69-76.

23. Boonamnuayvitayaa, V., Tayamanona, C., Sae-ungb, S., Tanthapanichakoon, W., "Synthesis and Characterization of porous media produce by a sol-gel method." Chemical Engineering Science (2006) 61 (5), 1686-1691.

24. Liang, R., Qiu, J., Cai. P.,"A novel amperometric immunosensor based on three-dimensional sol-gel network and nanoparticle self-assemble technique."Analytica Chimica Acta (2005) 534 (2), 223-229.

25. Gill, I., "Bio-doped Nnaocomposite Polymers : Sol-Gel Bioencapsulates". Chemistry of Materials (2001) 13 (10), 3404-3421.

26. Tsagkogeorgas, F., Ochsenkunh-Petropolou, M., Neissner, R., Knopp, D.," Encapsulation of Biomolecules for bioanalytical purposes: Preparation of diclofenac antibody-doped nanometer-sized silica particles by reverse micelle and sol-gel processing." Analytica Chimica Acta (2006) 573-574, 133-137.

27. Smarslya, B., Garnweitnera, G., Assinkb, R, Brinker, J.V., "Preparation and characterization of mesostructured polymer-functionalized sol-gel derived hin films." Progress in Organic Coatings (2003) 47 (3-4), 393-400.

28. Doherty, W.J., Armstrong, N.R., Saavedra, S.S., "Conducting Polymer Growth in Porous Sol-Gel Thin Films: Formation of Nanoelectrode Arrays and Mediated Electron Transfer to Sequestered Macromolecules." Chemistry of Materials (2005) 17 (14), 3652-3660.

29. Tanga, Z., Xiea, Y., Hawthorne, H., Nevilleb, A., Thammachartb, M., Troczynskic, T., Lic, G., Yang, Q., "Characterizing the microstructure and mechanical and elctrochemical properties of novel ceramic/polymer sandwich

structural coatings." Surface and Coatings Technology (2006) 200 (20-21), 5986-5974.

30. Sun, S., Murray, C.B., Weller, D., Folks, L., Moser, A., Science, 2000, 287, 1989-1992.
31. Wohltjen, H., Snow, A.W., Analytical Chemistry, 1998, 70, 28856-28859.
32. Asher, S.A., Alexeev, V.L., Goponenka, A., Sharma, A.C., Lednev, A.K., Wilcox, C.S., Finegold, D.N., Journal of American Chemical Society, 2003, 125, 3322-3329.
33. Velev, O.D., Kaler, E.W., Langmuir, 1999, 15, 3693-3698.
34. Gates, B., Xia, Y., Advance Materials, 2000, 12, 1329-1332.
35. Xia, Y., Gates, B., Yin, Y., Liu, Y., Advanced Materials, 2000, 12, 693-713.
36. Yang, P., Wirnsberger, G., Hunag, H.C., Codero, S.R., McGehee, M.D., Scott, B., Deng, T., Whitesides, G.M., Chmelks, B.M., Burratto, S.K., Stucky, G.D., Science, 2000, 287, 465-467.
37. Hatori, H., Advanced Materials, 2001, 13, 51-54.
38. Reculusa, S., Ravaine, S., Chemistry of Materials, 2003, 15, 598-605.
39. Wang, w., Gu, B., Journal of Physical Chemistry B, 2005, 109, 22175-22180.
40. Wang, W., Gu, B., Liang, L., Hamilton, W., Journal of Physical Chemistry B, 2003, 107, 3400-3404.
41. Korgel, B.A., Fullam, S., Connolly, S., Fitzmaurice, D., Journal of Physical Chemistry B, 1998, 102, 8379-8388.
42. Martin, J.E., Wilcoxon, J.P., Odinek, J., Provencio, P., Journal of Physical Chemistry B, 2000, 104, 9475-9486.

43. Sommer, A.P., Ben-Moshe, M., M.Mgdassi, S., Journal of Physical Chemistry B, 2004, 108, 8-10.

44. Fendler, J.H., Meldrum, F.C., Advanced Materials, 195, 7, 607-631.

45. Mahalingam, V., Onclin, S., Peter, M., Ravoo, B.J., Huskens, J., Reinhoudt, D., Langmuir, 2004, 20, 11756-11762.

46. Manoz, R., Frydman, E., Cohen, S.R., Sagiv, J., Advanced Materials, 2000, 12, 725-727.

47. Sagiv, J., Journal of American Chemical Society, 1980, 102, 92-98.

48. Wasserman, S.R., Tao, Y.T., Whitesides, G.M., Langmuir, 1989, 5, 1074-1087.

49. Strober, W., Fink, A., Bohn, J., Journal of Colloidal Interface Science, 1968, 26-62.

50. De, G., Karmakar, B., Ganguli, D., Journal of Materials Chemistry, 2000, 10, 2289-2293.

Chapter 4

Polymer-Facilitated Biofunctionalization of Magnetic Iron Nanoparticles

ABSTRACT

This work details the preparation of a group of polymers that was used to facilitate the attachment of proteins to the surface of magnetic (iron oxide) nanoparticles. In this scheme the nanoparticles were first prepared by precipitating the black iron oxide particles from a basic solution of Fe (II) and Fe (III). The magnetic nanoparticles were then exposed to solutions of aminopropyltrimethoxysilane, [redacted]yanatopropyltrimethoxysilane and various silane-containing polymers designed and prepared in-house. In all schemes, proteins successfully attached directly to the surface of the nanoparticles, which was confirmed by fluorescence spectroscopy. It is also worth noting that in the case where the proteins were attached to the polymer-coated nanoparticles, the fluorescence peak was at 330 nm, consistent with the fluorescence from protein in their native state, indicating that there was no evidence of protein denaturation. These findings are consistent with the polymer providing a protective underlayer to the protein, and thus preventing any adverse effects from the surface functional groups that could cause changes in the protein properties and its spectrum.

Introduction

In recent years a significant amount of research has been undertaken focused on the use of magnetic nanoparticles in fields as diverse as magnetic separation, to their use in medicine. While magnetic particles have been used in imaging techniques such as magnetic resonance imaging, new areas include magnetic particles in drug delivery, cancer therapy, bacteria detection and differentiation.

Nanoparticle are very small materials with dimension less than 100nm[1] which is particularly beneficial in that it allows for size-dependent properties that may not be observed or lost in the bulk. The high surface area-to-volume ratio provided by these materials also make them very attractive for use in biomedical applications, where materials of such small dimension can easily pass through the cell membrane into the cell body and deliver drugs or allowing for the imaging of the cell or a specific component of the cell. Nanoparticles of various materials (metals, metal oxides, and polymers) and possessing unique properties (magnetic, semiconducting) can be prepared by several different methods in the lab including simple wet chemical methods [2]. Judicious choice of materials and control of reaction conditions affect the size of the resulting nanoparticles.

Of particular interest in this work is the preparation of magnetic nanoparticles and their functionalization that allows for facile bio-modification of these materials.

The superparamagnetic properties of magnetic nanoparticles have made them very attractive candidates for use in medical imaging, such as contrast agents for magnetic resonance imaging (MRI), magnetic field assisted transport, separations and analyses. Lee *et al.* demonstrated that injecting polymerized magnetic nanoparticles into cancer cells improved the contrast between the cancer cells and surrounding tissue during MRI [1, 3]. Magnetic nanoparticles are also widely used in the separation and detection of proteins and bio-organisms [4].

A wide range of magnetic nanoparticles can be prepared and some common examples include those of iron oxide, cobalt ferrite, iron platinum, and manganese ferrite. Newer synthetic methods have also been developed to produce magnetic nanoparticles, usually prepared under high temperature, organic phase or aqueous conditions [5]. These nanoparticles can then be modified to create a core-shell structure that will help the particle retain its shape and stability. This modification typically involves coating the nanoparticle with polymer. The polymer acts as a scaffold for attachment of surfactants. Surfactants with functionalized groups are then used as a platform to simulate surface conditions needed for the particular study [6]. Other researchers have coupled quantum dots to the surface of thiol-modified polymer-coated superparamagnetic beads, using thiol-to-metal bonds to attach the quantum dots to the magnetic beads [7].

Recently, modification of magnetite nanoparticles by means of surface-initiated atom transfer radical polymerization (ATRP) was accomplished [8]. ATRP blocks copolymerization and allows polymerization of functional monomers like styrenes, acrylates, acrylamide, and acrylic acids. As a result, the manufactured polymers exhibit similar weights. The immobilization of an ATRP initiator on a functionalized iron oxide surface helps subsequent ATRP produce functional polymer brushes [9]. Because of the continued subsequent polymerization, the iron oxide nanoparticles form hybrids in conjunction with the present polymers. These hybrids can then be used to build novel iron oxide-based medical technologies and instruments.

Ferrofluids are colloidal suspensions of iron particles of nanometer dimension that exhibit a magnetic response in the presence of a magnetic field. Ferrofluids can be easily prepared by the co-precipitation of the salts of Fe^{2+} and Fe^{3+} most commonly ferric and ferrous chloride in the presence of a base. The resulting material is Fe_3O_4. Iron nanoparticles with diameters of 5 to 10 nm can easily be prepared. Since these nanoparticles are smaller than typical cells, bacteria and viruses, they are ideal candidates for use in biological studies as their small size allows them to readily access the target species. For example, Smith *et al.* found that aptamer-conjugated magnetic nanoparticles were able to infiltrate multiple

cancer cells and that infiltration of the nanoparticles into corrupted cells eventually allowed for a selective extraction and detection of the target cells [9-11].

Biofunctionalization of nanomaterials such as silica and magnetic nanoparticles has lead to extensive applications in the medical field. In order for this to be a success, there is a need of biocompatible materials as well as for facile approaches to allow the attachment of biological entities with the retention of bioactivity. [12-18]. Nanotechnology as applied to medicine is a very promising and active topic of research that bridges biology, chemistry and medicine. Procedures like photodynamic therapy and heperthermia have proven to be a hopeful advancement in the treatment of cancer [3,18-22].

In the work described here, the preparation of a group of silane-containing polymers that facilitate the attachment of proteins to the surface of magnetic particles in a simple process is presented. The polymer not only provides the skeletal support for the magnetic nanoparticles, but also protects the protein from denaturing as a result of the polar surface functionalities. Denatured protein loses its inherent structure and properties, thereby resulting in loss of cell activity or even death of the cell or organism. Therefore, for the purposes of protein/organism identification, it is important for the protein not to denature during the assay.

Experimental Methods

The preparation of the functionalized magnetic nanoparticles proceeded in four distinct steps. The polymers were first prepared by the radical polymerization of the monomers. Next, the magnetic nanoparticles were prepared by the coprecipitation of Fe (II) and Fe (III) from basic solutions. The nanoparticles were then functionalized with the polymers or silanes, and finally the proteins were attached to the polymer-modified nanoparticles. These steps are described in detail below.

Polymer Preparation

Four different co- and ter-polymers such as n-Phenylmaleimide-vinyltrimethoxysilane (NPM-VTMS), Chlorophenylmaleimide-vinyltrimethoxysilane (CPM-VTMS), Bromophenylmaleimide -vinyltrimethoxy silane (BrPM-VTMS) and ter-polymer [redacted]henylmaleimide-vinyltrimethoxysilane-Allylisothiocyanate (CPM-VTMS-AITC) were synthesized according to the procedure described in Chapter 2 of this dissertation. All polymers were used as described below to functionalize the magnetic nanoparticles.

Synthesis and Functionalization of Magnetite

A typical procedure for the preparation of the magnetic nanoparticles involves the coprecipitation of iron (II) and iron (III) in the presence of a strong base. More specifically, $FeCl_2 \cdot 4H_2O$ and $FeCl_3 \cdot 6H_2O$ were first dissolved in distilled water followed by the addition of ammonium hydroxide with stirring. After approximately

30 minutes of stirring, the supernatant was decanted, the product was then rinsed with ethanol and water, and re-suspended in ethanol and used in the functionalization steps as described below.

Magnetic Particle Functionalization

a) Polymer functionalization

A mass of 250 mg of the appropriate copolymer was dissolved in 15 mL of acetone to which 2 drops of concentrated HCl was added to facilitate the hydrolysis of the silane groups to the corresponding silanol groups. This solution was stirred for 10 minutes. The magnetite nanoparticles as prepared above were suspended in ethanol, followed by an addition of 5 – 7 mL of NH_4OH and stirred for 30 minutes. The polymer solution was then added drop-wise to the suspended nanoparticles while stirring continuously. FTIR spectroscopy was used to confirm the attachment of the polymer to the surface of the nanoparticles.

b) Attachment of other groups to magnetic particles

Amino (NH_2) terminal groups were introduced to the magnetic nanoparticles by first suspending the nanoparticles (plain or polymer-functionalized nanoparticles) in ethanol. A 5% ethanolic solution of 3-aminopropyltrimethoxysilane was then added to the suspension while stirring. The solution was stirred overnight and then collected for further use. FTIR spectroscopy was used to confirm the attachment of the silane groups to the nanoparticles.

Isocyanato (NCO) functionalization of the magnetic nanoparticles was accomplished by re-suspending the magnetic nanoparticles in ethanol. A 5% ethanolic solution of 1,6-diisocyanatohexane was then added and the suspension allowed to stir overnight. FTIR spectra were collected to confirm the attachment of the silane-functionalized iron nanoparticles with the NCO groups.

Protein Attachment

Subsequent to the functionalization of the magnetic iron nanoparticles as described above, a model protein (egg albumin) was used to demonstrate the biofunctionalization of protein to the surface of the nanoparticles. A solution of egg albumin was prepared by dissolving it in a 0.01M sodium borate buffer. The protein solution was divided into four equal portions, and the functionalized nanoparticles were added to each portion. In the case of the isocyanato-functionalized nanoparticles, the protein was attached to the particles via the formation of a urea linkage –N(C=O)N –.

In a second step, to illustrate a one-pot functionalization, the magnetite particles were mixed into a solution of 1,6-diisocyanatohexane to which the protein solution was added. Fluorescence spectra were collected to confirm the attachment of the protein to the magnetite.

Bio-Ferrograph Studies

In this experiment a Bio Ferrograph (Model # 2100, Guilfoyle Inc.) was employed for the analysis of the biofunctionalized magnetic iron oxide nanoparticles. This particular instrument allows for the online analysis where both magnetic deposition and imaging of the nanoparticles is possible. Using a pump, a small amount of the ferrofluid is introduced into the system and flows over an electromagnet with a field strength of 1.2 Tesla. The electromagnet generates a high gradient magnetic field resulting in the deposition of the magnetic particles in a size gradient along the microscope slide attached to the instrument.

Preparation of the IgG solution:

The IgG solution was prepared by diluting a commercially available 11.0 mg/ml solution of human IgG in 10 ml of 1X PBS buffer solution.

Preparation of the FTIC labeled anti-IgG solution:

The anti-IgG solution was prepared by diluting a commercially available 3.4 mg/mL solution in 5 ml of 1X PBS solution. The anti-IgG was purchased already labeled with FITC.

[redacted]tion of Dansyl Chloride Solution:

0.080925g of dansyl chloride is dissolved in 100 mL of Dimethylformamide by stirring and covered with aluminium foil as dansyl chloride is very sensitive to light.

[redacted]ration of the egg albumin solution:

The egg albumin was prepared by dissolving 0.0132 g of egg albumin in 1 mL of 0.01 borate buffer at pH 8.4. The egg albumin was subsequently labeled with dansyl chloride according to a procedure described in reference 1. Briefly, the egg albumin was stirred with a 0.003M solution of dansyl chloride egg albumin for 1.5 hours at 25^0C. During the labeling procedure the solution was wrapped in aluminum foil to avoid the photodegradation of the dansyl chloride. The resulting labeled egg albumin was stored at 15^0C until further studies.

[redacted]cation of the isocyanatopropyltriethoxysilane functionalized nanoparticles:

The isocyanato nanoparticles were prepared by stirring a specific amount of the ferrofluid with the isocyanatopropyltrimethoxysilane. The resulting particles were rinsed, collected and resuspended in an appropriate solution depending upon the further needs of the method.

[redacted] of the IgG-functionalized magnetic nanoparticles:

The IgG-functionalized particles were prepared by suspending the [redacted]natopropyltriethoxysilane functionalized nanoparticles prepared as described in the step above in a solution of IgG that had been prepared in 1X PBS solution. This magnetic nanoparticle-IgG mixture was allowed to stir in an ice bath for 2 hours. The [redacted]G-functionalized nanopartilces were collected, rinsed and stored at 15 ^{0}C until needed for further studies.

[redacted]ation of egg albumin-functionalized magnetic nanoparticles:

The egg albumin functionalized nanoparticles were prepared by suspending the [redacted]yanatopropyltriethoxysilane functionalized magnetic nanoparticles prepared as described above in a solution of egg albumin that had been prepared as described above. This mixture was allowed to stir at 25^{0}C for 2 hours. The resulting nanoparticles were stored at 15^{0}C until further studies.

[redacted]eparation of the ferrograph cassette:

In the first part of the ferrography experiment the five ports of the cartridge were prepared by introducing 0.3 mL of the various magnetic nanoparticles that were suspended in 1X PBS solution.

Port 1). IgG-functionalized magnetic nanoparticles (prepared as above)

Port 2). IgG-functionalized magnetic nanoparticles (prepared as above)

Port 3). IgG-functionalized magnetic nanoparticles (prepared as above)

Port 4). Isocyanato-functionalized magnetic nanoparticles (Control 1)

Port 5). Plain (unfunctionalized) magnetic particles (Control 2)

After the cassette had been prepared as described above, the second step was to determine if there was any biorecognition between the IgG functionalized magnetic nanoparticles and the anti-IgG. Ports 4 and 5 as described above were used as control. In port 4, the nanoparticles are only functionalized with [redacted]cyanatopropyltriethoxysilane to determine if there is any capture of anti-IgG by any unreacted isocyanato groups. Port 5 is plain magnetic nanoparticles.

[redacted]iorecognition experiment:

Next, the antibody (anti-IgG) and the control protein (egg albumin) were introduced into the ports as described below. The ferrography experiment was allowed to proceed and after drying, the magnetic particles were collected from the cassette and fluorescence spectra were collected in order to determine binding between the antibody and antigen. The control protein (egg albumin) was introduced to

determine if there was any non-specific binding to either the IgG or unreacted isocyanato groups.

For these experiments, ram on Ferrograph is programmed to introduce the samples at a flow rate of 0.5 mL/min. Additional sample was introduced during sequential runs.

Table 4.1: Shows the various experiments conducted in each port of the ferrograph cassette

Ports	Step 1	Step 2
Port 1	IgG-functionalized magnetic nanoparticles	FITC labeled anti-IgG introduced
Port 2	IgG-functionalized magnetic nanoparticles	Dansyl Chloride labeled egg albumin introduced
Port 3	IgG-functionalized magnetic nanoparticles	Mixture of labeled anti-IgG and labeled egg albumin introduced
Port 4	Isocyanato-functionalized magnetic nanoparticles (No IgG)	Mixture of labeled anti-IgG and labeled egg albumin introduced
Port 5	Plain (unfunctionalized) magnetic particles	Mixture of labeled anti-IgG and labeled egg albumin introduced

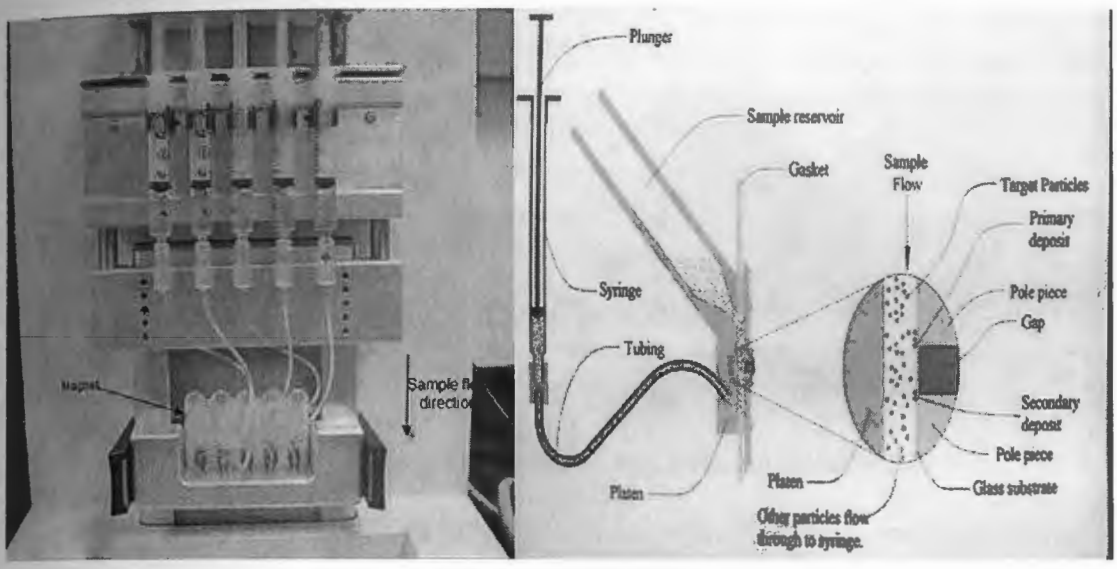

Figure 4.1: a) The Bioferrograph used for this experiment. b) Cross sectional view of the deposition cassette showing how the particles are attracted by magnet on the glass substrate.

At a flow rate of 0.5 mL/min, allowed the ferrograph to draw the sample fluids through the deposition cassette into the syringes. At this point, the magnetic particles labelled with their respective substances will collect into the deposition cassette via the force of the magnet. After this sequence is performed, add 0.150 mL of distilled water to each port as a transitioning fluid. This will ensure that the remaining residue from the previous solutions will be washed out of each port, allowing the Anti-IgG

solutions to make a clean entry into the ferrograph. Once all the transitional fluid has been drained from each port, and the fluid is collected in the syringes as well as the particles collected in the deposition cassette, the following solutions introduced into the ports in 0.3 mL increments as follows:

Port 1) FITC labeled anti-IgG introduced

Port 2) Dansyl chloride labeled egg albumin introduced

Port 3) Mixture of labeled anti-IgG and labeled egg albumin introduced

Port 4) Mixture of labeled anti-IgG and labeled egg albumin introduced

Port 5) Mixture of labeled anti-IgG and labeled egg albumin introduced

Again making sure the ferrograph is set at a flow rate of 0.50 mL/min. begin capturing the liquid into the syringes until each port is drained of all remaining solutions. Once completed, removed the deposition cassette from the ferrograph and collect the remaining particles for analysis.

The particles are scraped from the microscopic slide, suspended in the 1X PBS solution and analyzed by Fluorometer.

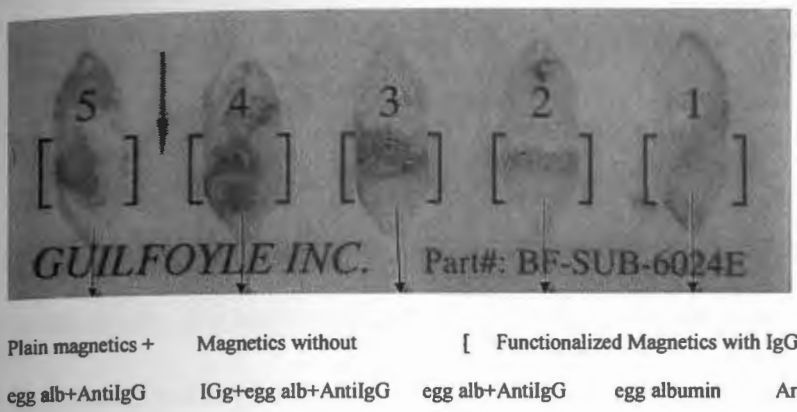

Figure 4.2: The glass substrate showing five ports from which the particles were scraped for further analysis.

RESULTS and DISCUSSION

The aim of the work presented in this paper is the development of simple chemistries that can be used for the facile biofunctionalization of nanoparticle. In this case, we have focused our attention to the functionalization of magnetic iron oxide particles. The functionalized magnetic nanoparticles can thus be used as multifunctional sensors in the capture and analysis of pathogens and particulates [10, 11]. Additionally, the ability to functionalize these materials with biological entities such as proteins and antibody can prove particularly attractive in the biomedical/bioimaging fields. For example, if these materials can be functionalized with a specific protein/antibody that can recognize a specific type of tumor, the it is conceivable that better images or medical decision can be made because only that specific tumor will be imaged since these "smart" nanoparticles can be directed to a specific target.

The preparation of the magnetic nanoparticles was accomplished by co-precipitation of Fe^{2+} and Fe^{3+} in the presence of ammonium hydroxide resulting in the formation of a blackish-brown precipitate, which was visibly attracted to an external magnet. Once the magnetic nanoparticles had been prepared they were then collected and functionalized in one of two schemes followed by attachment of a model protein (egg albumin). In the first scheme which is presented as Figure 4.3a, a polymer that had been synthesized to present terminal isothiocyanato groups was first attached to

the surface of the iron oxide nanoparticles by formation of bonds between the surface of the nanoparticle and the methoxysilane side groups of the polymer. In the second step presented as Figure 4.3b, the polymer-modified nanoparticle is then exposed to a solution of the egg albumin polymer that had been prepared in a buffered solution. In this scheme, the attachment of the protein to the nanoparticles is through the formation of a thiourea group between the amino terminus of the protein and the isothiocyanate group of the polymer.

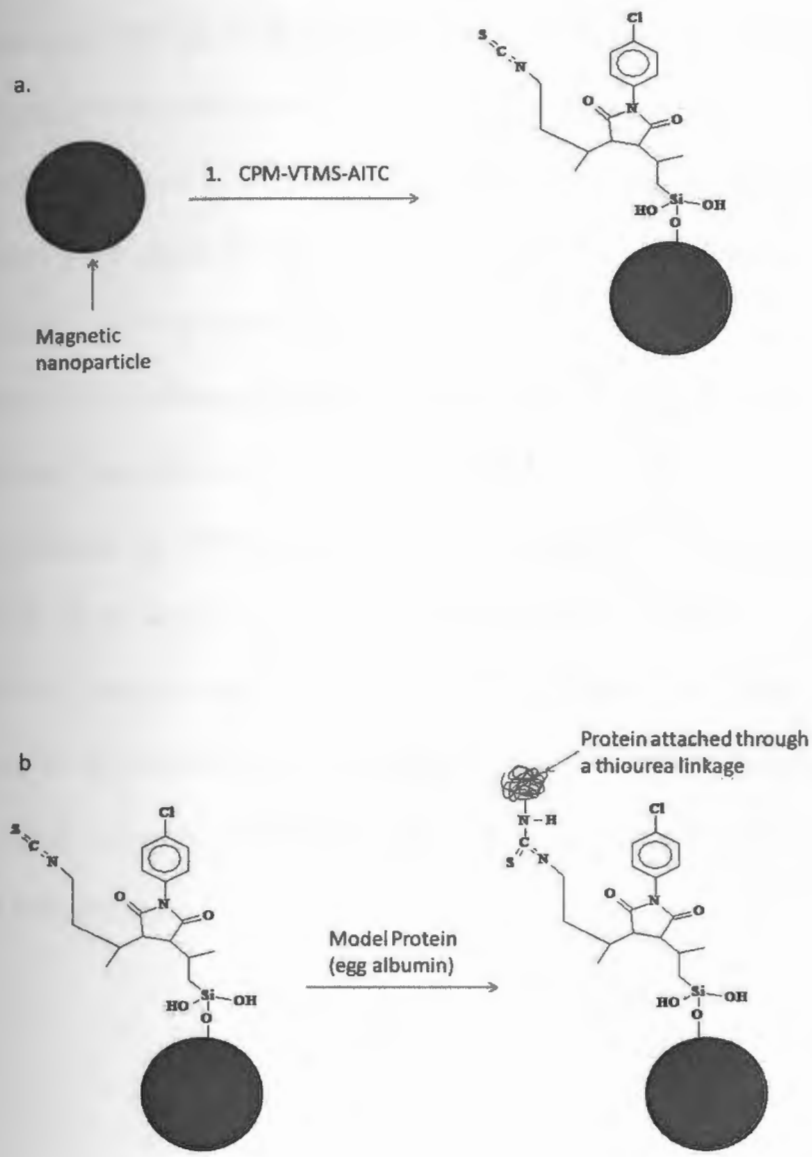

Figure 4.3 a. Modification of iron oxide nanoparticle with the polymer (NPM-VTMS-AITC). 4.3 b. Shows the attachment of the model protein to the polymer-modified iron oxide through the formation of a thiourea.

The amino terminal group allows for the attachment of the protein to the nanoparticles through the formation of an amide or urea linkage depending upon the linker group employed to anchor the protein. The purpose of the isocyanato group is to allow the attachment of the protein via urea linkages. The schematics present as Figure 4.4 a and 4.4 b show the functionalization of the iron oxide nanoparticle. In 6a, the nanoparticle is first modified with aminopropyltrimethoxysilane followed by the addition of 1,6-diisocyanatohexane which resulted in the change of color of the precipitate from blackish-brown to brownish-yellow. The functionalization step was also confirmed by FTIR spectroscopy. In this scheme, one of the isocyanato groups can link to the amino group of the aminopropyltrimethoxysilane, while the other isocyanato group is free for attachment to the protein. Schematic 4.4 b shows the attachment of the model egg albumin protein to the surface. The amino-terminus of the protein can react with the terminal isocyanato group through the formation of a stable urea-linkage.

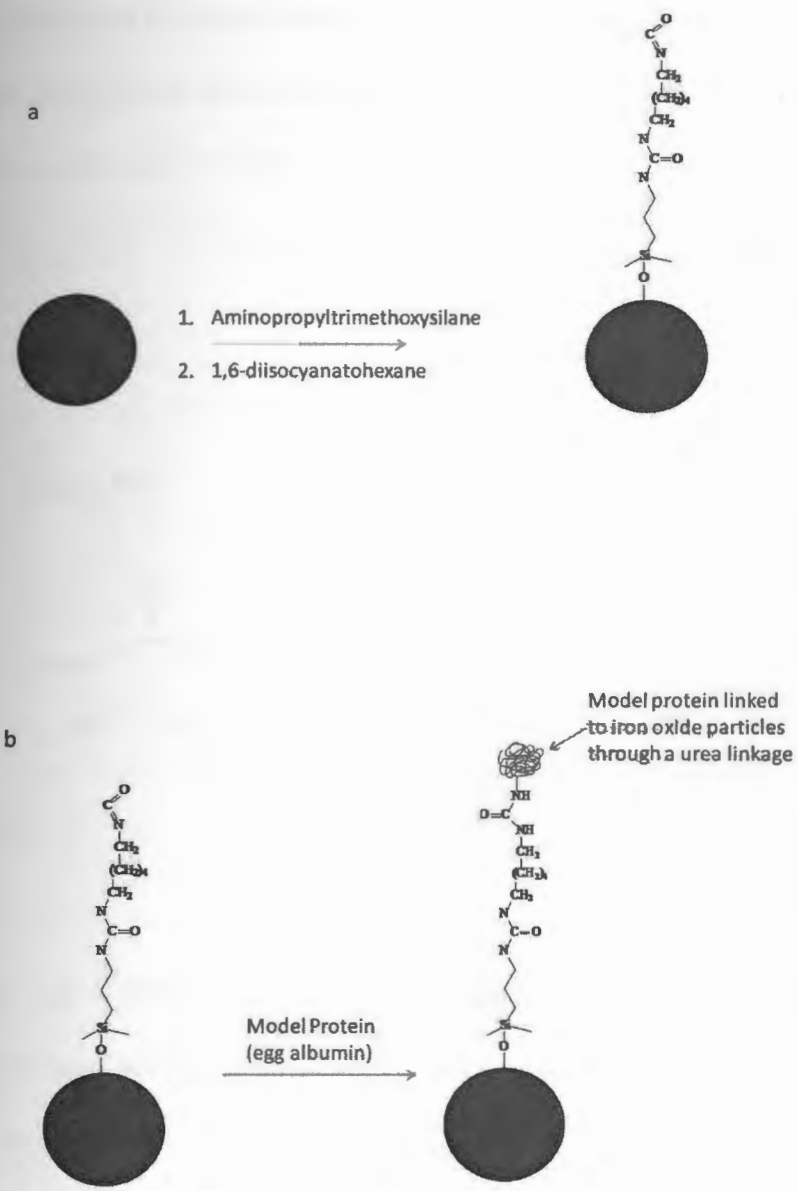

Figure 4.4 a. Iron oxide modification with aminopropyltrimethoxysilane and 1,6-diisocyanatohexane. 4.4 b show the attachment of the model protein through the formation of a urea-linkage.

Subsequent to protein modification, the nanoparticles were collected and analyzed further by FTIR and fluorescence spectroscopy to confirm the biofunctionalization of the iron oxide nanoparticles.

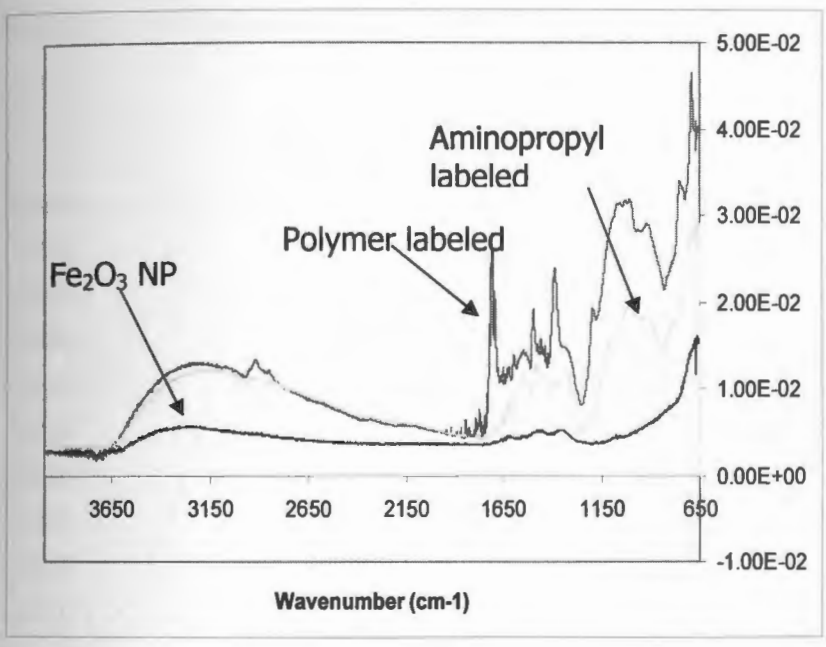

Figure 4.5 - FTIR spectra of iron nanoparticles, nanoparticles coated with polymer and with aminopropyltrimethoxysilane. The peak centered at ~ 1700 cm^{-1} is consistent with the carbonyl peaks of the maleimide in the polymer, confirming polymer modification.

Figure 4.5 is the FTIR spectra of the native iron oxide particle and also the modified iron oxide nanoparticles. In the spectrum of the polymer modified nanoparticle, the peak centered at approximately 1700 cm^{-1} is consistent with the carbonyl peak of the maleimide group of the polymer. This peak is taken as confirmation of the polymer modification of the magnetic nanoparticle.

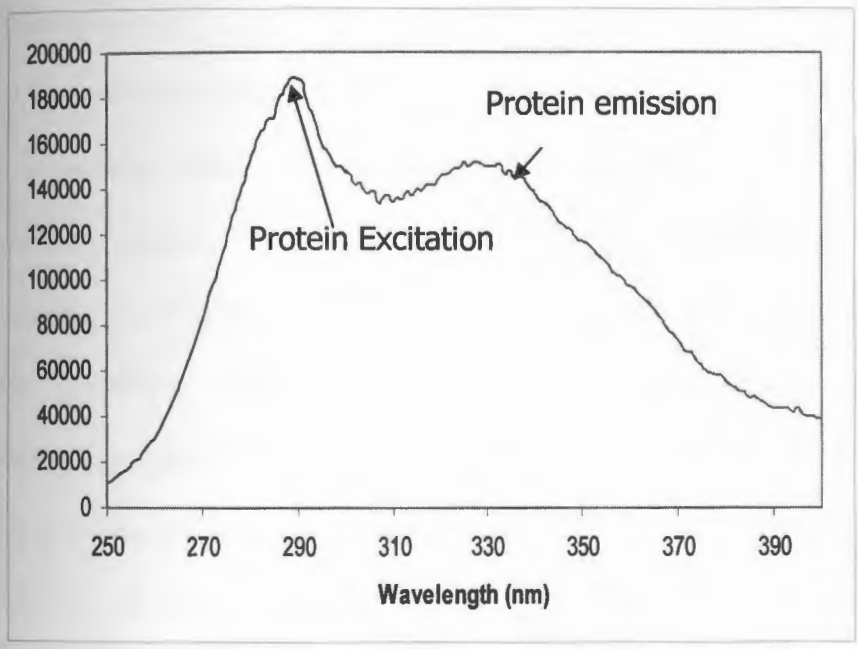

Figure 4.6 - Fluorescence from egg albumin functionalized iron nanoparticles. The nanoparticles had been coated with polymer before protein attachment.

Figure 4.6 is a fluorescence spectrum of the functionalized nanoparticle with the attached egg albumin. The fluorescence peak for protein at 330 nm is evidence that the protein was successfully labeled to functional ends of the magnetic nanoparticle. This peak which is associated with fluorescence from the tryptophan moiety of the

protein is also evidence of the fact that the proteins are not denatured under the modification conditions. In the even of protein denaturation this peak is typically red-shifted. In this case we feel that this finding is due to the cushion-like layer of the polymer that protects the protein from the surface of the nanoparticle. It should be noted that we have control over the thickness of the polymer layer by controlling the modification chemistry as well as the time of exposure of the nanoparticle to the polymer solution.

In the Bioferrograph biofunctionalization studies it was necessary to determine an appropriate ratio of isocyantopropyltrimethoxysilane to the protein to obtain a satisfactory signal. To accomplish this study the model protein (egg albumin) labeled with dansyl chloride was employed. Here, 3 separate 10 mL batch of ferromagnetic fluid particles was stirred with volumes of 1, 2 and 3 mL of [redacted]yantopropyltrimethoxysilane for 1 hour. These blends gave ratios of 10:1, 10:2 and 10:3 respectively. Subsequently, each batch of particle was collected and stirred with 1mL of dansyl-labeled egg albumin and stirred for 30 minutes. It was found in this study that the 10:3 ratio particles gave the most intense fluorescence signal. The increased signal scales with increasing ratio and is likely due to the increase in the number of reactive groups on the surface of the particles allowing for more efficient capture of the protein. Due to this finding all subsequent studies were performed using this 10:3 ratio. Figure 4.7 is the spectra collected after the danysl chloride-labeled egg albumin was exposed to the magnetic particles prepared at different ratio. The 10:3 ratio gives a much more intense signal. All spectra were collected for the particles suspended in 1X PBS buffer.

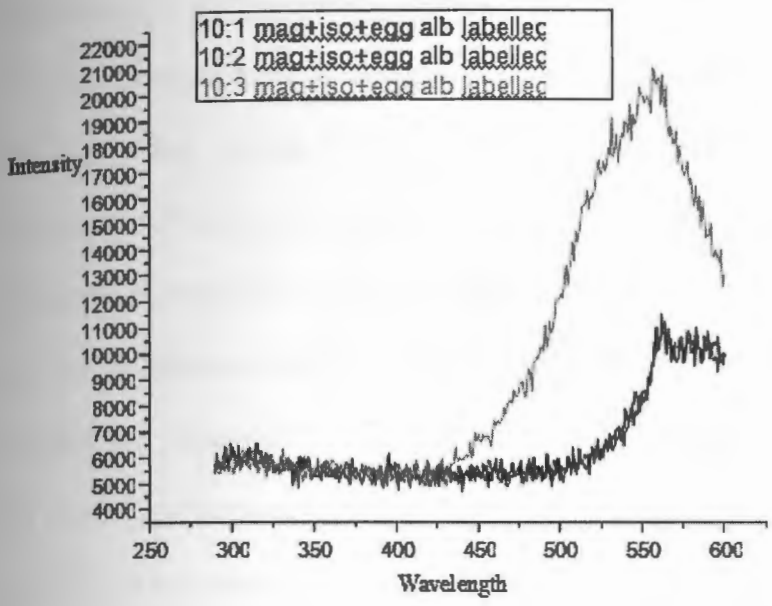

Figure 4.7: The 10:3 ratio of magnetic particles with isocyanato showed good signal of dansyl peak of egg albumin.

BioFerrography Experiment:

After the ferrography experiment is complete the cassette is disassembled and the glass substrate is collected and the magnetic particles adhered to the glass substrate is dried under vacuum using a pressure of 25 -30 inches of mercury. After the particles are dried they are then scraped from the glass substrate and resuspended in 1X PBS solution. These samples are then introduced into the fluorimeter and excited at the appropriate wavelengths.

The wavelengths chosen to excite the samples depended on the particular species being analyzed. In most cases the particles were excited at 280nm to look for

the presence of a protein peak. In the event the protein is attached a fluorescence peak centered around 330nm is observed indicative of a native (undenatured) protein. In the case when testing for the presence of the danysl chloride peak used to functionalize the egg albumin, an excitation peak of 340 nm is employed. It should be noted that in cases where dansyl chloride is present, if the protein peak is exited at 280 nm, the fluorescence from the danysl chloride is observed due to the energy transfer between the protein and dansyl chloride to the overlap between the emission peak of the protein and excitation peak of the dansyl chloride. When probing for the presence of FITC, an excitation wavelength of 480 nm is employed.

In the first experiment conducted in Port 1, the magnetic nanoparticles had been functionalized with the antigen IgG followed by exposure to the antibody anti-IgG. Fluorescence spectrum (data not included) collected from this sample however, revealed no presence of a FITC signal. However when the experiment is conducted in the solution phase, there is clear evidence of the binding event. Below Figure 4.8 is the fluorescence spectrum collected for the same experiment conducted in the solution phase using 1X PBS. Here the magnetic particle that had been functionalized with [redacted]yanatoproypyltrimethoxysilane followed by IgG and then anti-IgG. In this experiment the binding event is evident between the IgG and the anti-IgG as indicated by the FITC signal centered at 520nm after excitation at 480nm. The likely explanation for the lack of signal from the sample scraped from the ferrography substrate is due to the short exposure time of the sample to the anti-IgG solution. As mentioned previously a flow rate of 0.5mL/min was employed, which was likely not enough time for such a highly specific recognition event to be observed.

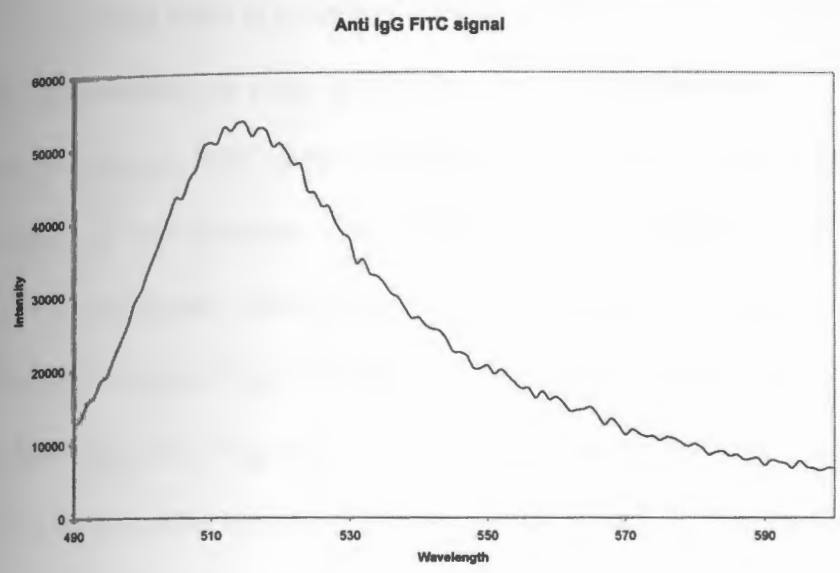

Figure 4.8: Binding Event confirmed by IgG and Anti IgG with the FITC signal centered at 520nm after excitation at 480nm.

The experiment conducted in Port 2 of the ferrograph was IgG-functionalized magnetic nanoparticles that was subsequently exposed to dansyl chloride-labeled egg albumin. In this experiment when the magnetic particles are collected from the ferrograph and analyzed by fluorescence spectroscopy there was evidence of a binding event as indicated by the fluorescence peak at approximately 580 nm as seen in the spectrum below. In this particular case an excitation of 280 nm was employed which excited the protein, leading to the fluorescence and subsequent energy transfer to the dansyl chloride moiety which explains the 580nm peak. It should be noted that the observe peak at 580 nm is much higher than that expected for the dansyl chloride moiety, however, this is undoubtedly due to solvent effects.

While there is a binding event evident in this particular experiment as evident by the fluorescence peak, it is unclear whether this binding is a result of non-specific binding to IgG (very unlikely) or due to any unreacted isocyanato groups still on the surface of the particles. The latter seems far more likely due to the fact that the isocyanato groups shows no preference for any particular protein to which it binds. Further studies are underway to discern the nature of this binding. It is very likely that a blocking step using a small amine after exposure to the IgG will solve the problem of this unwanted binding as the amine group will bind to any unreacted isocyanato groups rendering them deactivated.

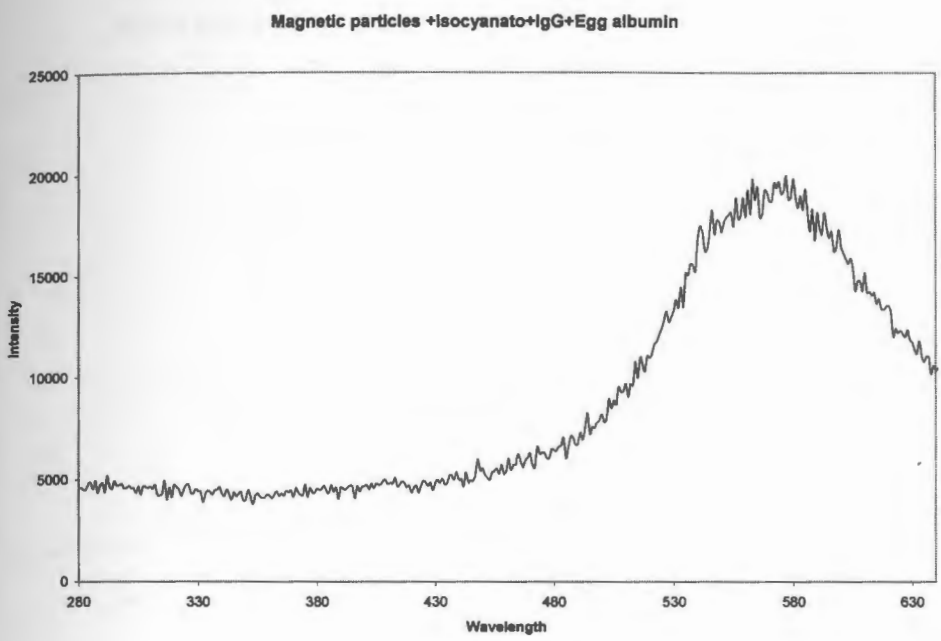

Figure 4.9: Excitation at 280nm excited the protein leading to energy transfer to the dansyl chloride moiety observed around 580nm.

The experiment in Port 3 involved the IgG functionalized magnetic nanoparticle followed by exposure to a mixture of the FITC-labeled anti-IgG and the dansyl chloride-labeled egg albumin. The spectrum collected below is the solution phase version of this experiment. In this case the sample is excited at 280 nm which is selected to selectively excite the protein. In the event there is any dansyl chloride moieties present there will be energy transfer from the protein to dansyl and lead to a fluorescence spectrum. It should be noted that when the sample was scraped from the glass substrate from the ferrograph, there was no detectable signal. This again is likely due to an insufficient amount of exposure time during the run.

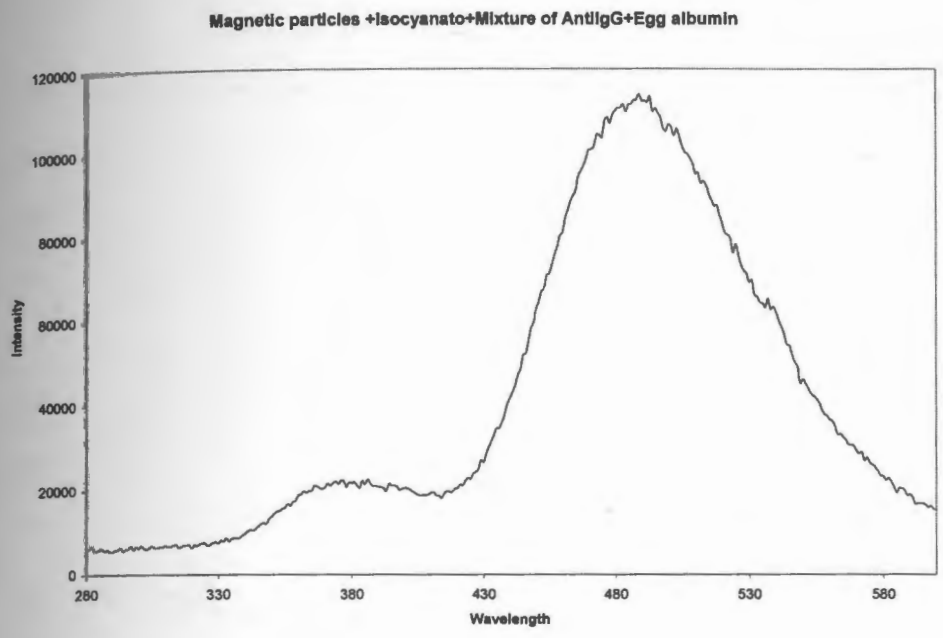

Figure 4.10: Sample excitation at 280nm excite the protein and energy transfer from protein to dansyl chloride is observed around 480nm.

The experiment in Port 4 was the magnetic nanoparticles that had only been functionalized with isocyanatopropyltrimethoxysilane but with no IgG. This port was subsequently exposed to a mixture of anti-IgG and egg albumin. Aim was to determine if there is any binding between the proteins, particularly the anti-IgG. The spectrum of the sample collected from the ferrograph cassette showed no evidence of binding of either the egg albumin or anti-IgG. This finding is likely due to the short exposure time of the protein solution to the sample.

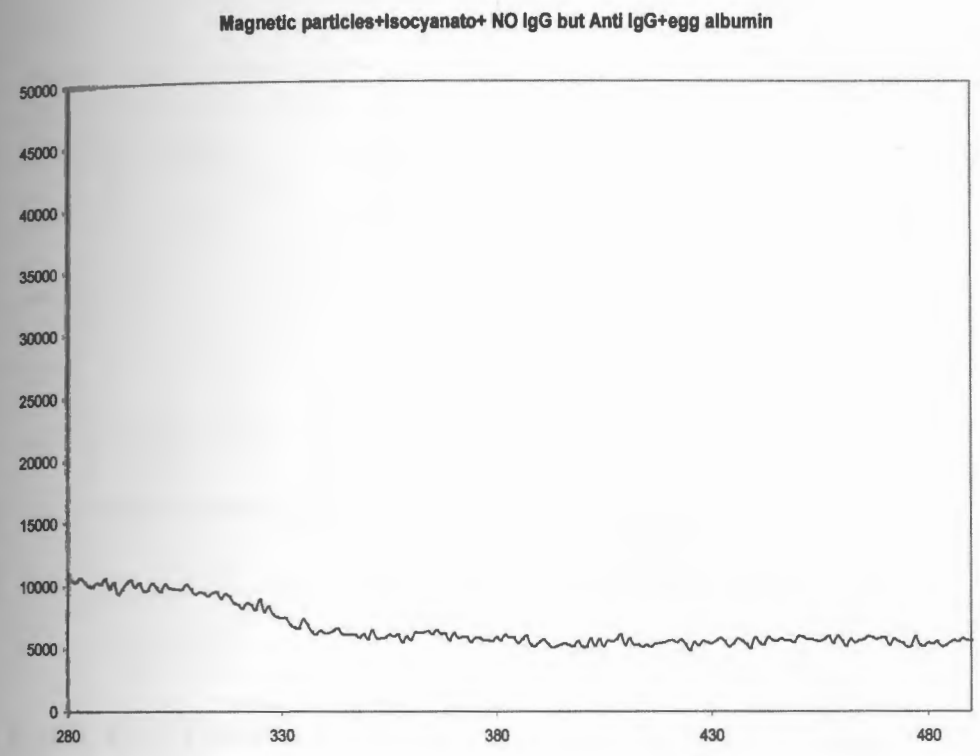

Figure 4.11: No signal of FITC and Dansyl Chloride confirms there is no binding of the proteins with functionalized magnetic nanoparticles without IgG.

The control experiment conducted in Port 5 involved the use of the plain unfunctionalized magnetic nanoparticles. This port was then exposed to the mixture of anti-IgG and egg albumin. In this case the fluorescence spectrum revealed no fluorescence peak as expected. This finding is consistent with the fact that there is no group capable of binding the protein to the surface of the magnetic nanoparticles. Below is the fluorescence spectra taken of the sample collected from the cassette of the ferrograph.

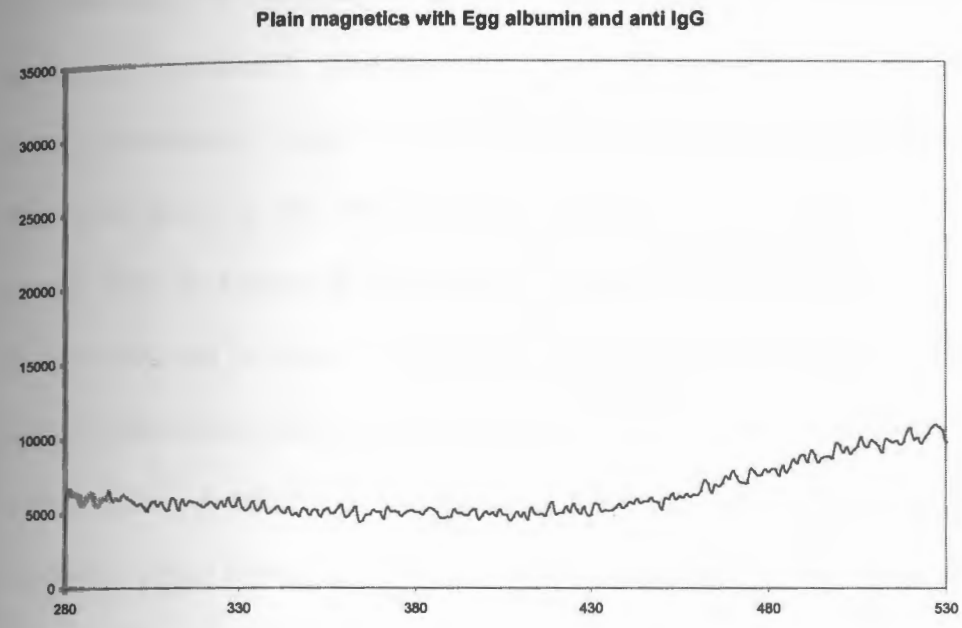

Figure 4.12: Confirms no binding of the protein to the surface of the magnetic nanoparticles.

CONCLUSION

In this work we have demonstrated facile methods for the preparation of biofunctionalized magnetic iron oxide nanoparticles. In one method we first modify the surface of the nanoparticle with aminopropyltrimethoxysilane followed by the addition of 1,6-diisocyanatohexane. In this route, the surface is modified to present a distal isocyanato group that can link to an amino group of a protein through the formation of a urea linkage. In the second route we have synthesized a novel terpolymer that present trimethoxysilane functionalities that facilitate direct attachment to the surface of the nanoparticle and also isothiocyanato groups that are used to anchor the protein through formation of a thiourea. Spectral data confirm the

modification of the nanoparticle and fluorescence spectroscopy was used to confirm the protein attachment. The fluorescence from the protein showed no evidence of protein denaturation based upon the peak position of the tryptophan group. This finding we feel to be associated with polymer providing a cushion layer separating the protein from the surface of the nanoparticle. The simple modification steps presented in this work can be used to selectively/specifically modify these nanoparticles for specific applications, where a specific antibody can be attached to the nanoparticle that will facilitate it attaching to a specific target for imaging and/or quantification purposes. Using Bioferrograph for biofunctionalization studies we observed some solvent effects and non-specific adsorption. In other work currently underway is to allow the functionalized magnetic particles to flow at a very low flow rate to allow sufficient time for efficient binding. And an approach to block the several active sites offered by surface functionalization such as by using ethylamine to prevent protein adsorption.

References

1). Lee, H.; Lee, E.; Kim, D. K.; Jang, N. K.; Jeong, Y. Y.; Jon, S. Antibiofouling Polymer-Coated Superparamagnetic Iron Oxide Nanoparticles as Potential Magnetic Resonance Contrast Agents for in Vivo Cancer Imaging. *J. Am. Chem. Soc.* **2006**, *128*, 7383-7389.

2) .Latham, A. H.; Williams, M. E. Controlling Transport and Chemical Functionality of Magnetic Nanoparticles. *Acc. Chem. Res.* **2008**, *41*, 411-420.

3) .Ito, A.; Shinkai, M.; Honda, H.; Kobayashi, T. Medical Application of Functionalized Magnetic Nanoparticles. *Journal of Bioscience and Bioengineering* **2005**, *100*, 1-11.

4) .Gu, H.; Xu, K.; Xu, C.; Xu, B. Biofunctional Magnetic Nanoparticles for Protein Separation and Pathogen Detection. *Chem. Commun.* **2006**, 941-949.

5) .Shukoor, M. I.; Natalio, F.; Therese, H. A.; Tahir, M. N.; Ksenofontov, V.; Panthöfer, M.; Eberhardt, M.; Theato, P.; Schröder, H. C.; Müller, W. E. G.; Tremel, W. Fabrication of a Silica Coating on Magnetic γ-Fe2O3 Nanoparticles by an Immobilized Enzyme. *Chemistry of Materials* **2008**, *20*, 3567-3573.

6) .Matyjaszewski, K.; Xia, J. Atom Transfer Radical Polymerization. *Chem. Rev.* **2001**, *101*, 2921-2990.

7) .Wang, D.; He, J.; Rosenzweig, N.; Rosenzweig, Z. Superparamagnetic Fe2O3 Beads−CdSe/ZnS Quantum Dots Core−Shell Nanocomposite Particles for Cell Separation. *Nano Letters* **2004**, *4*, 409-413.

8) .Zhou, Y.; Wang, S.; Ding, B.; Yang, Z. Modification of Magnetite Nanoparticles Via Surface-Initiated Atom Transfer Radical Polymerization (ATRP). *Chem. Eng. J.* **2008**, *138*, 578-585.

9) .Smith, J. E.; Medley, C. D.; Tang, Z.; Shangguan, D.; Lofton, C.; Tan, W. Aptamer-Conjugated Nanoparticles for the Collection and Detection of Multiple Cancer Cells. *Anal. Chem.* **2007**, *79*, 3075-3082.

10). Meyer, D. M.; Tillinghast, A.; Hanumara, N. C.; Franco, A. Bio-Ferrography to Capture and Separate Polyethylene Wear Debris from Hip Simulator Fluid and Compared with Conventional Filter Method. *Journal of Tribology* **2006**, *128*, 436-441.

11). Meyer, D. M.; Hanumara, N. C.; Tillinghast, A.; Franco, A. In *In Polyethylene wear debris from hip simulator fluid captured and separated using bio-ferrography;* 2004 ASME/STLE International Joint Tribology Conference; American Society of Mechanical Engineers, New York, NY 10016-5990, United States: Long Beach, CA, United States, 2004, pp 1755-1763.

12). Michael Giersig, Michael Hilgendorff, Magnetic Nanoparticle Superstructures; European Journal of Inorganic Chemistry, 2005, 18, 3571-3583.

13). P. Stephen Williams, Francesca Carpino., Maciej Zborowski., Magnetic Nanoparticle Drug Carriers and their study, Molecular Pharmaceutics., 2009, 6(5), 1290-1306.

14). Q A Pankhurst, J Connolly, S K Jones and J Dobson., Applications of Magnetic Nanoparticles in Biomedicine, Journal of Applied Physics., 36, 2003.

15). Magnetic Nanoparticle Metrology, Material and Science Engineering Laboratory, 2006.

16). Science News., Magnetic Nanoparticles Assemled into long chains., Science Daily, Oct 23, 2005.

17). Ganesan Balasundaram, Thomas J Webster., Applications of Magnetic Nanoparticles., Materials Research Society, 2005.

18). Misra, R.D.K., Magnetic nanoparticle carrier for targeted drug delivery: perspective, outlook and design., Materials Science and Technology, Volume 24, Number 9, September 2008 , pp. 1011-1019(9).

19). Boris Polyak, Ilia Fishbein, Michael Chorny, Ivan Alferiev., High field gradient targeting of magnetic nanoparticle-loaded endothelial cells to the surfaces of steel stents., Proceedings of National Academy of Sciences., 105, 698-703, 2008.

20). Stuart C McBain, Humphrey HP Yiu, Jon Dobson., Magnetic Nanoparticles for Drug Delivery., Dove press, 2009, Volume 4.

21). Tetsuya Osaka, Tadashi Matsunaga, Takuya Nakanishi, Atsushi Arakaki, Daisuke Niwa and Hironori Iida., Synthesis of Magnetic Nanoparticles and their applications in bioassays ., Analytical and Bioanalytical Chemistry, 384, 2006.

22). Magnetic Nanoparticles helps in detecting cancer., Nanotechnology Development News., June 2008.

CHAPTER 5

Surface Modification of Microfluidic Devices

ABSTRACT

The goal of the project presented in this chapter is the development of novel and facile ways of functionalizing microfluidic systems for bioanalysis. Functionalization is achieved by employing a variety of silane-based materials, primarily copolymer that are prepared in-house that can be used to tailor the structural, physical, and chemical properties of the device. In addition to polymeric materials, surface modification with silica nanoparticles and *in-situ* monolith preparation appears to be a promising avenue to provide an excellent interface to increase the surface roughness and area within the device, as well as serving as an inert site for attachment of the biological entities being employed in these systems. In this work we describe the biofunctionalization of microfluidic chips using facile surface modification schemes. In one instance, an antigen (bovine IgG) is attached to the surface modified microfluidic chip via urea linkage and successful binding of antigens and antibodies is observed. Preservation of the bioactivity is evident based upon the observed binding activity as indicated by the detected fluorescence signal within the chip after the binding event of the labeled antibody (bovine anti-IgG) captured by the antigen within the channel. This study can be extended for a high-throughput system for bio-marker proteins.

INTRODUCTION:

Miniaturized instrumentation and reactors have attracted great interest in the last decade. The first reported use of a microchip was in 1979, when a gas chromatograph air analyzer was fabricated on a silicon wafer. It was not until several years later, when flow injection analysis was performed on a chip, that microchips gained attention. Over the last decade, research in integrated microfluidic devices (which are typically referred to as lab-on-a-chip devices or micro total analysis systems [μTAS]) has expanded to include sample preparation, fluid handling, microreactors, separation systems, cell handling, and cell culturing. The incorporation of these techniques has led to microfluidic devices that have been used to perform capillary electrophoresis-based separations, magnetic microparticle-based separations, immunoassays, DNA analysis, and clinical diagnostics, along with the design of highly efficient microreactors. They have been applied in medical analysis, environmental monitoring, biochemical analysis, and microchemistry[1].

Microfluidics is the science of designing, manufacturing, and formulating devices and processes that deal with volumes of fluid on the order of nanoliters (10^{-9} liter) or picoliters (10^{-12} liter). The devices themselves have dimensions ranging from millimeters (mm) down to micrometers.

Microfluidics – a multidisciplinary field involves the formation of micron sized channels, electrodes, wires and other novel features in chemically-resistant wafers. Fluids are then introduced into the channels and moved to regions of the wafer that perform functions such as mixing, filtering, reaction, product separation and analysis. Thus, the devices automate and integrate many steps that are currently

performed in distinct, time-consuming steps by skilled and expensive laboratory technicians[2].

Advantages of such systems include high performance, design flexibility, reagent economy, miniaturization, and automation. The use of small flow channels, typically between 1 and 100 μM is important when considering the networks of microscopic channels in substrates in which analytes are transported, mixed, and separated. Miniaturization allows high-throughput screening, portability, and high-density arrays on a small scale. By decreasing the dimensions of devices, space, time, and the amount of analyte decrease. Smaller apparatuses are lower in cost, consume less energy and material, and are minimally invasive when referring to a biological application. The use of less material is protecting our limited resources and the disposability of the microdevices helps to avoid contamination. It has also been reported that microchannels can improve the speed and accuracy of chemical reactions, as well as the speed, sensitivity, and repeatability of many assays[3].

With a few exceptions, microfluidics is at an earlier stage of development for life science applications and, despite the potential, looks set to take a while to really invoke a paradigm shift [4].

Microfluidic Lab-on-a-chip Devices

The purpose of these devices is to manipulate and process solution based samples and systems by carrying out typical procedures such as mixing, heating and separation. Processed samples may be delivered to some form of detector that subsequently transmits data. These devices typically consist of a monolithic material

that is patterned with microscale channels and features such as mixers, valves, injectors and separators that can assume the role of equivalent macroscopic laboratory equipment. Appropriate connection to the macroscale world for inputs and outputs (not trivial) is required and so the microfluidic device is likely to be part of a system[4].

Typically, materials used are either glass or polymer although some hybrid silicon components may also be used. Microfluidic technology allows the reliable handling of smaller samples and provides greater control over a process with increased safety. True lab-on-a-chip devices would also incorporate some means of detection thus providing a 'reagents in – data out' apparatus although the material output of processed reagents may be desired[4]. The use of microfluidic devices is making rapid inroads in the modern analytical laboratory, primarily because of their small physical footprint, speed and efficiency of chemical separations, and reduced reagent consumption[5].

Materials Employed in Making of Microfluidic Devices:

Traditionally, lab-on-a-chip devices have been manufactured in silica due to its well understood surface chemistry and favorable micromachining techniques that are ubiquitous in the microelectronics industry. These techniques are typically based on silica etching which is time consuming, requires specialized resources, and utilizes a large amount of chemical solvents that pose unique safety and environmental hazards. Recently researchers have begun to utilize devices fabricated from polymer substrates as an alternative to glass. Reasons include reducing the total cost and the ability to tailor physical and chemical properties which may include surface roughness, surface

charge, optical clarity, and tensile strength. For example, polymer substrates typically have greater impact resistance than glass and when one considers mass production, the cost of polymer substrates are a fraction of the cost of glass which leads to a large amount of savings. The past two decades have seen rapid advancement of Lab on a Chip (LOC) system with applications ranging from gas chromatography to capillary electrophoresis, and more recently to high-pressure chemistry and single cell analysis. For many applications in clinical medicine, biology and chemistry, silicon and glass may still be the preferred materials. The mechanical rigidity, chemical resistance, and low permeability properties of silicon and glass, combined with the optical transparency of glass, make them a good choice for many demanding LOC applications. The large and well developed silicon and glass micromachining toolbox provide the capability to obtain microstructures with high precision and repeatability. In addition, scaling device dimensions down to the nanometer scale is relatively straight forward using silicon and glass micromachining, which is important for emerging fields, such as nanofluidics and nanosensing[5].

However, some of the advantages of using polymers are negated by the traditional microfabrication techniques used to manufacture metal or silicon molds which are subsequently utilized to fabricate polymer devices by imprinting or injection molding. The primary negative associated with manufacturing molds in the laboratory by traditional methods is the time commitment for the production of the original mold and the inability to modify the mold. This proves to be costly and time consuming. In a research and development environment it is important that researchers have access to fabrication techniques that are rapid and easily implemented with a variety of

substrates. In addition it is important that changes in the fluidic circuit be implemented with minimal cost and limited time investment[5].

Microfluidic devices can perform multiple laboratory functions on a single, compact, and fully integrated chip. However, fabrication of microfluidic devices is difficult, and current methods, such as glass-etching or soft-lithography in PDMS, are either expensive or yield devices with poor chemical robustness. Hence a simple method that combines the simple fabrication of PDMS with superior robustness and control of glass was developed by Researchers Keith E. Herold and Abraham Rasooly, Dept. of Bio-Engineering, University of Maryland. They coat PDMS channels with a functionalized glass layer. The glass coating greatly increases the chemical robustness of the PDMS devices. As a demonstration, they produce emulsions in coated channels using organic solvents. The glass coating also enables surface properties to be spatially controlled. As a demonstration of this control, they spatially pattern the wettability of coated PDMS channels and use the devices to produce double emulsions with fluorocarbon oil[5].

The use of thermoplastic polymers as microfluidic substrates is a robust and growing area of research, with important implications for the development of low cost disposable microfluidic devices for a host of bioanalytical applications. Substrate bonding is a critical step required for the formation of sealed microchannels within thermoplastic chips. Unlike silicon and glass, the diverse material properties of thermoplastics opens the door to an extensive array of substrate bonding options, together with a set of unique challenges which must be addressed to achieve optimal sealing results[5].

While the use of glass or hard plastic is still employed in the design of microfluidic devices, many researchers have turned to poly dimethylsiloxane (PDMS), a rubbery material also used to make soft contact lenses as an alternative. According to Whitesides, who heads one of two groups that first worked with the polymer, "PDMS has become a popular choice for microfluidic device fabrication for its ease of use"[6].

In certain instances, glass is the most popular material employed for the fabrication of microchip such is the case when designing electrophoresis-based devices. This choice is primarily due to the similarity of the glass surface to that of fused-silica capillaries. In addition, glass has many other positive attributes for microchip electrophoresis applications, including good mechanical and optical properties, high electrical insulation, and low chemical reactivity. Glass microchips are usually fabricated using classical photolithography combined with wet chemical etching .Some disadvantages of glass chips are that they are expensive and relatively difficult to fabricate. Production of these chips requires access to a clean room and the use of corrosive etching solutions. In addition, the thermal bonding technique which is often used in the fabrication of glass microchips is time-consuming and often irreproducible[7]. Glass and hard plastics are easy to break and hard to etch and bond. Glass, however, being susceptible to breakage, cracking, scratching and chipping, is a difficult material to process and handle. Bonding of glass plates can also be achieved at room temperature 20^0C. This is based on hydrogen bonding at the glass interface, which has been achieved only after rigorous cleaning. And also during sealing of glass plates leads to thermal degradation of a chemically modified layer[6].

The above outlined disadvantages related to glass microfabrication procedures have led scientists to investigate alternative materials for microchip fabrication. In particular, the production of microfluidic devices using polymeric substrates has generated significant interest due to their superior biocompatibility, greater flexibility, reduced cost, and ease of processing[8]. Additional advantages of polymers are that they are inexpensive, large numbers of microdevices can be fabricated from a single master, and the production of these devices does not require a clean room environment[7]. PDMS is the most popular polymer for microfluidic applications. It is elastomeric, inexpensive and possesses good optical clarity. Another significant advantage of PDMS is its ability to generate a tight seal to itself or other flat surfaces, reversibly or irreversibly, without distortion of the microchannels. An essential element of PDMS prototyping is the fabrication of a master template. This master is commonly fabricated in photoresist (such as SU-8), silicon, or nickel[7]. Disadvantages of PDMS include its hydrophobicity, which can lead to analyte adsorption. PDMS is just very easy to work with. There's a very simple procedure to go from design to master to mold, and you can seal the layers together almost effortlessly. A rubbery elastomer, PDMS won't break if dropped. It also breathes, so gases can exchange with the environment beyond the chip, while the material's springiness enables pneumatic control[3].

Applications of Microfluidic devices:

Microfluidic systems have diverse and widespread potential applications. Some examples of systems and processes that might employ this technology include

inkjet printers, blood-cell-separation equipment, biochemical assays, chemical synthesis, genetic analysis, drug screening, electro chromatography, surface micromachining, laser ablation, and mechanical micro milling. Not surprisingly, the medical industry has shown keen interest in microfluidics technology[9].

Lab-on-a-chip (LOC) technology has the potential to greatly simplify analytical analysis by providing a platform for chemical and biochemical reactions as well as the analysis of such reactions without a laboratory. Another advantage of performing the reactions in a microfluidic device is the large surface area-to-volume ratios in the chip[7]. The benefits of microfluidics experienced by R&D chemists are now being extended to R&D biologists involved in life science technologies such as genomics, proteomics, high throughput screening and molecular diagnostics[10]. Microfluidics has facilitated major biochemical application advancements in point-of-care diagnostics, bioterrorism detection, and drug discovery. There are numerous potential applications in biotechnology, pharmaceuticals, the life sciences, defense, public health, and agriculture. Microfluidic lab-on-a-chip (LOC) technologies represent a revolution in laboratory experimentation, bringing the benefits of miniaturization, integration, and automation to many research-based industries[11].

Microfluidic devices have a broader range of applications than DNA microarrays as they can be used for applications that include: chemical reactions (e.g. microreactors), biological assays, sample preparation, sample purification, sample analysis and diagnostics.

There are a number of reasons for the slow progress of microfluidic devices for life science applications. From a user's point of view, awareness of the technology

requires further effort and microfluidics currently represents a different and novel way of doing things which creates potential difficulty of translating day-to-day activities to these new systems and a poor understanding of the benefits that can be realised. Only by a growing experience of these technologies can the scope and limitations of these technologies be understood and exploited. There is some uncertainty with the choice between standardized products and the use of bespoke devices that are designed specifically for a particular function. Whereas the first are cheaper and more versatile, performance is compromised. Performance is not an issue with the second but bespoke devices would require a good understanding of what is to be achieved (only possible with experience) and will be more expensive and less versatile. Integrating detection into a lab-on-a-chip device may result in the introduction of detection techniques that are not in standard use which may take time to be adopted by users. Some routine analytical techniques cannot be integrated into a lab-on-a-chip device due to technical or cost issues [12].

The benefits of microfluidics are reduced reagent consumption, improved accuracy and control, and the prospect of automated high throughput screening and optimization. Although the field of microfluidics is still very much in its infancy, the keen interest currently being shown in this field can only help to drive this technology forwards to enable potential productivity improvements in drug discovery to be realised[13].

From a supply point of view, there continues to be a proliferation of technical solutions and microfluidic components that serve to increase choice (and confuse) but few of which have been proven in real applications or manufacturing environments.

Each of these developments is typically a component or part of a required solution and more effort is required to integrate these components into functional devices and move from proof of concept to prototype. With respect to manufacturing, microfluidic devices often use processes that originate from the semiconductor industry which seeks high volume 'killer' applications for cost competitiveness. The desire for a high volume killer application is at odds with the life science microfluidics market which is likely to be typified by a large number of modest volume markets with a limited product lifetime. Only diagnostic applications are likely to achieve the desired high volumes (probably polymer based) and these will only evolve fully once the lower volume applications have resulted in an adequate understanding of biological systems[14].

The current use of robotic laboratory systems in conjunction with microtitre plates is well established and ongoing incremental developments allow this incumbent paradigm to remain competitive. Only when microfluidics offers a distinct and proven advantage over these solutions can they start to be replaced[15].

A glass surface is hydrophilic, meaning it attracts water. This is often an advantage when working with glass microfluidic chips, but in certain applications you would need the surface to be hydrophobic or modified with a coating that prevents adsorption of small molecules[16].

In drug development, for instance, compounds can be screened using microfluidic chips. In order to prevent compounds to stick in the channel, a coating should be applied to the channel walls.

To have different application of PDMS in micro fluidics and bioengineering, it is necessary to modify the PDMS surface nature to improve wetting characteristics, have control in nonspecific binding of proteins and cells, and increase adhesion. The surface grafted by water-soluble polymer chains is highly resistant to protein adsorption and this is important for suppressing biofouling proteins and cell engineering and, pharmaceutics, and biotechnology. The use of poly (ethylene oxide) (PEO) or alternatively called polyethylene glycol (PEG), is very common in the above-mentioned applications for reducing nonspecific adsorption of proteins and cells[17].

The prevention of surface fouling by protein adsorption has been an elusive research goal. The current ideas in this domain assume two different directions. One focuses on correlating protein adsorption with surface properties of the PDMS. The second approach involves tailoring the molecular interactions between the adsorbing proteins and the surface.

Experimental:

Preparation of PDMS based Microchannel:

Microfluidic devices based on elastomeric materials such as polydimethylsiloxane (PDMS) are rapidly becoming a ubiquitous platform for applications in Biotechnology, Chemistry and Engineering fields. Recent growth in the field of PDMS microfluidics has far outpaced that in alternative device technologies based on glass and silicon, due in large part to significantly simpler and less expensive fabrication procedures as well as the possibility of easily incorporating integrated mechanical microvalves at extremely high densities[11]. We believe that the field of chemistry could benefit tremendously from the development of an elastomeric microfluidic device technology PDMS microfluidics with the additional feature of surface modification[11,12].

PDMS is cast from more commonly used Dow Corning Sylgard 184 contains PDMA Elastomer (Component A) and the curing agent (Component B). Sylgard is a two part resin system containing vinyl groups (Part A) and hydroxysilane groups (Part B) shown in **Scheme 5.1** below. Mixing the two resin components together leads to a cross-linked network of dimethyl siloxane groups. Because this material is flexible, it can be peeled off from the SU-8 master, leaving the master intact and ready to produce another device. Upon curing, the PDMS elastomer or pre-polymer is cross-linked by the curing agent which is a platinum-based catalyst[13, 15, 16].

Scheme 5.1: PDMS cross linking.

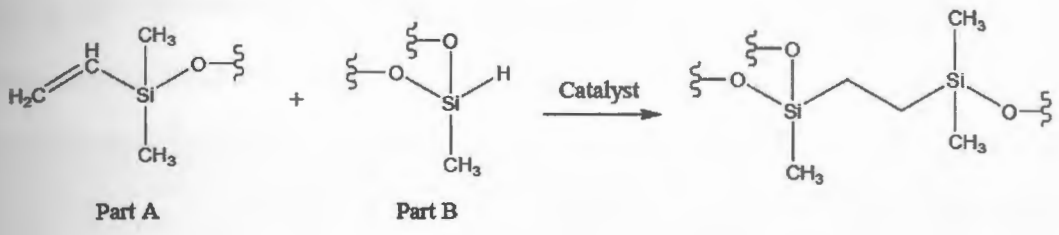

Part A Part B

Component A and B are mixed in a definite ratio (10:1) . PDMS is poured on each mold and degassed using a vacuum chamber for 15 minutes to remove air bubbles. And the molds are heated at 60^0 C for 30 minutes. Then the second layer of PDMS poured on to the same mold and degassed and heated at 60^0 C for 2.5 hours. As the baking of PDMS is done using a scalpel, cut out the required shape and peeled off the silica wafer. A biopsy punch is used is used to cut out the holes for the ports.

Activated Surface Bonding:

Using a plasma asher create plasma activation on the surface of glass, silica wafer and PDMS. A plasma asher is intended for use with RIE (Reactive Ion Etching) as well as plasma cleaning. We were able to create oxygen free radicals on the surface of glass and PDMS then place the surfaces together for a permanent bond.

After plasma ashing gently press the PDMS layers against the wafer so there are no air bubbles between the PDMS. And bake them again with the PDMS facing up at 85^0C for 80 minutes.

To ensure a better reversible seal between PDMS with glass, a mixing ratio of 20:1 used, because this produces a less rigid polymer replica. More rigid PDMS chip, the sealing to another PDMS remained good. The PDMS channel slab bonded to a

cover substrate in order to create a sealed chip. This is achieved by irreversible bonding after oxidation of the PDMS layer to create the silanol groups. The PDMS surfaces are oxidized in an O_2 plasma[6].

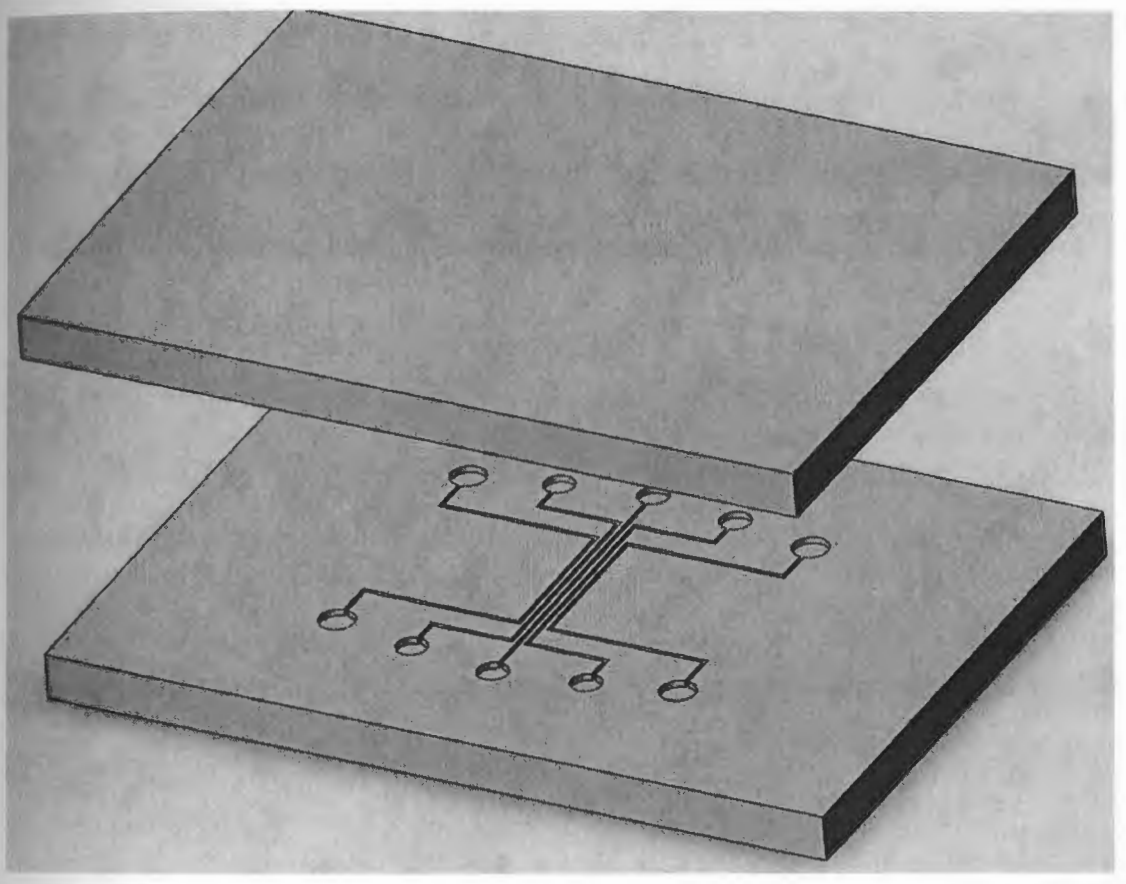

Figure 5.1: 3-D view of the microfluidic channel used for biofunctionalization studies.

Zeiss Axioplan 2 light microscope:

Zeiss Axioplan 2 Imaging system incorporates a research quality light microscope which enhances imaging capability with various filter sets. Image acquisition is achieved with the Zeiss AxioCam digital camera. Image Acquisition, processing and analysis are achieved using ZEISS AxioVision software. This

microscope is used for the examination of proteins, antigens and antibodies that are labeled with one or more fluorescent probes.

Fluorescence Spectrometer:

The fluorometry analysis was performed on Photon Technology International Spectrometer for measurements of fluorescence signals, excitation and emission spectra, and fluorescence suppression of fluorophores attached to proteins.

Typhoon Laser:

The typhoon imager offers multi-color fluorescence and provides better resolution. The machine's dual lasers and two detectors enable the investigator enables to choose from a wide range of fluorescent probes. This variable mode imager is used for automatic scanning of the fluorophores attached to proteins. The attachment of two or more fluorophores to a particular protein is confirmed.

Silica modified microchannels.

The immobilization of biological entities such as proteins, enzymes, cells is of great importance for the development of biosensors, immunoassays and bio-microfluidic devices. In this work, we study the *in-situ* bio-functionalization and cell adhesion in microfluidic channels. Here we are looking to develop a facile route to covalently anchor antibodies (bovine IgG) to the channel surface while retaining their biofunctionality[24]. In this scheme, a silica based monolith is grown directly within the channel. In order to prepare the monolith, a solution of ethanol, ammonium hydroxide

and water was prepared. A second solution of ethanol and and tetraethoxyorthosilane was added to the first solution above. These sol-gel precursors are mixed and stirred for 2 hours *ex-situ* and then injected into the microchannels and left overnight to cure.

Preparation of Bovine IgG (antigen):

Commercially available Bovine IgG of concentration 11.0mg/ml is used. The 10µl bovine IgG diluted with 10ml of 1X PBS buffer solution. And stirred in a beaker of ice for 30 min. Due to the denaturation of proteins at high temperatures, all mixing was performed under ice cold conditions.

Preparation of AntiBovine IgG labelled with Fluoro isothiocyanate (FITC):

Commercially available AntiBovine IgG of concentration 3.4 mg/ml is used. The 5µl bovine IgG diluted with 10ml of 1X PBS buffer solution. And stirred in a beaker of ice for 30 min. At room or higher temperatures protein degenerates so mixing process done in ice cold conditions.

Preparation of 3.00e-6M egg albumin solution:

0.0132g of egg albumin is dissolved in 1mL of 0.01 borate buffer with pH 8.4. This solution was subsequently stored in the refrigerator.

0.003M solution of dansyl chloride:

0.080925g of dansyl chloride is dissolved in 100 mL of Dimethylformamide.

Labelling egg albumin solution with dansyl chloride:

1 mL of 0.003M dansyl chloride solution is mixed with 1 mL of 3.00e-6M egg albumin solution and stirred for one and half hours in an aluminum foil covered vial. The mixture was stored in the refrigerator.

RESULTS and DISCUSSIONS:

As previously mentioned, the goal of this work is to develop a facile route to the modification of PDMS microfludic devices that allow for their biofunctionalization. The ability to biofunctionalize these devices opens up the possibility for the development of microdevices that can be used to rapidly and cheaply develop medically relevant devices where sample requirements can be kept at a minimum. Additionally, the ability to modify these devices in a facile manner also opens up the possibility of design coatings to prevent the biofoulding that is typically encountered in these devices.

The most reliable method to covalently functionalize PDMS is to expose it to an oxygen plasma, whereby surface Si-CH_3 groups along the PDMS backbone are transformed into Si-OH groups by the reactive oxygen species in the plasma **Figure 5.2.** These silanol surfaces are easily transformed with alkoxysilanes to yield many different chemistries as shown below in **Scheme 5.2**[17,18].

Scheme 5.2. Silanization of plasma-exposed PDMS.

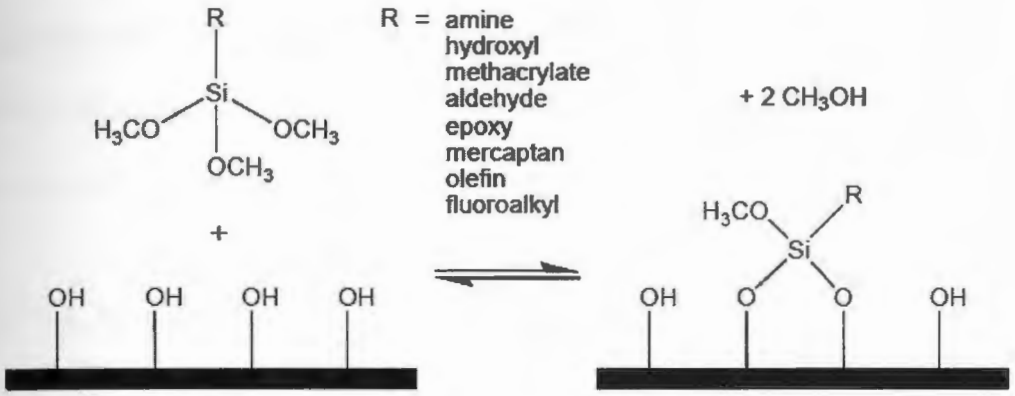

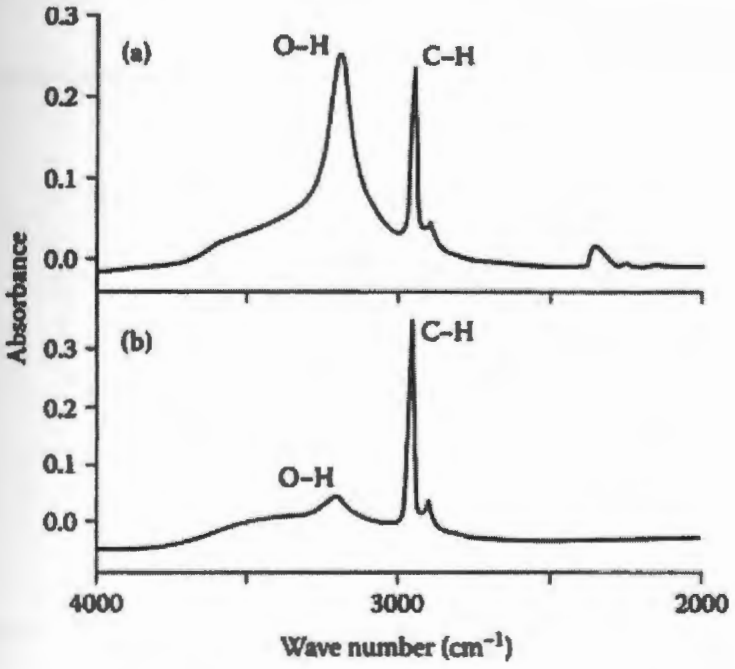

Figure 5.2: Measurement of IR Absorbance of PDMS by ATR. (a). A PDMS substrate immediately after treatment with oxygen plasma. (b) A PDMS substrate treated with an oxygen plasma and then in air for 3 hours.

Although PDMS is swollen in many organic solvents, it is unaffected by water, polar solvents (ethylene glycol) and perfluorinated compounds. It was found that non-

swelling solvents include water, nitromethane, DMSO, ethylene glycol, acetonitrile, fluorotributylamine, perfluorodecalin, and propylene carbonate. The compatibility of PDMS to other organic solvents can be improved by coating the PDMS surface by sodium silicate.[6]

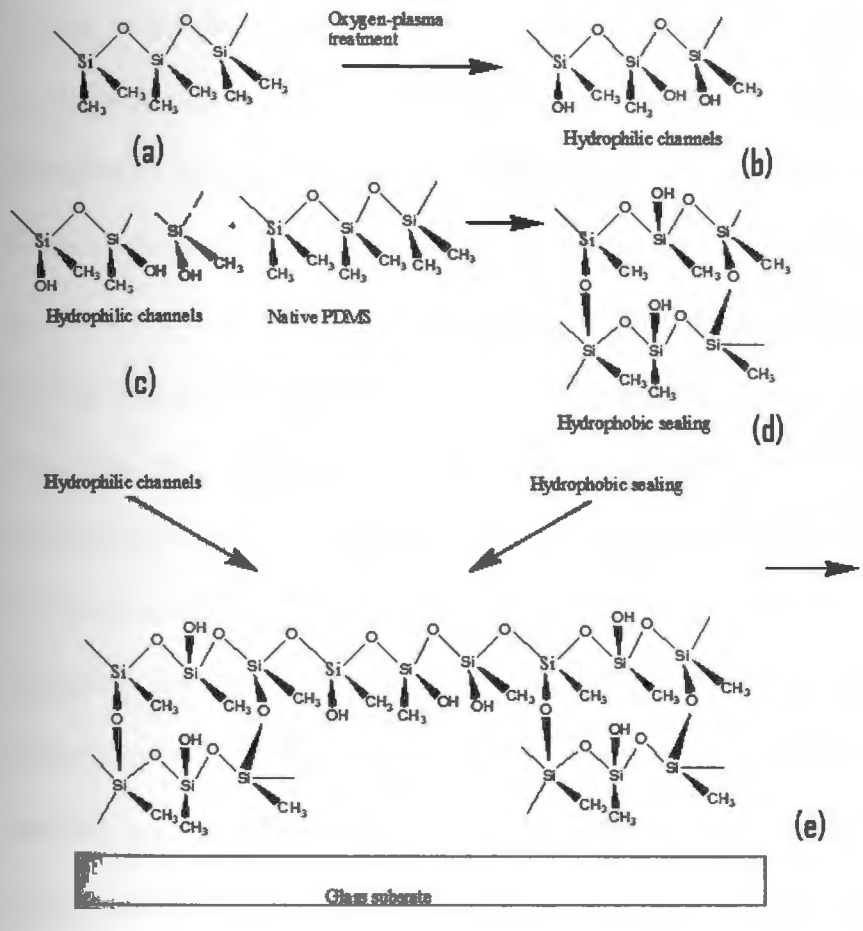

Figure 5.3: Creation of Hydrophilic PDMS channel with hydrophobic sealing. (a). Native PDMS surface with methyl groups. (b). After treatment with O_2 plasma- hydrophilic surface with -OH groups is obtained. (c). Hydrophilic PDMS surface is in contact with a native PDMS surface. (d). Rearrangement of PDMS surface to its hydrophobic recovery. (e). A hydrophilic channel with hydrophobic sealing is obtained[16].

Silica modified microchannels

Modification of the device is also possible by growing silica nanoparticles and silica monoliths *in*-situ within the channels. In this scheme a precursor mixture containing tetraethoxyorthosilicate (TEOS) is injected into the microfluidic channels and left overnight. Over time the TEOS solution undergoes a gelation step where the TEOS molecules crosslinks to form rigid three-dimensional silica particles. As the gel formation is left overnight further crosslinking of particles lead to monolith formation within channel and cured for few days for reaction to complete. When observed under microscope shrinkage away from the wall is observed which allows flow to occur through and around monolith. The monolith within the channel serves to (1) increase the surface area of the channel allowing for the attachment of the biological entities and (2) it can serve as a source of electroosmosis within the channel. The second benefit is particularly important due to the fact that the native PDMS is incapable of generating electroosmotic flow due to its lack of surface hydroxyl groups that are needed. By introducing a silica monolith into the channel, electroosmotic flow can be realized, because when the pH is greater than 3 as is required to work with the proteins/antibodies, the surface silanol groups of the monolith are deprotonated and allow for the development of an electrical double layer necessary for electroosmotic flow.

Subsequent to the monolith preparation within the channel, it is further modified with aminopropyltrimethoxysilane and diisocyanatohexane to provide an active site for protein attachment via urea linkage.

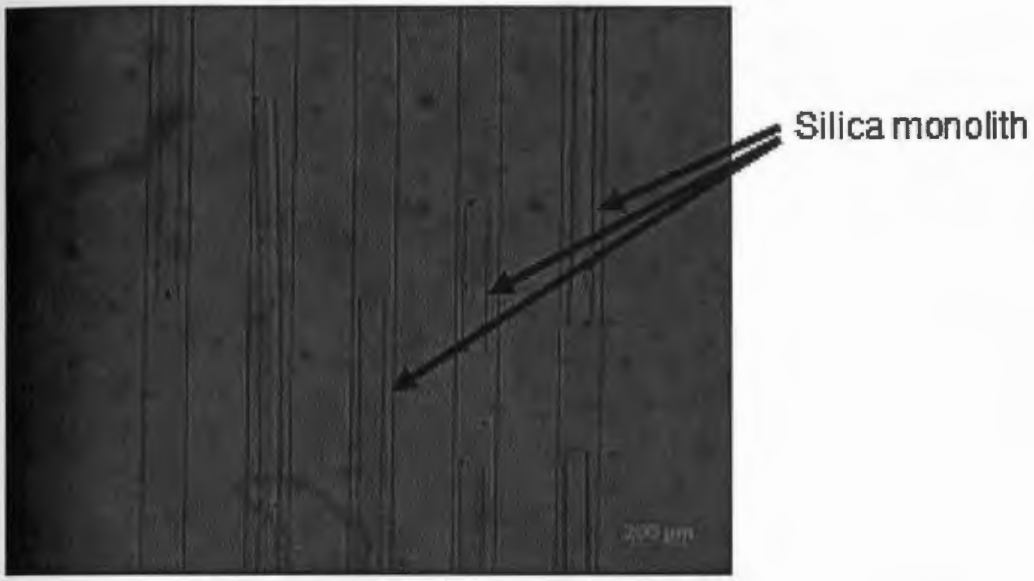

Figure 5.4: Silica nanoparticles injected in the microchannels showing the formation of monolith.

Microscopic images taken of the channel confirmed the formation and shrinkage of monolith away from the walls. To confirm that flow is still possible through the channel with monolith a solution of quantum dots is injected. As evident in the fluorescence microscopic image below, the entire channel becomes filled with the solution and the solution exits the other end of the channel.

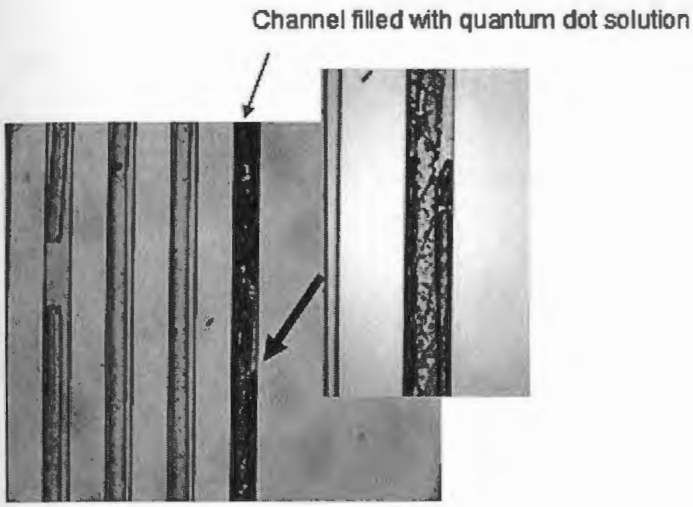

Fig 5.5: Channel filled with quantum dot solution. Flow is still possible through and around monolith.

A model protein (egg albumin labeled with dansyl chloride) was attached to silica nanoparticles that had been modified with aminopropyltrimethoxysilane and 1,6-isocyanatohexane. The linkage chemistry is the same as that within the monolith modified channel mentioned above. Here, the isocyanato group is capable of reacting with the N-terminus of the protein leading to the formation a stable urea moiety. The linkage chemistry is depicted below in Scheme 5.3

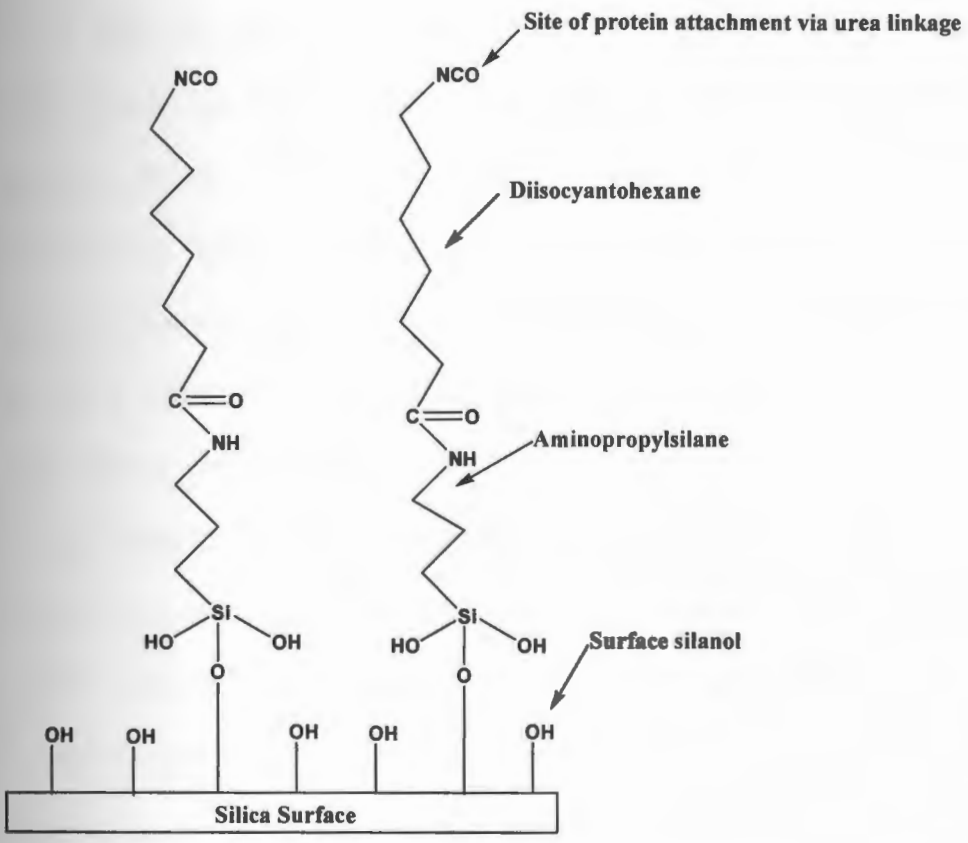

Scheme 5.3: Surface linkage Chemistry

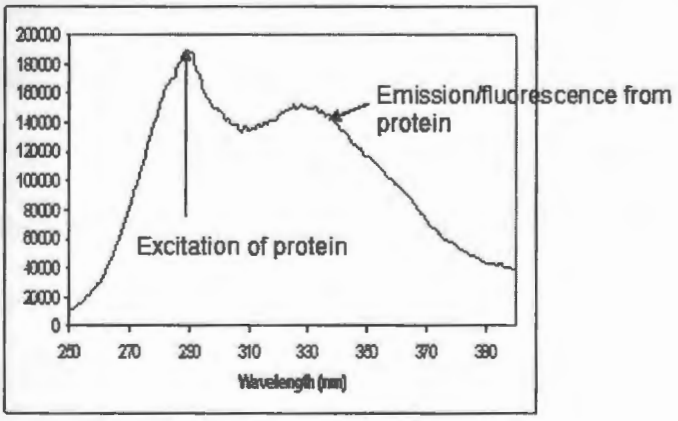

Fig 5.6: Fluorescence from protein-labeled Nanoparticle – No denaturing of proteins

From the Figure 5.6 it is evident that there is no protein denaturation when the silica particles are modified with aminopropyl silane and 1,6-Diisocyanato hexane and attached protein egg albumin labelled with dansyl chloride (fluorophore). Modification with aminopropyl silane and 1,6-diisocyanato hexane serves as extra spacer so that the protein are not affected by the surface of the particles which may adversely affect the biofunctioning of the proteins and possible leading to their denaturation. In this scheme, the protein is excited at 290 nm and an emission peak centered around 330 nm is observed – Figure 5.6. The emission peak not only confirms the attachment of the protein to the particles, but also reveals that the protein is still in its native/non-denatured state. Once it was confirmed that the proposed linkage chemistry was successful as evident by the attachment of the egg albumin, the work is continued further to determine the antigen-antibody interactions. As the monolithic columns formed in the channels, the surfaces are modified with aminopropyltrimethoxysilane and 1,6-diisocyantohexane. The antibody bovine IgG is injected into the channels and allowed to react at an optimum temperature overnight. Subsequent to the antibody attachment into the channel, the antigen (bovine anti-IgG) labeled with FITC is introduced into one of the channel and left for 2-3 hours. With the fluorescence microscope detection, from Figure 5.7 [D], the first 4 channels on the left hand side which has IgG shows no fluorescence but the channel with AntiIgG labelled with FITC shows signal, confirming the binding interaction of IgG and AntiIgG.

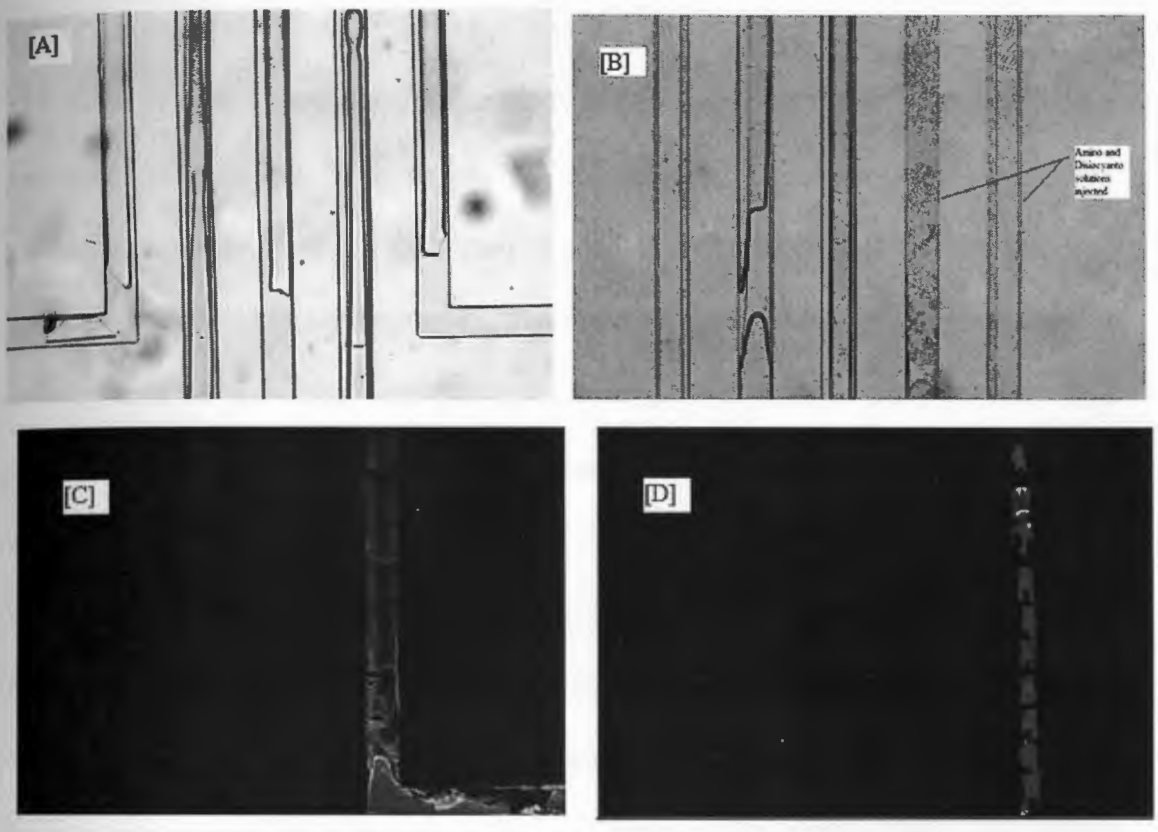

Figure 5.7: [A].Showing the formation of Silica Monoliths **[B].** In the right two channels aminopropyltrimethoxysilane and 1,6-Diisocyantohexane were injected and allowed to sit over night **[C].** Egg albumin labeled with Dansyl chloride showing fluorescence indicates that the protein is linked to the silanes **[D].** All the channels filled with IgG and last channel injected Anti-IgG labelled with FITC shows fluorescence – suggests the successful linkage of antigen to the silanes and binding with antibody.

CONCLUSION

In this work we have successfully demonstrated a facile approach to the functionalizaton of PDMS substrates that allow for their efficient modification with biological entities. Here we have used various silanes as well as polymers prepared in-house in the modification schemes. To accomplish an increased surface area within the channels we have use a sol-gel protocol to grow silica nanoparticles and silica monoliths *in-situ*. Further modification of the monolith and nanoparticles allows for the facile attachment of biological entities within the channels. In the first case we have used a model protein to study the preservation of the biofunctionalization of the protein after adsorption onto the surface of the silica particles. By varying the length of the space chain as well as using a polymer underlayer allows for the preservation of biofunctioning, mostly likely due to the isolation of the protein from the surface charges on the particles that would likely lead to the denaturation of the protein. Subsequent to this study the channels were labeled with an antigen followed by introduction of an antibody that was labeled with a fluorophore. It was confirmed by the fluorescence image that only the channels that had been modified with the antigen lead to the observation of a fluorescence signal. This signal is indicative of the antibody-antigen interaction. This work points to the ability to develop these systems in a facile manner where biofunctioning can be preserved. By choosing an appropriate biorecognition element (enzyme, antibody, etc) holds the potential for further development of these devices into cheap and readily available biomedical detection systems for a variety of diseases.

REFERENCES:

1. Shelley D. Minteer ., Christine M. Moore. "Overview of Advances in Microfluidics and Microfabrication."Microfluidic Techniques. doi: 10.1385/1592599974.

2. Microfluidics: Impact on Drug Discovery by Gillian Davis at the Dolomite centre Ltd.

3. [illegible]tech.edu/Microfluidics/chapter1.html

4. An Overview of DNA Analysis and Microfluidic Lab-on-a-Chip for Life Science Applications, Medical Representative News Letter, 2004.

5. A textbook on Lab on a chip Technology (Vol. 1) Fabrication and Microfluidics, Keith E.Herold, chapters 3, 5, 7, and 12.

6. T.B. Microfluidic lab-on-a-chip for chemical and biological analysis and discovery By Paul C. H. Li

7. Wendell Karlos Tomazelli Coltro,[1,2] Susan M. Lunte,[2] and Emanuel Carrilho, Comparison of the analytical performance of electrophoresis microchannels fabricated in PDMS, glass, and polyester-toner.

8. Procedure for making PDMS micro-channel chips. Zhang's group.

9. T.B. Fundamentals and Applications of Microfluidics.

10. Biological Applications of Microfluidics, Frank A. Gomez (Editor), ISBN: 978-0-470-07483-1

11. McDonald, J. C.; Duffy, D. C.; Anderson, J. R.; Chiu, D. T.; Wu, H.; Schueller, O. J.; Whitesides, G. M., Fabrication of microfluidic systems in poly(dimethylsiloxane). [illegible]*ectrophoresis* **2000,** 21, (1), 27-40

12. Makamba, H.; Kim, J. H.; Lim, K.; Park, N.; Hahn, J. H., Surface modification of poly(dimethylsiloxane) microchannels. *Electrophoresis* **2003,** 24, (21), 3607-19.

13. *Silicon Compounds: Silanes and Silicones*. Gelest, Inc.: Morrisville, PA, 2004; p 560.

14. Hermanson, G. T.; Mallia, A. K.; Smith, P. K., *Immobilized Affinity Ligand Techniques*. Academic Press: San Diego, CA, 1992; p 454.

15. Wendell Karlos Tomazelli Coltro,[1,2] Susan M. Lunte,[2] and Emanuel Carrilho, Comparison of the analytical performance of electrophoresis microchannels fabricated in PDMS, glass, and polyester-toner, Electrophoresis. 2008 December; 29(24): 4928–4937.

16. Vikash Sharma, Marshal Dhayal, Govind, S.M. Shivaprasad and S.C. Jain, Surface characterization of plasma-treated and PEG-grafted PDMS for micro fluidic applications, Vacuum Volume 81, Issue 9, 25 May 2007, Pages 1094-1100.

17. Grafted poly(ethylene oxide) brushes as nonfouling surface coatings Leckband, D.; Sheth, S.; Halperin, A. Journal of Biomaterials Science, Polymer Edition, Volume 10, Number 10, 1999 , pp. 1125-1147(23)

CHAPTER 6

Functional Maleimido-Polymers for Amine Sensing and Discrimination: The Mechanism of the Color Change

Abstract

In this work we report the fluorogenic nature of a group of maleimido-containing polymers in the presence of aliphatic amines. In the presence of amines, the originally colorless polymer solution typically becomes a very intense deep pink, red or purplish color depending upon the functional moieties incorporated into the polymer chain. The polymer-amine solution initially exhibit an intense fluorescence peak centered 580nm with excitation of 470nm. In addition to the ability to sense the presence of amines, these polymers are also able to differentiate between the various classes of amines (primary, secondary, tertiary) as evidenced by the change in color from the initial pink/red/purple color after sitting. In the case of primary amines, the color changes to an intense yellow solution (λ_{ex} = 470nm, λ_{em} = ~520nm). In the presence of secondary amines the solution changes to orange (λ_{ex} = 470nm, λ_{em} = ~560nm). In the presence of tertiary amines, no change in color was typically observed from the original color (λ_{ex} = 470nm, λ_{em} = ~580nm). Finally, it was observed that when a drop or two of concentrated acid was added to the solution the original colorless solution was obtained and when subsequently exposed to amines the

colored fluorescent solutions could be again obtained. This process can be repeated multiple times.

Introduction

Recent advances in sensor research have yielded innovative applications that have been of tremendous value to our national security, healthcare, environmental safety, and energy resource management[1]. Sensors are the key input devices for effective monitoring and control, which leads to highly efficient and productive industrial operations, biological and chemical operations[2]. Sensors have made serious inroads into automotive, medical, industrial, pharmaceutical, biological and aerospace applications[3]. Chemical Sensing is part of an acquisition process in which some insight is obtained about the chemical composition of the system in real time. Generally, it consists of two distinct steps: recognition and amplification. The coupling of the chemically selective layer to the physical part of the sensor is very important. There are different types of sensors such as thermal sensors – to determine the temperature of the object to which the sensor is in contact[4], gas sensors- to detect the presence of gases such as CO, NO, NO_2, CO_2 and Hydrocarbons[5], Optical Sensors – for industrial, environmental and diagnostic applications[6], Chemical Sensors – to detect specific molecules in gas phase or solution phase. Fiber optic chemical sensors offers an innovative line of modular fiber optic chemical-sensing systems for dissolved and gaseous oxygen, p^H and dissolved CO_2[7].

Lately, chemical sensors are attracting great interest in early detection of smoke/fire as well as hazardous chemical agents to provide safety and security in public places and mass transportation systems. The chemical sensors interacts with the analyte molecule giving a measurable signal in response.

Chemical sensors based on conjugated polymers have received a grat deal of attention due to their ability to detect analytes at low concentrations[8]. Fluorescence intensity and quenching provides an effective means for detection because of the extreme sensitivity and simple detection[9, 10]. Often chromatographic methods such as HPLC, Column Chromatography and spectrometric methods such as MS, NMR, IR used for detection of small organic molecules. And these techniques are time consuming and expensive. Chemical sensors based on conjugated polymers can quickly detect trace amounts of organic molecules in both gas phase and solution phase and are important in areas such as forensics, industrial processing, food packaging and distribution, etc.

Polymer based sensors are now commonly used in detection of biological molecules by fluorescence based has become rapidly developing field[11, 12]. Despite the continuing demand, for commercial success, major advances in these sensors are required in terms of easy to handle, lower cost, selectivity, reliability and durability. However, there has already been research and development integrating polymer sensors into practical applications.

The Johns Hopkins University Applied Physics Lab has developed molecularly imprinted polymers (MIP), a class of synthetic polymers that may be tailored to selectively detect a particular substance. The molecular imprinting technique involves

a polymer, which has been synthesized in the presence of a target molecule, being used to separate a target molecule from other species[13]. Molecular recognition is an important aspect of any biosensor system. Due to increased stability in a variety of environmental conditions, molecular imprinted polymer (MIP) technology is an attractive alternative to biological-based recognition. This is particularly true in the case of improvised explosive device detection, in which the sensor must be capable of detecting trace amounts of airborne nitroaromatic compounds[14] and explosives such as smokeless powder, black powder, PETN, C4, Nitrobenzene, Nitrotoluene, Picric acid, TNT, and sodium/potassium chlorates etc. The polymers are now being used in the environmental and food sciences which helps in early detection before any sustainable damage occurs to drinking water[15, 16] or sea food[17].

In this work, the preparation of a variety of silane based polymers which are used for the detection of amines is reported. The important advantage of these polymers are that they are stable over a period of time, inexpensive, simple and cheap starting materials, cost efficient, can easily detect the presence of amines while avoiding the use of expensive and time consuming detection techniques. A change in the color of the polymer solution upon the addition of an amine gives a preliminary idea if the amines present or not. Over time, the amine-polymer solution changes color which affords discrimination between the classes of amines, i.e. primary, secondary or tertiary. In the case of a primary amine, the originally non-fluorescence polymer changes to a deep pink/reddish color and eventually turns to an intense yellow color with a fluorescence signal shifted from the original 580 nm down approximately 520 nm. In the presence of secondary amines, the intense pink/reddish

color after exposure changes to an orange color over time. When exposed to tertiary amines, the solution remains the intense pink/reddish color over time. The focus of this work is to elucidate the species that are responsible for these observations and the mechanism by which they are formed.

Experimental

Polymer preparation:

All polymers employed in this study were synthesized in-house through radical polymerization of *n*-phenylmaleimide (NPM) with various comonomers, namely allyl- or vinyltrimethoxysilane (ATMS or VTMS), allyl- or vinyltriethoxysilane (ATES or VTES), and allylisothiocyanate (AITC). In all cases the syntheses were performed using chloroform as solvent and AIBN (2,2'azobisisobutyronitrile, 1 – 10mol%) as radical initiator. Polymer syntheses and characterization has already been mentioned in Chapter 2. Figure 6.1 depicts a representative copolymer. Acronyms for the various polymers were developed by combining the various acronyms of each monomer as presented above. For example a copolymer prepared from *n*-phenylmaleimide and vinyltrimethoxysilane is given the acronym (NPM-VTMS). Similar acronyms will be employed throughout the remainder of the chapter.

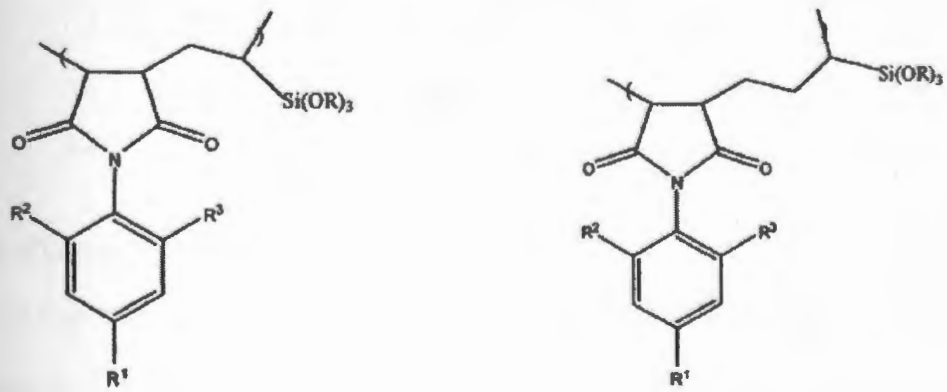

Where: R = -CH_3, -CH_2-CH_3, $R^2 = R^3$ = H, -CH_3, NO_2, R^1= H, -CH_3, Cl, Br, CN, NO_2, $NHCOCH_3$

Figure 6.1: General chemical structure of the Polymers

Table 6.1: List of amines studied and their abbreviations used

Name of the Base	Abbreviation
Propyl Amine	PA
Di Propyl Amine	DPA
Tri Propyl Amine	TPA
Isopropyl Amine	IPA
DiIsoPropyl Amine	DIPA
Aniline	-
Pyridine	-
3,5-Di methyl Aniline	-
Ammonium Hydroxide	NH_4OH
Sodium Hydroxide	NaOH

Preparation of Polymer solution

0.5w/v% stock polymer solutions were prepared by dissolving the various polymers in acetone. Equal volumes (10 mL) of each of the stock polymer solution were introduced into separate vials to which a test solution (0.1 ml) was added. The various test solutions and their corresponding abbreviations employed are listed in Table 6.1

Separate solutions were prepared for studying the effect of polymer concentration keeping the base concentration constant. Three different solutions with 0.5g, 0.1g and 0.01g of the polymer NPM-VTES dissolved in 10 ml of acetone were prepared in separate vials to which 0.1 ml of the primary amine propylamine was added.

To compare the intensities of various polymer solutions with different bases, 0.1g of each polymer was dissolved in 10 ml of acetone in separate vials and .1 ml of propyl amine was added to each vial and the fluorescence intensity measured.

pH changes were observed for a 0.1% solution of 4-Cl-PM-VTES in acetone. 0.01 ml DPA was added to 10 ml of the polymer solution and pH recorded. 0.01 ml of 4M HCl was added to this pink colored solution to see if the solution became colorless. More HCl was added (0.03 ml) to the solution to become colorless. At this point 0.01 ml DPA was added to get a colored solution.

Results and Discussion

The aim of the work presented in this paper is to explore the possible mechanism of the fluorogenic and sensing properties of the polymers that were prepared within our lab. The originally non-fluorescent and colorless polymer solutions exhibited significant fluorescence centered at approximately 580 nm when excited at 470 nm in the presence of amines (primary, secondary and tertiary). In addition to the spectral data, in the presence of the amine regardless of class all solutions turned a deep pink/fuschia/red/purple color, where the color and intensity depended upon the polymer side chain. For example, the methoxysilane polymer

(NMP-VTMS, NPM-ATMS) typically gave much deeper colors and higher spectral fluorescence intensity relative to their ethoxysilane counterparts (NPM-VTES, NPM-ATES).

The unique nature of these polymers to act as amines sensors lies in the fact that in addition to the fluorogenic response in the presence of amines, when the polymer-amine solution is allowed to sit, the solutions undergo further color changes as well as spectral changes that depend on the class of the amines. In the case of primary amines, the polymer solutions change from the pink/red/purple color to a bright yellow accompanied by a significant increase in fluorescence intensity (often saturating the detector) centered at ~520nm. In the case of a secondary amine, the original pink/red/purple solution changes to orange with a peak centered at ~560nm. In the case of the tertiary amine, the solution typically retains its original pink/red/purple color. In this way, it is possible to distinguish between the different classes of amines.

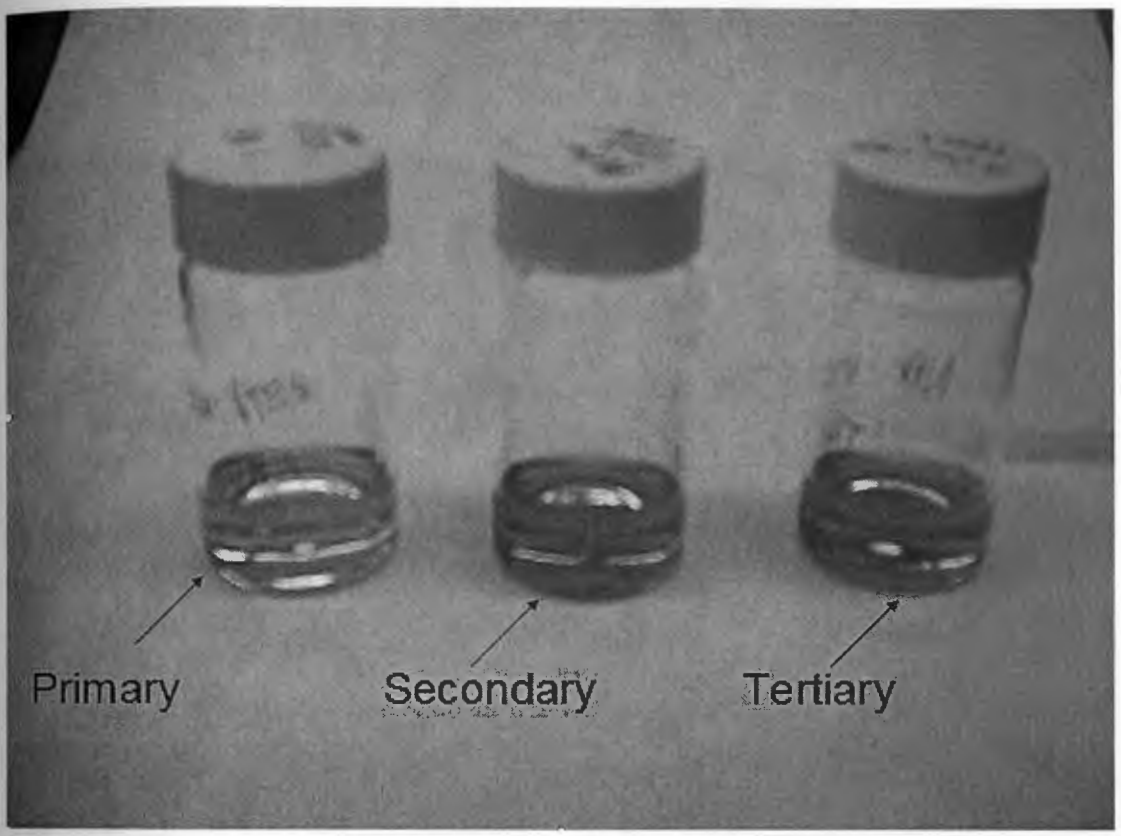

Figure 6.2: Colors of polymer solutions exposed to different amines with different colors to distinguish the type of base added.

Subsequent to synthesis, the polymers were all collected as powders from hexane, air-dried and analyzed by GPC and FTIR, ^{1}H- and ^{13}C-NMR spectroscopies. GPC data (not presented) revealed molecular weights between 5,000 and 25,000 g/mol, where the molecular weight depends upon the amount of the initiator used. Examination of the FTIR spectra of the polymers reveals bands characteristic of the functional groups of the polymer, e.g. the carbonyl stretch, aromatic stretches, etc (complete assignment not given). The FTIR spectra (Figure 6.3) also reveal that under synthetic and ambient conditions the polymers are not subjected to hydrolysis of the alkoxysilane groups indicating the stability of the polymers. The characteristic broad –OH stretch of the Si–OH group centered around 3200 cm^{-1} as well as the Si-O stretch

of the Si-OH centered at approximately 950 cm^{-1} are both absent, however the Si-OC of the Si-OR centered about 1072 cm^{-1} is evident. These pieces of data are taken as confirmation of the lack of hydrolysis of the alkoxysilane. It should be noted that when the polymers are subjected to hydrolysis of the alkoxysilane groups there is a significant broad OH peak at 3200 cm^{-1} as well as a characteristic shift of the peak at 1072 cm^{-1} down to ~950 cm^{-1} consistent with the conversion of Si-OR to Si-OH. Additionally, when the polymers are hydrolyzed and crosslinked to form the corresponding siloxanes, the polymers fall out of solution and are no longer soluble.

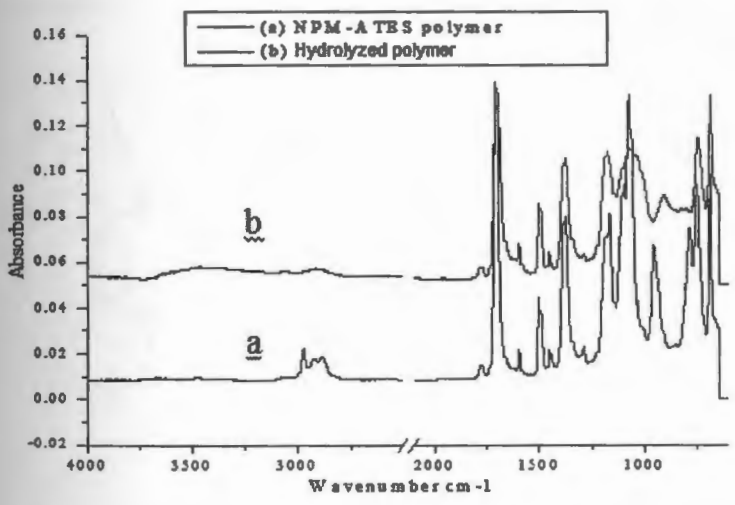

Figure 6.3: FTIR spectrum of the polymer a) and the subsequent conversion of alkoxy silane groups Si-OR to Si-OH.

Detection of primary amines:

When the polymer solution is exposed to a primary amine, the solution immediately turns to an intense deep pink/reddish color with an intense fluorescence peak centered about 580 nm. The broad nature of the fluorescence peak is suggestive of the formation of a complex of some kind. The proposed species leading to the

formation of this fluorescent species is the formation of an imine which results from the reaction of an amine with a carbonyl compound.

The proposed mechanism of the imine formation is due to a nucleophile attack on the carbonyl group by the lone pair electrons centered on the nitrogen of the amine group which leads to a dipolar tetrahedral intermediate. During this process, a proton transfer from the nitrogen of the amine to the oxygen yields a neutral carbinolamine. The proposed mechanism is depicted below. Figure 6.4 depicts the initial attack on the carbonyl center by the amine. Figure 6.5 depicts the mechanism of the imine formation.

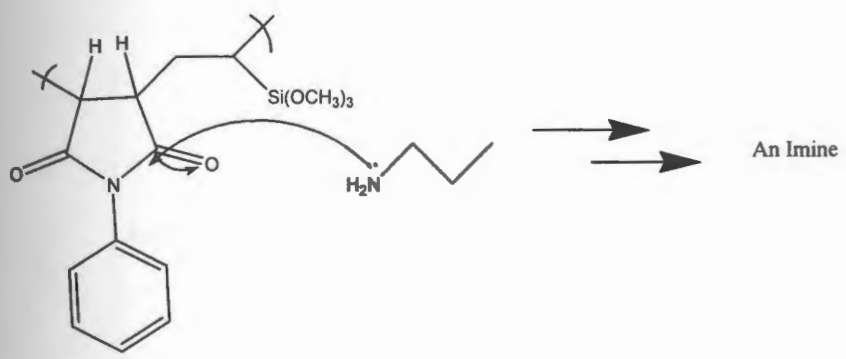

Figure 6.4. Initial amine attack on the carbonyl center

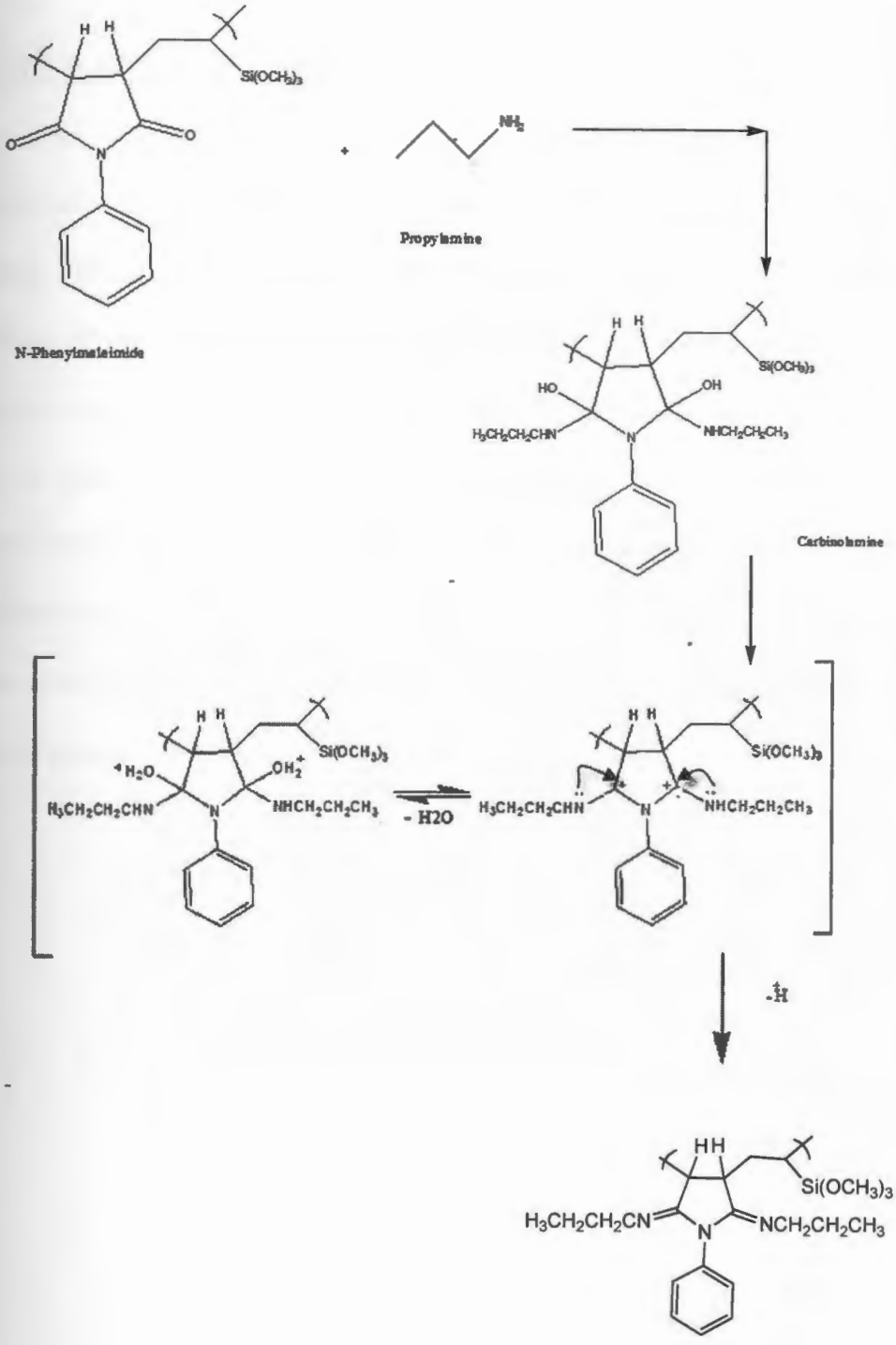

Figure 6.5. Mechanism of imine formation.

^{1}H-NMR of NPM-VTMS Polymer:

The ^{1}H-NMR spectrum of the NPM-VTMS polymer reveals bands characteristic of the functional groups present in the polymer. For example, the spectrum shows a broad peak with chemical shift at δ = 7.1 to 7.6 ppm (peaks b, c, d) indicative of the aromatic protons from the phenyl ring. Succinimide protons were observed at δ = 2.2 ppm (peak e), where the chemical shift can vary with cis (3.2 ppm) or trans (2.7 ppm). Methylene and methyl peaks associated with the vinyltrimethoxysilane monomer after the polymerization with the maleimide can be found with chemical shifts around δ = 1.4ppm (peak f) and δ = 1.7ppm (peak g). The terminal methoxy groups (–OCH3) (peak a) show their resonance at δ = 3.5ppm. Peak assignment can be seen on the spectrum below.

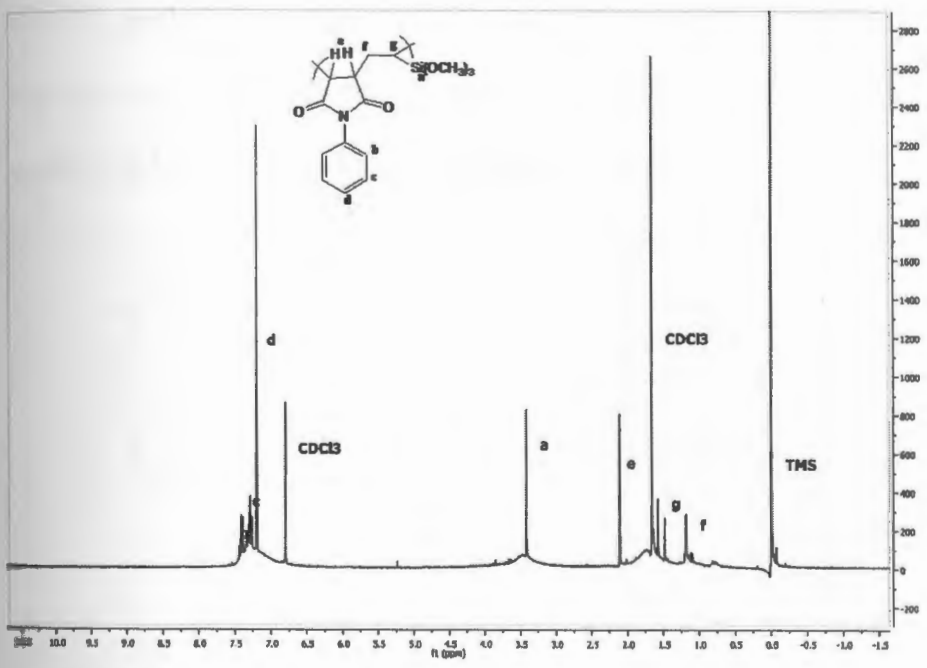

Figure 6.6: ^{1}H NMR of Polymer n-Phenylmaleimide-vinyltrimethoxysilane

^{13}C-NMR of NPM-VTMS Polymer:

The ^{13}C-NMR of the NPM-VTMS polymer was also collected and similar to the proton NMR, the spectrum reveals peaks characteristic of the functional groups as expected. The spectra Figure 6.7 shows the representative peaks of the phenyl ring at δ = 126 to 135ppm (peaks b, c, d and h). The carbonyl and succinimide carbons on

the maleimide ring were detected at δ = 170ppm (peak i) and δ = 31(peak e) respectively. The silane peaks are also visible with a slight chemical shift difference at δ = 65 (peak a). Successful preparation of the copolymer is also confirmed through the loss of vinyl moiety and peaks from the –CH2 and –CH around δ = 25 ppm (peaks f, g) between the maleimide and alkoxysilane.

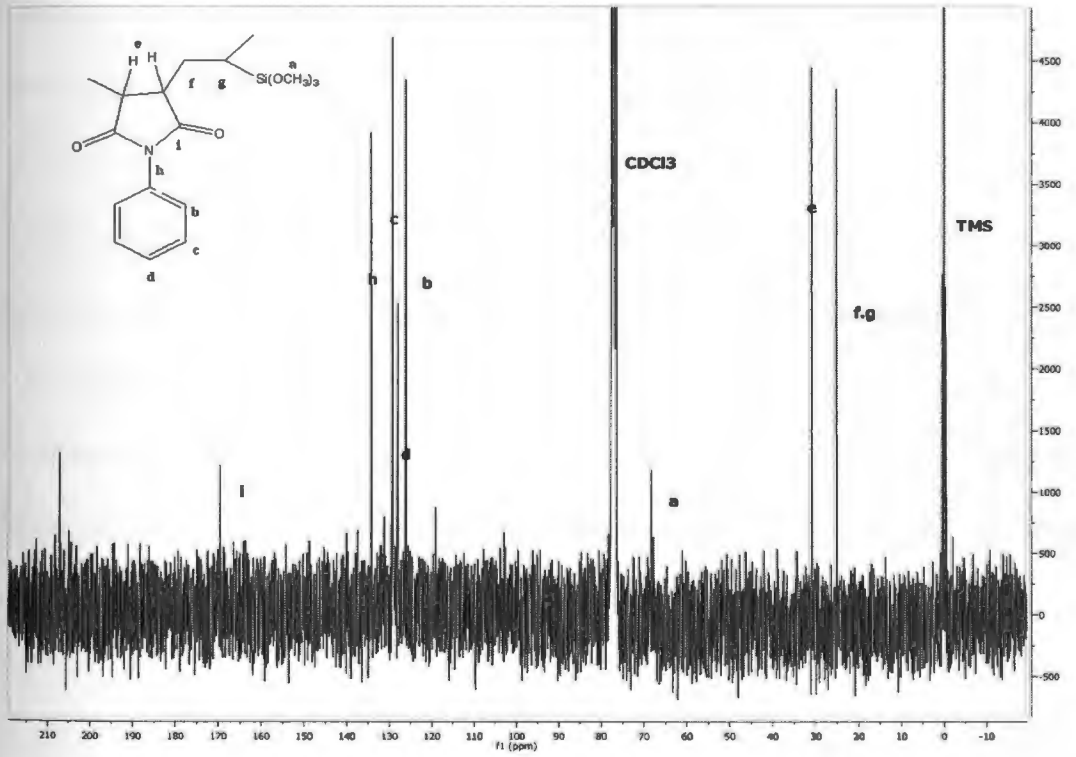

Figure 6.7: ^{13}C NMR of Polymer n-Phenylmaleimide-vinyltrimethoxysilane

^{1}H-NMR of Polymer with Propylamine confirming the formation of Imines:

NMR spectrum collected after the reaction of the polymer with the primary amine Figure 6.8 confirms the formation of imines (Schiff's base) between *n*-phenylmaleamide-co-vinyltrimethoxysilane and the primary amine (propylamine). The terminal methyl protons of the primary amine were observed as a triplet at $\delta = 0.96$ (peak h). The methylene protons of the amines were observed as a multiplet at $\delta = 1.4$ (peak i) and $\delta = 2.5$ (peak j). The typical aromatic proton resonance observed at $\delta =$ 7.2 to 7.6 (peaks b, c, d) confirms the successive formation of imines with the carbonyl group of maleic acid to the –NH2 group of primary amine. If there was no formation of imines the aromatic proton resonance shift would be seen at $\delta = 4.95$ to 5.75. Succinimide protons were observed at $\delta = 1.7$ (peak e) proving the disappearance of alkene during the polymerization process. Terminal methoxysilane groups are intact as evidenced by their resonance at $\delta = 3.5$ ppm (peak g). Peak assignment is given in the figure below.

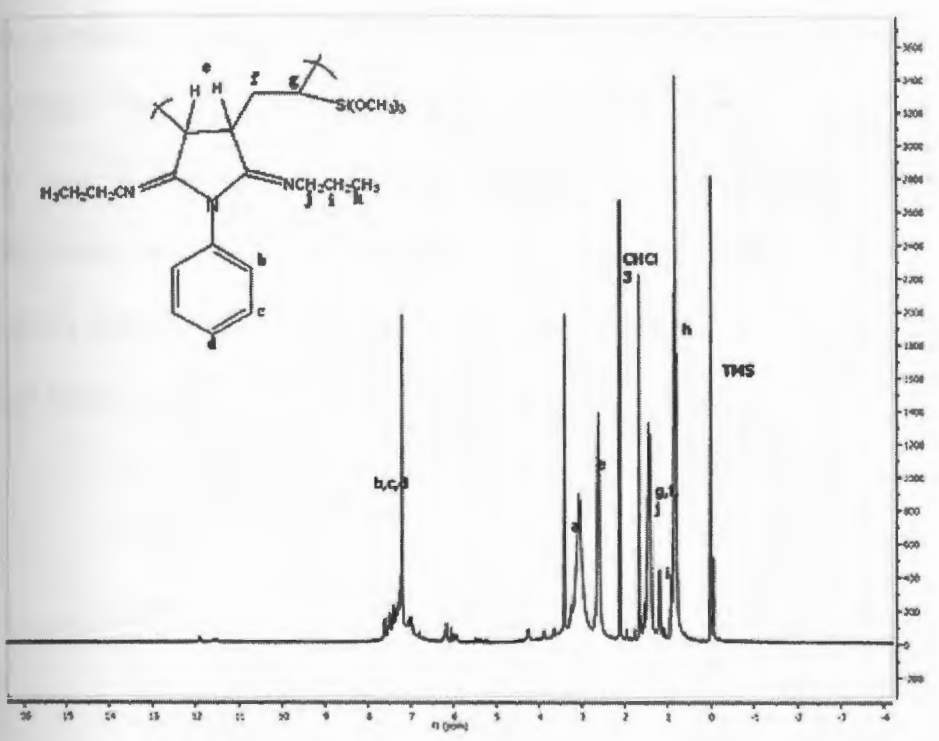

Figure 6.8: ^{1}H NMR conforming the formation of Imine

^{13}C-NMR of Polymer with Propylamine confirming the formation of Imines:

^{13}C-NMR spectrum Figure 6.9 and 6.10 collected after the reaction of the polymer with the propyl amine shows the typical aromatic carbon resonance at δ = 119 to δ = 129 ppm (peak b,c,d, in spectrum) . The methyl carbon resonance of the amine were observed at δ = 11.70 (peak h). The methylene carbons resonance were observed at δ = 25.18 (peak i) and –N-CH2- at δ = 49.0 (peak j). The formation of imine i.e., the conversion of carbonyl group of maleamide to –C==N is confirmed by

the presence of peak at δ = 164 (peak l). The intensity of the –C=O is strong in the polymer ^{13}C NMR spectrum and the intensity of –C=N peak is low. The silane peaks are also visible with a slight chemical shift difference at δ = 56.49 (peak a). Successful preparation of the copolymer is also confirmed through the loss of vinyl moiety and peaks from the –CH2 and –CH around δ = 20 ppm between the maleimide and alkoxysilane.

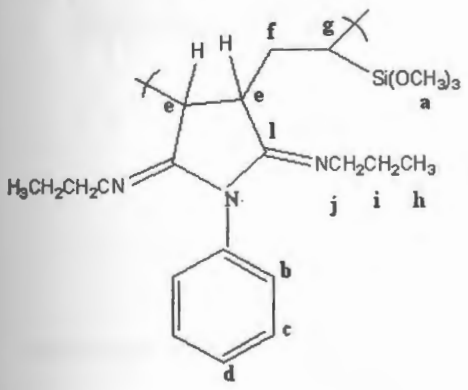

Figure 6.9: Structure of Imine

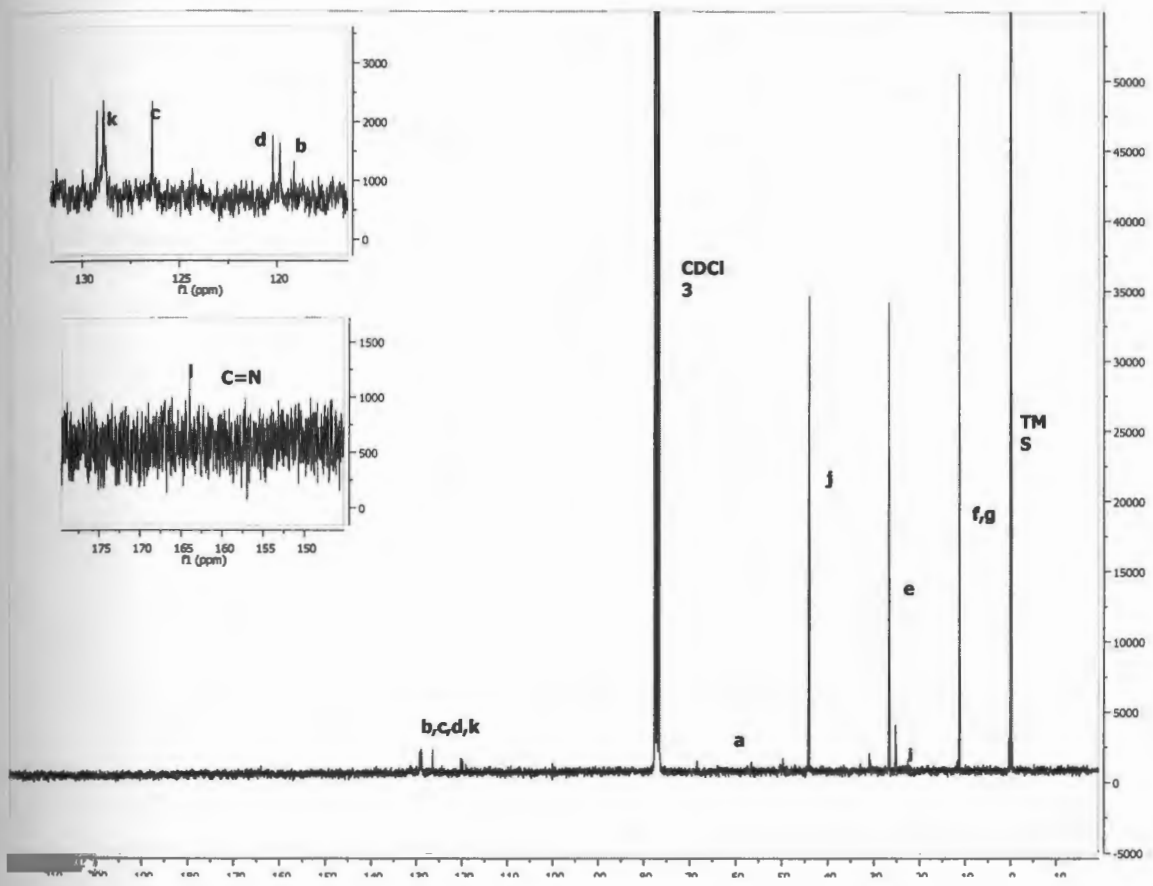

Figure 6.10: ^{13}C NMR of Imine formation

Reaction of Carbonyl Group with Secondary Amines:

Figure 6.11: Mechanism of Enamine Formation

The nucleophilic attack of lone pair of electrons of the nitrogen atom on the carbonyl group of the polymer resulted in the abstraction of allylic proton present in the maleimide ring and rearrangement followed a proton shift and a loss of water molecule resulted in the formation of Enamine.

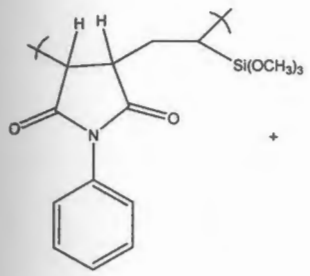

n-Phenylmaleimide-
vinyltrimethoxysilane

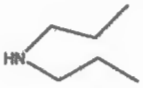

Dipropylamine
(secondary amine)

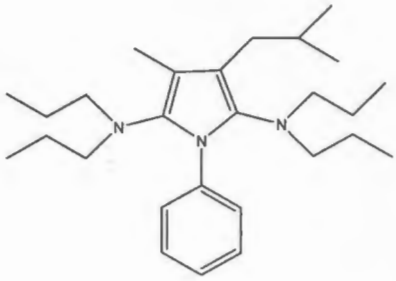

Enamine

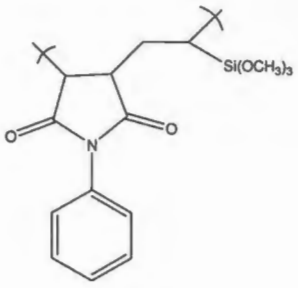

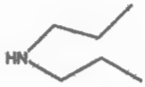

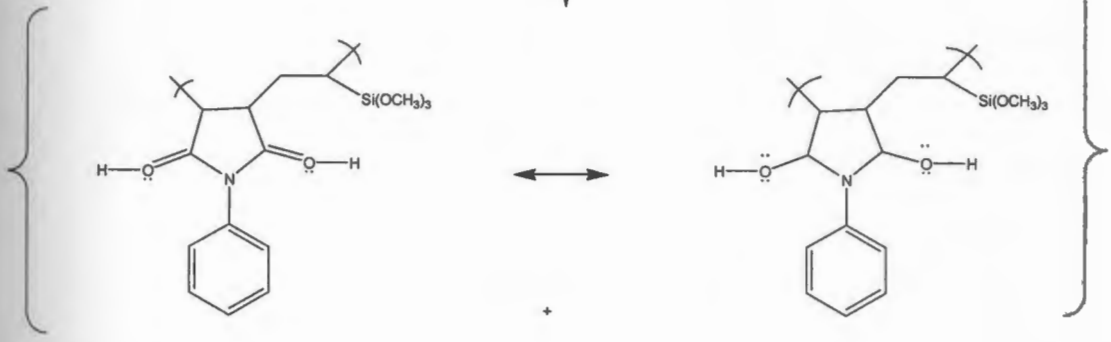

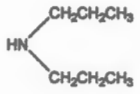

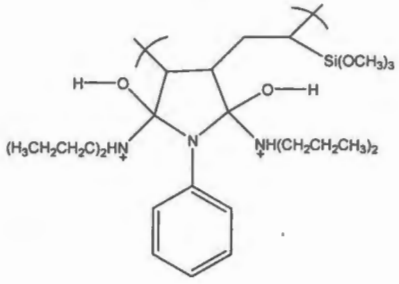

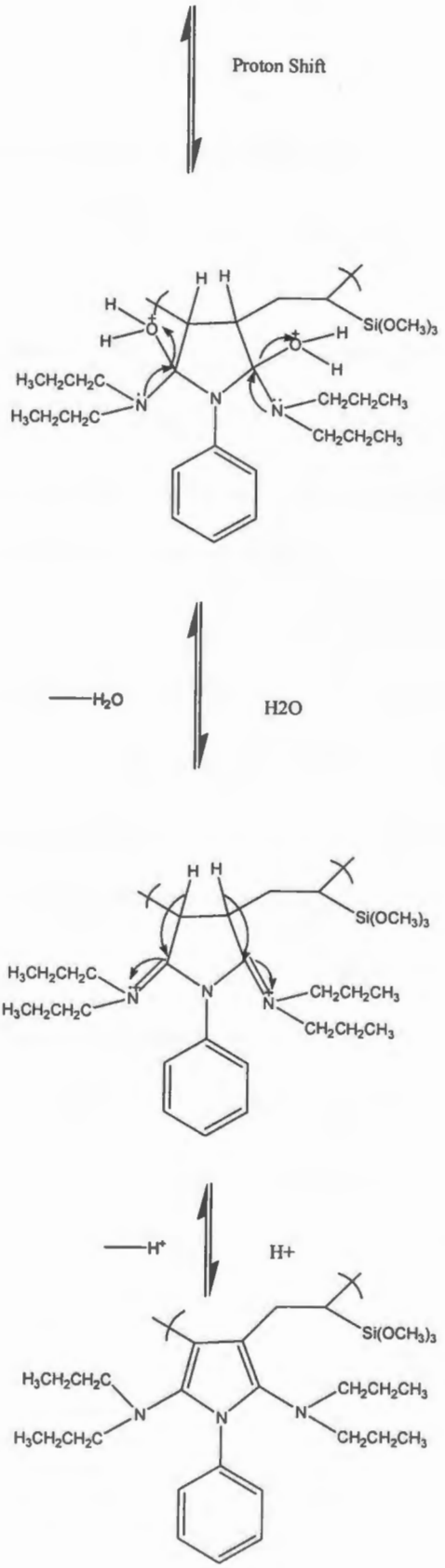
Proton Shift
Si(OCH3)3
H3CH2CH2C
H3CH2CH2C
CH2CH2CH3
CH2CH2CH3
—H2O
H2O
—H+
H+

Secondary Amine Detection – Enamine Formation:

^{1}H-NMR of Polymer with Secondary amine (dipropyl amines) forming Enamines:

The spectrum Figure 6.12 shows the successful formation of enamines between n-phenylmaleimide and vinyltrimethoxysilane and secondary amine (dipropylamine). The terminal methyl protons of the secondary amine were observed as a triplet at δ = 0.96 (peak h). The methylene protons adjacent to the methyl group are observed as a multiplet at δ = 1.53 (peak i). The second set of methylene protons adjacent to amino group is seen as a triplet at δ = 2.98 (peak j). All these peaks of the secondary amine confirm that they are intact with the amino group and do not undergo any hydrolysis during the reaction. A single peak at δ = 7.3 (peaks b, c, d)is typical aromatic proton resonance confirms the successive formation of enamines at the carbonyl oxygen region. If the secondary amine is attached to the para position of the phenyl ring we would see the aromatic resonance proton peaks at two regions δ = 6.57 and δ = 7.46, which are absent in the ^{1}H NMR, thus confirming the formation of enamine in the maleamide ring. Terminal methoxy silane groups are intact through resonance at δ = 3.5 ppm (peak a). The vinyl groups are observed as a singlet at around δ = 1.9 to 2.6 ppm (peaks f and g).

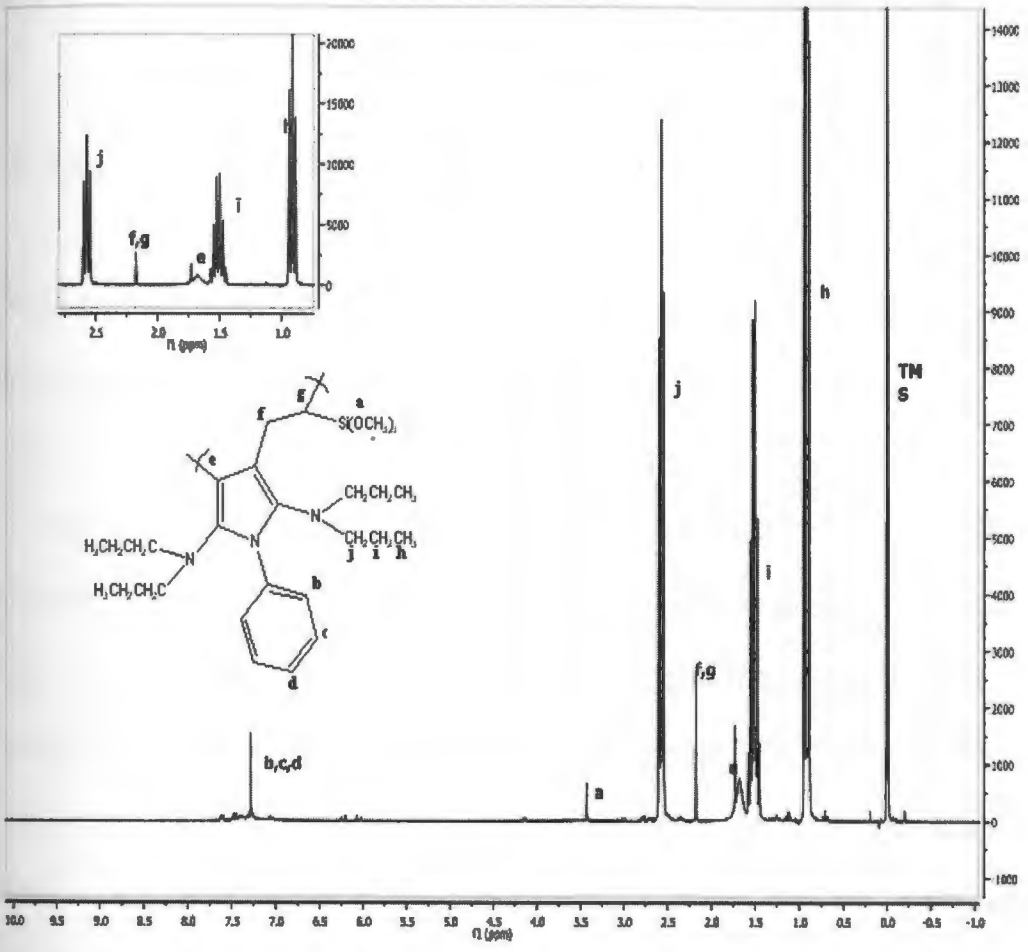

Figure 6.12: ^{1}H NMR of Enamine formation

^{13}C NMR of Polymer with Secondary amine (dipropylamine):

The spectrum Figure 6.13 shows the typical aromatic carbon resonance at δ = 120 to δ = 140 (peaks b, c, d, l and h). The methyl carbon resonance of the amine were observed at δ = 11.80 (peak i). The methylene carbons resonance were observed at δ = 21.47 (peak j)and –N-CH2- at δ = 53.15 (peak k). The formation of enamine i.e., the conversion of carbonyl group of maleamide to –C=C-N is confirmed by the presence of peak at δ = 119 (peak h). The silane peaks are also visible with a slight chemical shift difference at δ = 57.0. Successful preparation of the copolymer is also confirmed through the loss of vinyl moiety and peaks from the –CH2 and –CH around δ = 20 ppm between the maleimide and alkoxysilane. The other possibility of the attack of secondary amine at the phenyl ring is ignored because if the amine is attached to the para position of the phenyl ring would result strong peak at δ = 176 suggesting the presence of carbonyl group and the aromatic carbons resonance peaks are observed beyond δ = 140.

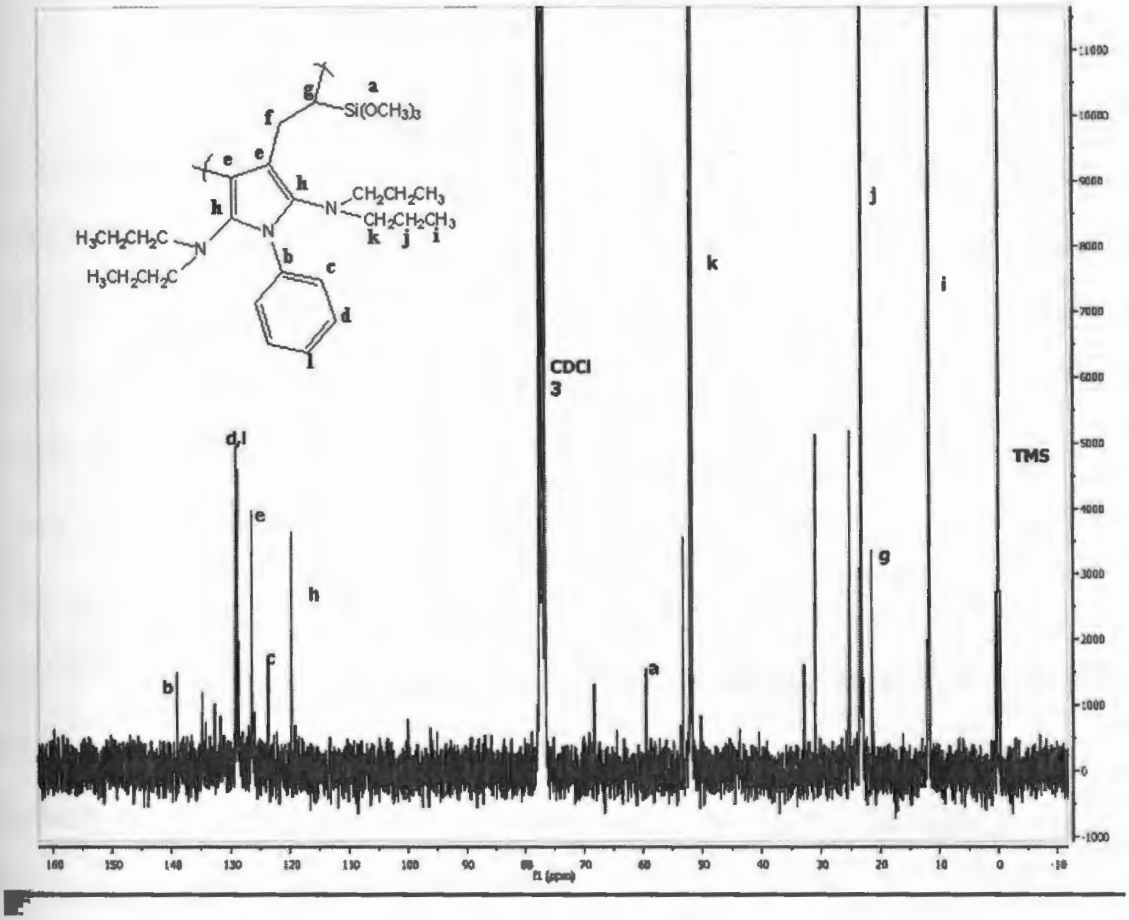

Figure 6.13: ^{13}C NMR of Enamine formation

Conclusions :

This work studies the changes in color associated with the addition of various classes of amines to solution of polymer prepared within the Major Lab. The polymer solutions which were nominally non-fluorescent exhibited a fluorogenic response in the presence of amines. The colorless solution turns an intense pink/reddish color in the presence of the amines. This color is reversible by addition of an acid (turns colorless) and further addition of a base (turns colored). This allows reuse of the

polymer solution for detection. So the same polymer can be used for more than one sample to be detected for amines. The polymer-amine solution initially exhibits an emission in the red region in the visible spectrum and shows a marked blue shift spectroscopically after sitting. There is also a visual color change as well that allows for the discrimination between the classes of amines. These solutions were studied over time in an attempt to reveal the species likely responsible for the variation in the color of the polymer solution in the presence of the various base. Our initial assumption of imine and enamine formation between the amines and the carbonyl center of the maleimide is confirmed by NMR spectra. We rationalize that due to the distinctly different species formed with primary, secondary and tertiary amines, these differences gives rise to the variation in the observed color.

Appendix

Chapter 6

Included in this appendix are the NMR spectra of the monomers as well as the estimations of the NMR spectra calculated using ChemDraw software. These estimations were used in confirmation of the structure assignment for the structures of the species formed upon the reaction of the amines with the polymers.

^{1}H-NMR of Monomer N-PhenylMaleimide :

The spectra Figure A-1shows the typical aromatic proton resonance at δ = 7.36, 7.34 and δ = 7.46. The maleimide protons were observed as a singlet at δ = 6.836 indicating the successful attachment of maleic anhydride moiety and functionalized aniline with a complete ring closure reaction of maleamic acid.

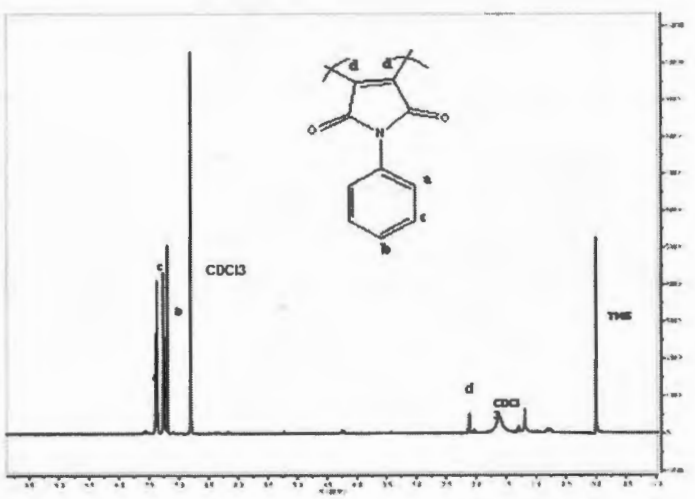

Figure A-1: ^{1}H NMR of monomer n-Phenylmaleimide

^{13}C NMR of Monomer N-Phenyl Maleimide :

The spectra Figure A-2 shows the typical aromatic carbon resonance at δ = 124 to 132. The peak at δ = 170 confirms the presence of carbonyl group of maleimide ring. The aliphatic protons on the maleamide ring were observed at δ = 138.

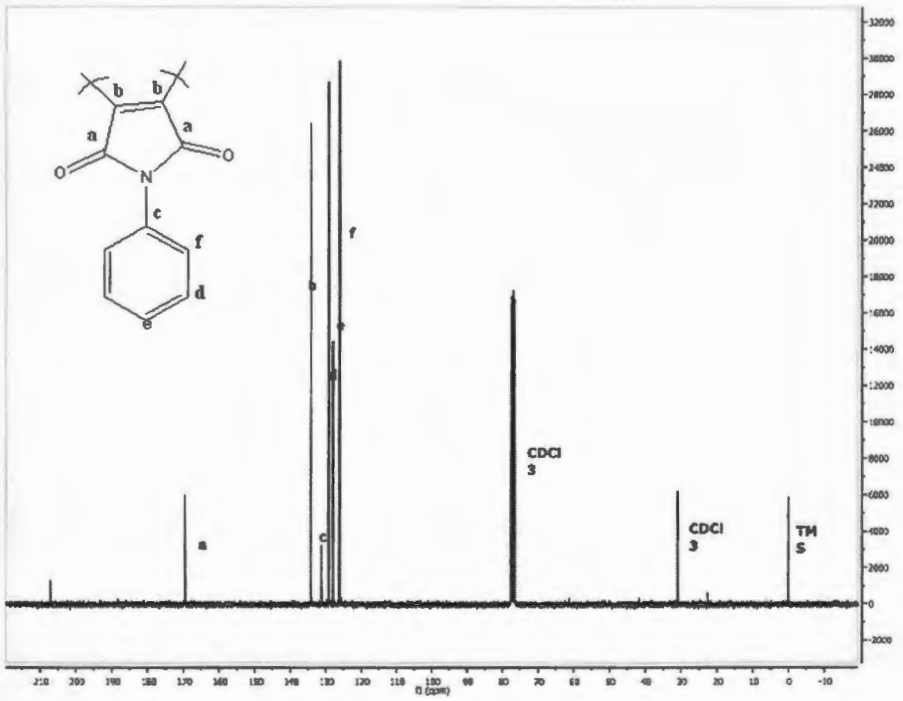

Figure A-2: ^{13}C NMR spectrum of monomer n-Phenylmaleimide

1. ^{1}H-NMR estimation for the NPM monomer.

ChemNMR H-1 Estimation

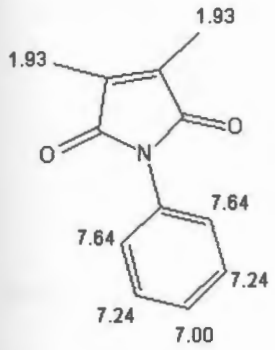

Monomer - NPM

Estimation Quality: blue = good, magenta = medium, red = rough

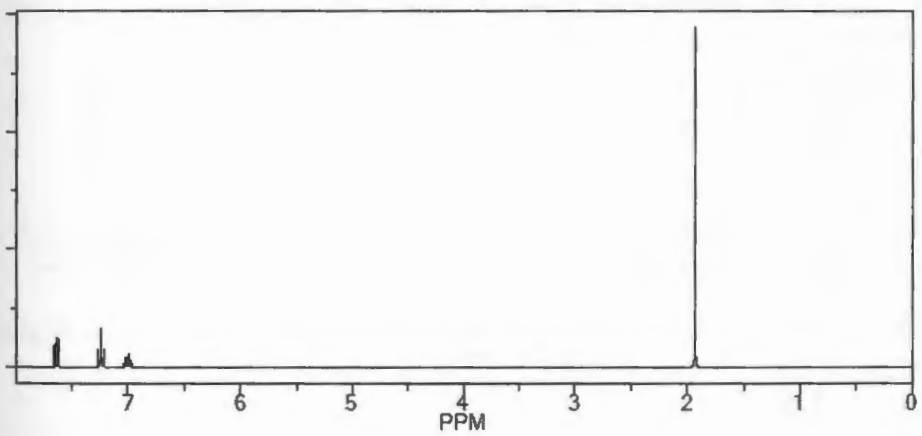

Figure A-3: ^{1}H NMR ChemDraw Estimation of monomer n-Phenylmaleimide

ChemNMR C-13 Estimation

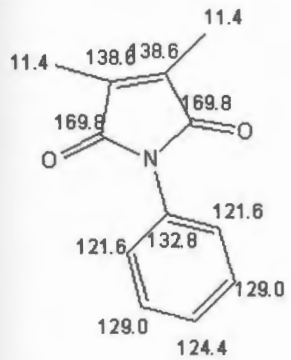

Estimation Quality: blue = good, magenta = medium, red = rough

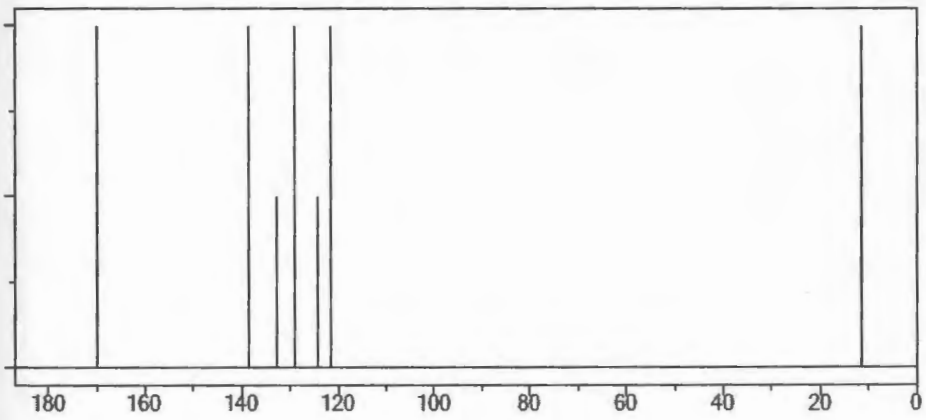

Figure A-4: ^{13}C NMR ChemDraw Estimation of monomer n-Phenylmaleimide

[1]H-NMR estimation of the polymer NPM-VTMS

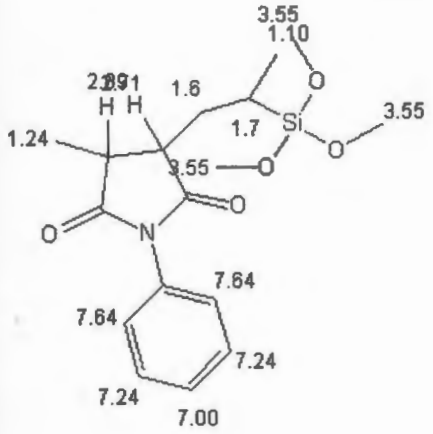

Polymer proton NMR

Estimation Quality: blue = good, magenta = medium, red = rough

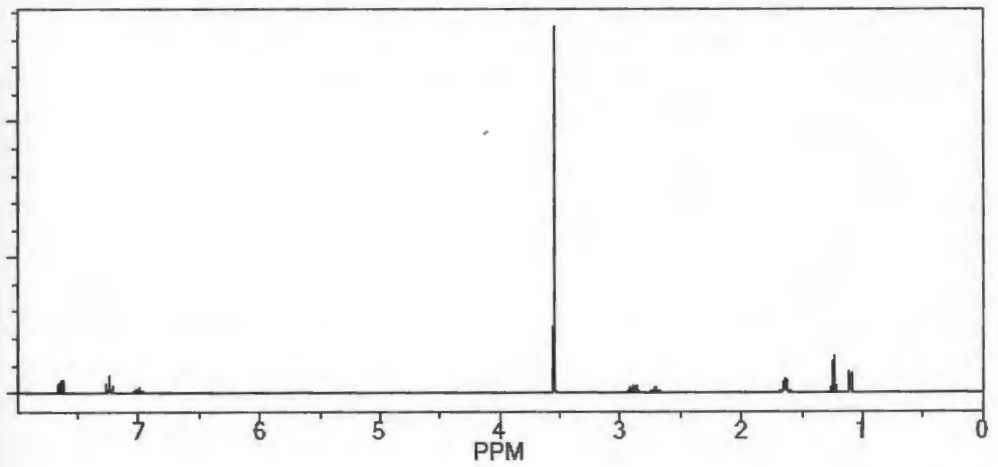

Figure A-5: [1]H NMR ChemDraw Estimation of Polymer n-Phenylmaleimide-vinyltrimethoxysilane

^{13}C-NMR estimation of the NPM-VTMS polymer

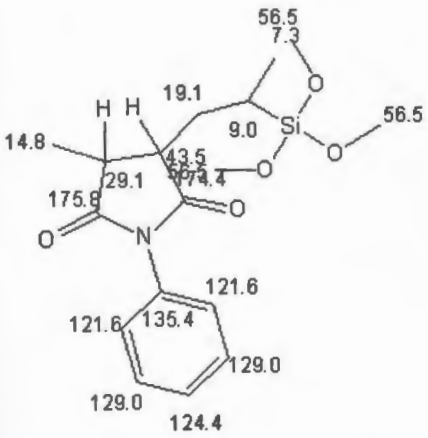

Polymer carbon 13 NMR

Estimation Quality: blue = good, magenta = medium, red = rough

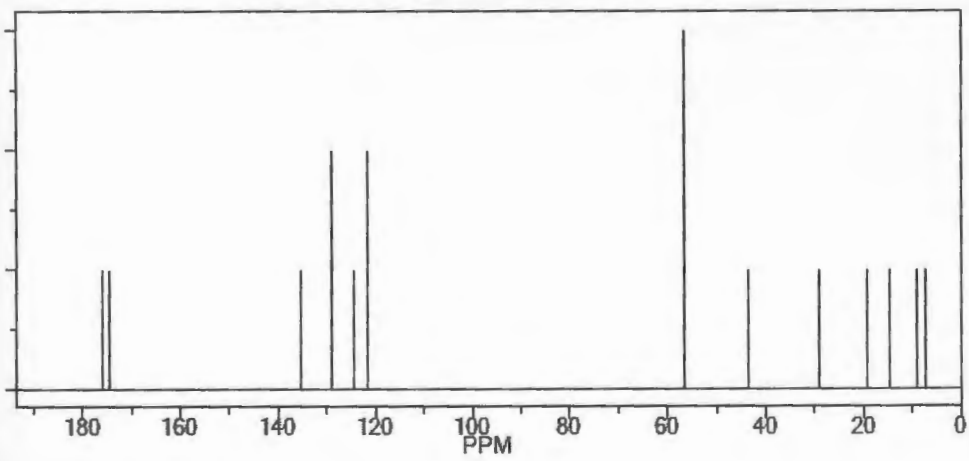

Figure A-6: ^{13}C NMR ChemDraw Estimation of Polymer n-Phenylmaleimide-vinyltrimethoxysilane

^{1}H-NMR estimation of the NPM-VTMS polymer showing imine formation with propylamine

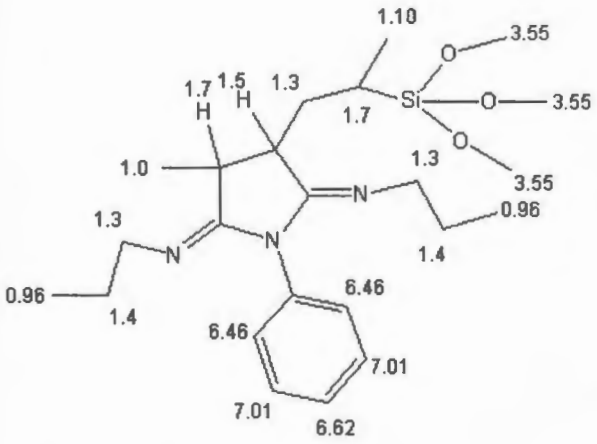

Polymer with Propylamine proton NMR

Estimation Quality: blue = good, magenta = medium, red = rough

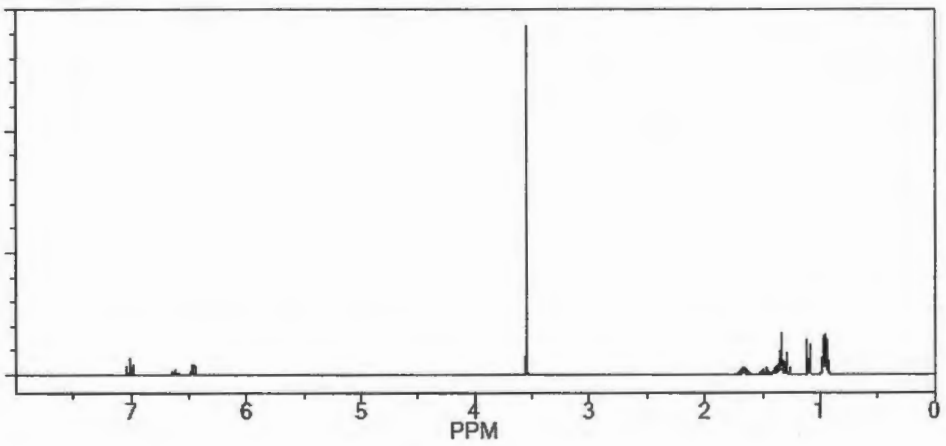

Figure A-7: ^{1}H NMR ChemDraw Estimation of Imine formation

^{13}C-NMR estimation of the NPM-VTMS polymer showing imine formation with propylamine

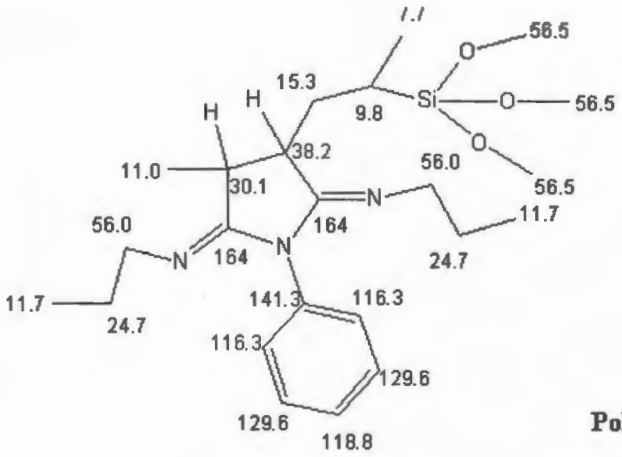

Polymer with propylamine carbon NMR

Estimation Quality: blue = good, magenta = medium, red = rough

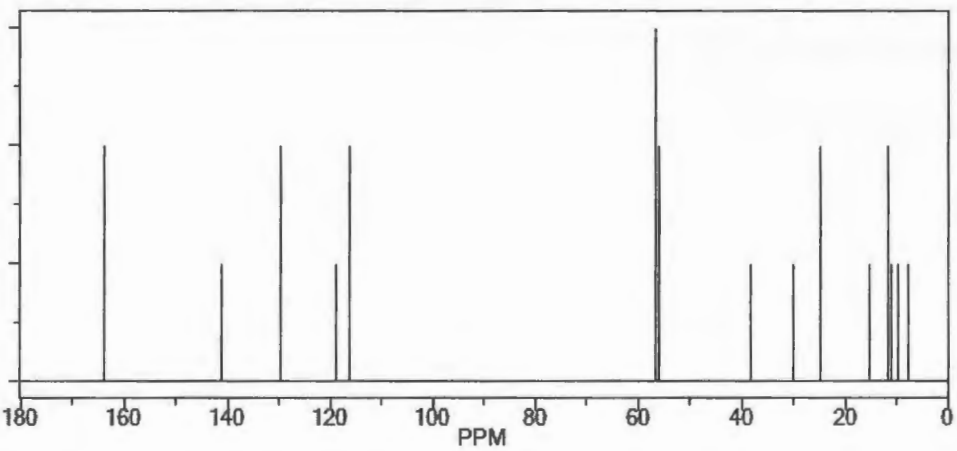

Figure A-8: ^{13}C NMR ChemDraw Estimation of Imine formation

^{1}H-NMR estimation of the NPM-VTMS polymer forming enamine with dipropylamine

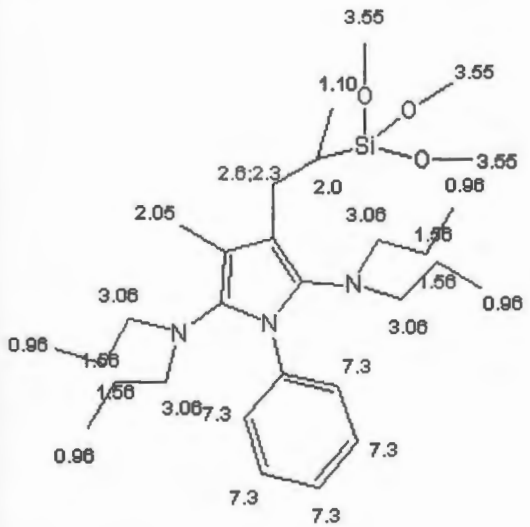

Polymer with dipropylamine proton NMR forming Enamine

Estimation Quality: blue = good, magenta = medium, red = rough

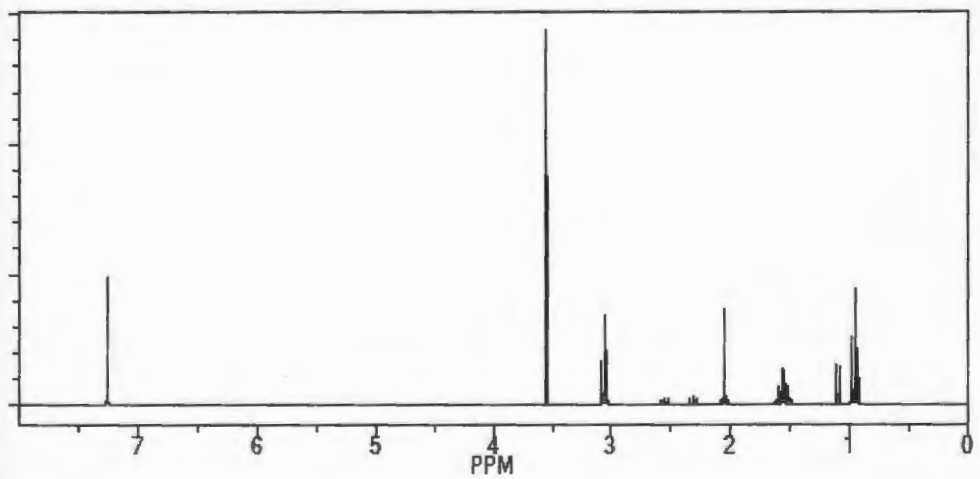

Figure A-9: ^{1}H NMR ChemDraw Estimation of Enamine formation

^{13}C-NMR estimation of the NPM-VTMS polymer forming enamine with dipropylamine

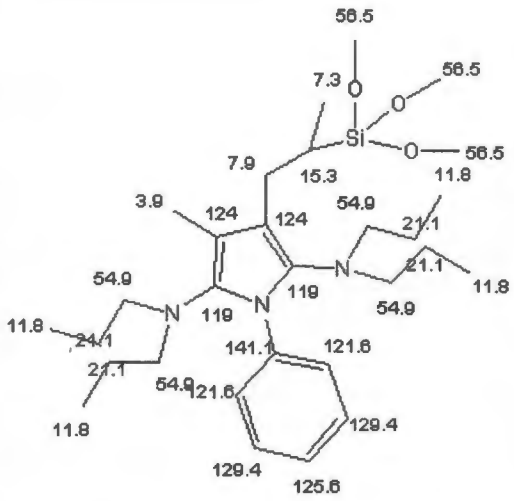

Polymer with dipropylamine forming enamine carbon NMR

Estimation Quality: blue = good, magenta = medium, red = rough

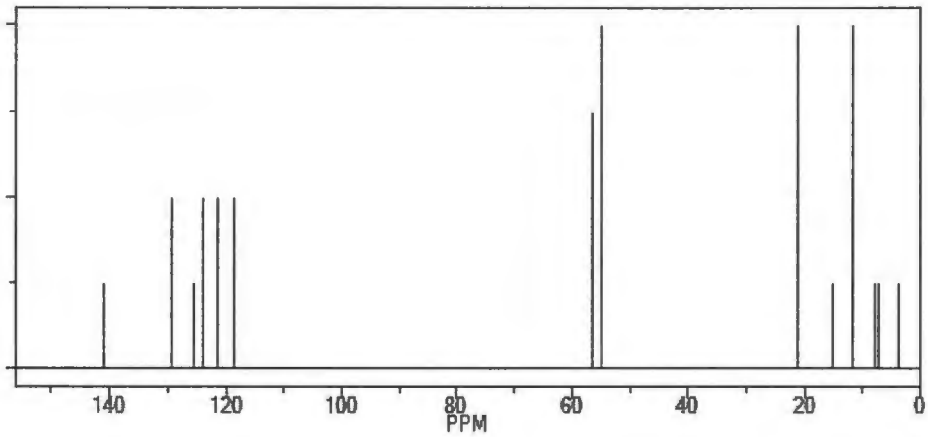

Figure A-10 : ^{13}C NMR ChemDraw Estimation of Enamine formation

Fluorescence Data

Polymer solutions with Primary, Secondary and Tertiary amines shows the λ_{max} at around 580 nm. But after some time when the polymer solutions with primary amines becomes yellow shows λ_{max} at 530 nm showing blue shift. And secondary amine changing from pink, deep red to orange shows first red shift and finally blue shift to λ_{max} of around 560 nm. Tertiary amines stay pink color for long period of time and do not show any change in λ_{max}.

Initial Spectra

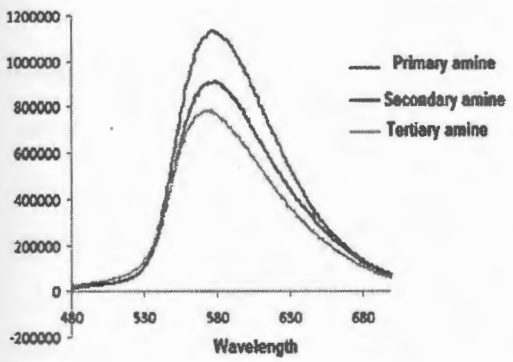

Spectra after the color changes

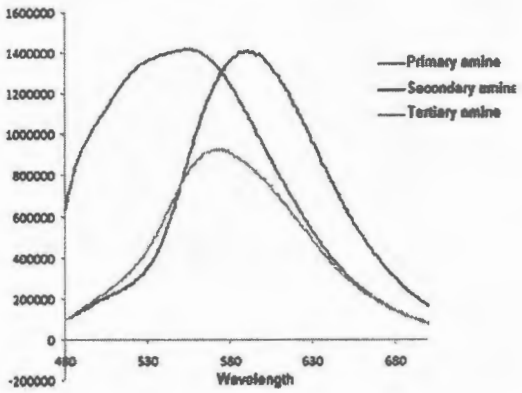

Figure A-11: Polymer spectra showing change in λ_{max} after adding amines over a period of time.

Spectrum with Primary amine

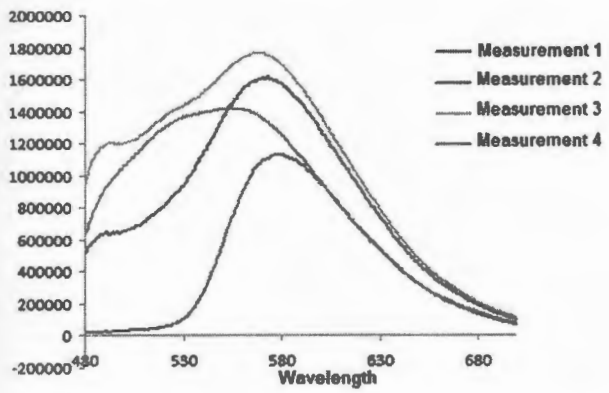

Spectrum with Secondary amine

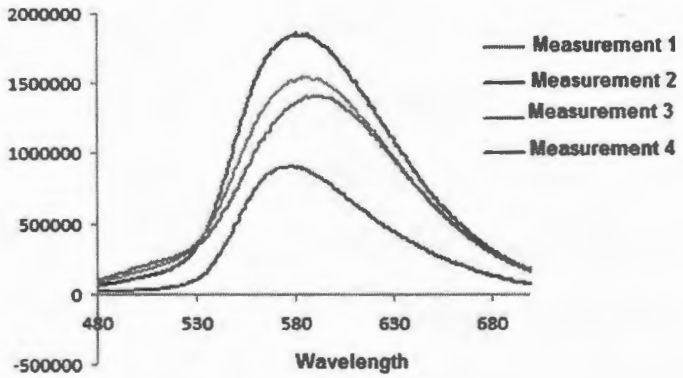

Spectrum with Tertiary amine

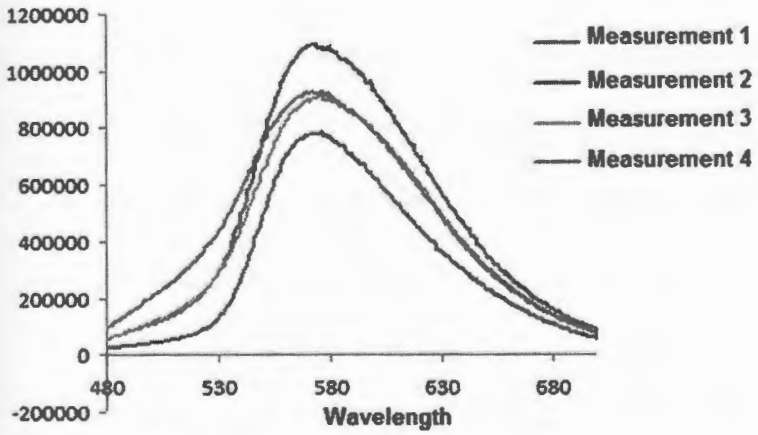

Figure A-12: Polymer solutions showing change in shifts when primary, secondary and tertiary amines were added.

References

1. Sensors and Related Research , FY 2007 Budget Request to Congress, Sensor-IED Narrative 01-23-06.doc
2. Vereshchagina, E.; Gardeniers, J. G. E., Development of Hot-Surface PolySilicon-Based Chemical Sensor and Actuator with Integrated Catalytic Micropatterns for Gas sensing Applications, Olfaction and Electronic Nose: Proceedings of the 13th International Symposium, 1137, 406-408.
3. The Future of Sensors, Electronic Design, The Authority on Emerging Technologies for Design Solutions, July 5, 2004.
4. K. Maruszewski, D. Andrzejewski and W. Strek., Thermal Sensor based on luminescence Rhuthenium bipyridine entrapped in sol-gel glasses, Journal of Luminescence., 72-72, 1997, 226-228.
5. A Textbook by Jiri Janata, Principles of Chemical Sensors.
6. A textbook by Rameier Narayanaswamy, Optical Sensors: Industrial, Environmental and Diagnostic Applications.
7. V. Liberali, F. Maloberti, and D. Tonietto, "Sigma-delta processing in multisensor systems for carbon monoxide detection", *Proceedings of IEEE International Symposium on Circuits and System (ISCAS `96)* , vol. *IV, Atlanta, USA, pp. 376-379, 1996.*
8. McQuade, T.D., Pullen, A., Swager, T.M., Chemical Review, 2000, 100, 2537-2574.
9. Lakowicz, J.R., Principles of Fluorescence Spectroscopy, Plenum Press: Newyork, 1983.

10. Czarnik, A.W., Fluorescence Chemosensors for Ion and Molecule Recognition., American Chemical Society, Washington, 1993.

11. Yang, W., Hamers, R.J., Applied Physics Letters, 2004, 85, 3626-3628.

12. Jones, R.M., Lu, L., Helgeson, R., Bergstedt, R.S., McBranch, D.W., Whitten, D.G., Proceedings of National Academy of Sciences, 2001, 98, 14769.

13. Molecularly Imprinted Polymer Sensors , The John Hopkins University, Applied Physics Laboratory.

14. Stringer, R.Cody., Gangopadhyaya Shubra., Grant, Shiela, A., Fluorescent imprinted polymers for detection of explosive nitro-aromatic compounds, Proceedings of the SPIE, 7303, 2009.

15. Tzouros, N.E., Arvanitoyannis, I.S., Food Review International, 2000, 16, 273.

16. Bastos, C., Mgan, N., Sensors and Actuators, B. Chemical, 2006, 116, 151.

17. Ailamaki, A., Faloustos, C., Fischbeck, P.S., Small, M.J., Small, J., Sigmod Record, 2003, 32, 47.

CHAPTER 7

Conclusions and Future Work

Conclusions

The research work presented in this dissertation is aimed at designing at new materials and facile assembly strategies for the design of materials that will find use in biofunctionalization studies, surface modification of microfluidic devices, chemical sensing and separations. We were able to manipulate the properties of the materials in a controlled way and also demonstrated various levels of control. First, we have successfully demonstrated a simple method to prepare a library of silane based polymers. We were able to tune the properties of the polymer by varying the identity of functional groups incorporated into the matrix of the materials by varying the substituted aniline used to prepare the maleimides. Secondly the conversion of polymers into various forms such as silica particles and silica-polymer composite particles to modify substrates by a simple dip-coating and spin-coating methods. Modified various substrates like glass, silicon by covalent linkage adopting a facile layer-by-layer approach. Since the polymers were covalently linked by strong siloxane bonds Si-O-Si the layers built on the substrates as well as multilayers were very robust under very harsh oxidizing conditions. We have observed that in the case of polymer modified interface there is significantly higher amount of particle deposition relative to the polymer-free interfaces. This finding we have rationalized in the context of the increased surface area provided by the polymer chains on the surface. This ability to

control the loading density opens whole new avenues towards design of materials which can be used as sensors for detecting amines and nitro compounds.

In the other research work detailed the polymer facilitated protein functionalization of Magnetic Iron Nanoparticles as the polymer not only provides the skeletal support but also protect the protein from denaturing as a result of the surface polar functionalities. In this work, research goal is aimed at ability to attach proteins, antigens and antibodies to the functionalized magnetic nanoparticles in such a way that the protein retains its native properties and to prevent non-specific adsorption of proteins in a biological specific antigen-antibody interaction.

The other work employed in our research is to perform the surface modification in the microfluidic channels. Biofunctionalization is achieved in microfluidic chips using facile surface modification schemes by using in-house prepared polymers and C18 materials. This work is a promising avenue to provide an excellent interface to increase the surface roughness and area within the device, as well as serving as an inert site for attachment of the biological entities being employed in these systems. This study can be extended for a high-throughput system for bio-marker proteins.

The last part of this research was application of the polymers prepared as sensors. The polymers are found to be sensitive to the presence of aliphatic amines, aromatic amines and weakly basic aromatic amines. The polymer solutions were intensely colored and fluorescence intensity increases in the presence of polymers. And by changing the nature of groups on the phenyl ring of the polymers, the sensitivity can also be tuned. An important feature associated with these polymers was

their reusability as detectors for amines. The polymer solutions with base added can be made reverse and colorless by adding an acid and can reuse again to detect another base. Successfully we were able to synthesize and characterize a library of versatile polymers and studied their potential applications in this work.

Future work

The work we present in this dissertation serves as an opening to a variety of novel areas that will be further explored within the Major group in future.

With respect to conversion of polymers into various superstructures and developing a layer-by-layer approach our work currently underway to determine the influence on hydrophobic character and polymer distribution on the surface as a function of film thickness and exploring the possibility of organization of these particles at the polymer-modified interfaces by heating the interface to the T_g of the polymer chains. It is expected that at the polymer T_g when the polymer chains "melt" and begin to flow, this will facilitate particle rearrangement into a more favorable configuration leading to organized arrays that do not require labor-intensive lithographic techniques.

With respect to synthesis of polymers, by modifying the phenyl ring with various groups, these polymer can be made to sense other organic groups as well. For instance, by adding a boronic acid moiety to the phenyl ring, these polymers can be made to detect both amines and carbohydrates.

Another area where the polymers reported can be used is to detect explosives. Since the polymers with base added have been found to be fluorescent, the presence of

any explosive can bring this fluorescence down and show a positive result. Not only as sensors, as these polymers are also being used to make columns (monolithic as well as HPLC) within the Major group, introduction of selective groups in the polymer can enhance the properties of these columns for selective as well as biological separations.

Magnetic Nanoparticles which are sub-micron size particles being smaller than typical cells, bacteria and viruses, they are ideal candidates for use in biological studies as their small size allows them to readily access the target species. The magnetic particles can be functionalized to attach antibodies labelled with fluorophores which can selectively attach to cancerous cells by recognizing the antigens via urea linkage. Upon magnetic resonance imaging, the magnetics can successfully help in the visualization of target cells. The magnetic particles modified biologically with drugs can be a promising treatment for cancer by Magnetic Resonance Imaging.

Simple maleimide chemistry used through out the research, combined with siloxane chemistry can also be used to prepare quantum dots whose surface is modified with known or unknown sequences of DNA oligonucleotides. These quantum dots can be linked to any of the surface used within the lab via Si-O-Si bonds. The size of the quantum dot can identify its position with the help of fluorescence.

Bibliography

Warren Gerhardt, Matija Carne, and MarcusW eck., Multifunctionalization of Synthetic Polymer Systems though Self-Assembly., Chemistry-A European Journal., 10, 24, 6212-6221.

Koutny, L. et al. Eight hundred base sequencing in a microfabricated electrophoretic device. Analytical Chemistry 72, 3388-3391 (2000).

Fan, Kee Ryu, Kashan Shaikh, David Bullen., Chang, Liu., Jack, Chen., Polymer Micromachining and Applications in Sensors, Microfluidics, and Nanotechnology. Journal of Micromechanics and Engineering, 2000, 10, 80-84.

Abhikit, Biswas., The challenge of fabricating nanocomposite thin films, Nanowerk., July 10, 2007.

Robert, Cammaratta., Processing and Mechanical Behavior of Nanocomposite Thin Films, Material Science and Engineering, Seminar, 2006.

Major, J.S., Blanchard, G.J., Strategies for Covalent Multilayer Growth.1. Polymer Design and Characterization, Chemistry of Materials, 2002, 14, 2567-2573.

Hodgson, R.J., Chen, Y., Zhang, Z., Tleugabulova, D., Long, H., Zhao, X., Organ, M., M.A., Brennan, J.D., Protein-doped monolithic silica columns for capillary liquid chromatography prepared by the sol-gel method : applications to frontal affinity chromatography, Analytical Chemistry, 2004, 76, 2780-2790.

Buchmeiser, M.R., New synthetic ways for the preparation of high-performance liquid chromatography supports, Journal of Chromatography A, 2001, 918, 233-266.

Constantin, S., Freitag, R., Solignac, D., Sayah, A., Gijs, M.A., Utilization of the sol-gel technique for the development of novel stationary phases for capillary electrochromatography on a chip, Sensors and Actuators B: Chemical, 2001, 78, 267-272.

Xia, Y., Gates, B., Yin, Y., Liu, Y., Advanced Materials, 2000, 12, 693-713.

Reculusa, S., Ravaine, S., Chemistry of Materials, 2003, 15, 598-605.

De, G., Karmakar, B., Ganguli, D., Journal of Materials Chemistry, 2000, 10, 2289-2293.

Marxer, S.M., Schoenfisch, M.H., "Sol-gel derived potentiometric pH sensors." Analytical Chemistry (2005) 77 (3), 848-853.

Parashar, V.K., Sahaya, A., Pfefferb, M., Schochb, F., Gobrechtc, J., Gijsa, M.A.M., "Nano-replication of diffractive optical elements in sol-gel derived glasses."Microelectronic Engineering (2003), 67-68, 710-719.

Jones, R.M., Lu, L., Helgeson, R., Bergstedt, R.S., McBranch, D.W., Whitten, D.G., Proceedings of National Academy of Sciences, 2001, 98, 14769.

Stringer, R.Cody., Gangopadhyaya Shubra., Grant, Shiela, A., Fluorescent imprinted polymers for detection of explosive nitro-aromatic compounds, Proceedings of the SPIE, 7303, 2009.

Bastos, C., Mgan, N., Sensors and Actuators, B. Chemical, 2006, 116, 151.